JANUARY 2019 Ph. D. in Electrical and Electronics Engineering MEHMET ARICI

REPUBLIC OF TURKEY

GAZİANTEP UNIVERSITY

GRADUATE SCHOOL OF

NATURAL & APPLIED SCIENCES

ADAPTIVE AND ROBUST CONTROL STRATEGIES FOR SYSTEMS WITH ACTUATOR FAILURE

Ph. D. THESIS

IN

ELECTRICAL AND ELECTRONICS ENGINEERING

BY

MEHMET ARICI

JANUARY 2019

ADAPTIVE AND ROBUST CONTROL STRATEGIES FOR SYSTEMS WITH ACTUATOR FAILURE

Ph. D. Thesis

in

Electrical and Electronics Engineering

Gaziantep University

Supervisor

Asst. Prof. Dr. Tolgay Kara

by

Mehmet Arıcı

January 2019

REPUBLIC OF TURKEY
GAZİANTEP UNIVERSITY
GRADUATE SCHOOL OF NATURAL & APPLIED SCIENCES
ELECTRICAL AND ELECTRONICS ENGINEERING

Name of the thesis: Adaptive and robust Control Strategies for Systems with Actuator Failure

Name of the student: Mehmet ARICI

Exam date: 25.01.2019

Approval of the Graduate School of Natural and Applied Sciences

Prof. Dr. A. Necmeddin YAZICI
Director

I certify that this thesis satisfies all the requirements as a thesis for the degree of Doctor of Philosophy.

Prof. Dr. Ergun ERÇELEBİ
Head of Department

This is to certify that we have read this thesis and that in our consensus opinion it is fully adequate, in scope and quality, as a thesis for the degree of Doctor of Philosophy.

Asst. Prof. Dr. Tolgay KARA
Supervisor

Examining Committee Members:	Signature
Prof. Dr. L. Canan DÜLGER	…………………..
Prof. Dr. Arif NACAROĞLU	…………………..
Prof. Dr. Ergun ERÇELEBİ	…………………..
Asst. Prof. Dr. Murat FURAT	…………………..
Asst. Prof. Dr. Tolgay KARA	…………………..

I hereby declare that all information in this document has been obtained and presented in accordance with academic rules and ethical conduct. I also declare that, as required by these rules and conduct, I have fully cited and referenced all material and results that are not original to this work.

Mehmet ARICI

ABSTRACT

ADAPTIVE AND ROBUST CONTROL STRATEGIES FOR SYSTEMS WITH ACTUATOR FAILURE

ARICI, Mehmet
Ph. D. in Electrical and Electronics Engineering
Supervisor: Asst. Prof. Dr. Tolgay KARA
January 2019
74 pages

In the present study, it is aimed to design a novel controller that is tolerant to actuator faults. The designed controller that uses robust adaptive control scheme maintains the system stability and desired closed-loop performance in the case of actuator faults. In the view of the control goal, a quadruple-tank system which comprises of two liquid pumps and level sensors is used as testbed. The system gives opportunity to obtain various plant structures being widely used in the literature by simply changing valve position of tank interconnections. A modified output-feedback multivariable model reference adaptive control (MRAC) scheme is proposed for the system that is prone to actuator faults. A unified comprehensive actuator fault model is presented. Then, some existing proper modifications that allow MRAC to gain the ability of actuator fault compensation controller is constructed by utilizing existing results and a new adaptation law that is based on a method first used for optimization purposes. The stability of proposed controller is proved and process simulation results are given to exhibit the effectiveness of the proposed scheme. The final control scheme, with some robustness modification by considering practical issues, is applied to the real process and it is shown that the control system leads to a faster smooth postfault transient response compared with similar methods. In addition it generates a smooth control signal without high frequency oscillations making the system less vulnerable to actuator damages

Key Words: fault tolerant control, multivariable adaptive control, actuator faults, robustness, nonlinear process, output feedback, dynamical inertial system, optimization

ÖZET

EYLEYİCİ ARIZALI SİSTEMLER İÇİN UYARLAMALI VE GÜRBÜZ DENETİMCİ STRATEJİLERİ

ARICI, Mehmet
Doktora Tezi, Elektrik ve Elektronik Mühendisliği
Tez Yöneticisi: Dr. Öğr. Üyesi Tolgay KARA
Ocak 2019
74 sayfa

Bu çalışmada, eyleyici arızası meydana gelmesi muhtemel sistemlerde, hedeflenen sistem performansının karşılanmaya devam edilmesini sağlayacak gürbüz ve uyarlanır karaktere sahip yeni bir denetimci tasarımı amaçlanmıştır. Öncelikle, olası eyleyici arızalarının büyük çoğunluğunu kapsayan bir genelleştirilmiş eyleyici arıza matematik modeli sunulmuştur. Çıkış geri beslemeli model referanslı uyarlamalı denetim yöntemi ana yaklaşım olarak belirlenip eyleyici hata/arıza kompanzasyon yeteneğini uyarlamalı denetimciye kazandırmak için bazı mevcut geliştirmeler denetimciye eklenmiştir. Bahsedilen geliştirmelerin yanında eniyileştirme temelli bir uyarlama mekanizması yardımıyla önerilen denetimciye son hali verilip, özgün denetimcinin kapalı çevrim kararlılığı ispatlanmıştır. Literatürdeki farklı sayıdaki ara bağlantılı sıvı tanklarını vanalar vasıtasıyla elde etmeye elverişli, iki adet sıvı pompası ve seviye algılayıcıları bulunan dörtlü tank deney düzeneği, tasarlanan denetimcinin kapalı çevrim sisteminin performansını gözlemlemek amacıyla kullanılmıştır. Kapalı çevrim sistem başarımı bilgisayar benzetimlerinin yanında, test düzeneğine gerçek zamanlı olarak uygulanmış; benzer denetim yöntemlerine kıyasla daha hızlı arıza sonrası geçiş tepkesine sahip olduğu ve bunun yanında eyleyicilerin daha az yıpranmasına olanak veren yumuşak geçişli ve az salınımlı denetim işareti ürettiği gösterilmiştir.

Anahtar Kelimeler: Hata toleranslı denetim, çok değişkenli uyarlamalı denetim, eyleyici hataları, gürbüzlük, doğrusal olmayan proses, dinamik eylemsizliksel sistem, eniyileştirme

''Dedicated to my family''

ACKNOWLEDGEMENTS

I would like to thank my supervisor, Dr. Tolgay Kara for his guidance and support throughout the study. I am thankful for his encouragement and motivation.

I would like to express my love and gratitude to my family for their support, always best wishes.

This work is supported by The Scientific and Technological Research Council of Turkey (TUBİTAK), through project 116E020.

TABLE OF CONTENTS

Page

LIST OF FIGURES

Page

LIST OF TABLES

Page

LIST OF SYMBOLS/ABBREVIATIONS

A/D	Analog to Digital
B-SPM	Bilinear Static Parametric Model
CE	Certainty Equivalence
D/A	Digital to Analog
DC	Direct Current
DIN	Dynamic Inertial System
FD	Fault Detection
FDD	Fault Detection Diagnosis
FDI	Fault Detection and Isolation
FTC	Fault Tolerant Control
g-DIN	Generalized Dynamic Inertial System
ISE	Integral Square Error
ISR	Interrupt Service Routine
LQR	Linear Quadratic Regulator
LTI	Linear Time Invariant
MIMO	Multi Input Multi Output
MRAC	Model Reference Adaptive Control
MSE	Mean Square Error
PDJ	Positive Diagonal Jordan
PEA	Parametric Eigenstructure Assignment
PSUPA	Power Supply/Power Amplifier Unit
SISO	Single Input Single Output
SPR	Strictly Positive Real

CHAPTER I

INTRODUCTION

1.1 Motivation of Study

Due to increasing demand on performance and economic benefits in production, modern technical processes become more complex and require precise system control. Production and environment safety is an important topic for the technical processes existing in industries such as petro-chemical, paper production, food processing, pharmaceutical, nuclear and chemical reactors, water treatment facilities [1-6]. In such safety critical systems, a small variation in plant parameters can result in undesired system behavior and instability. Actuators are important vulnerable industrial plant components and any malfunctioning in these components may well cause the same catastrophic consequences. Actuator failure may occur in systems at uncertain time in different ways such as lock-in-place, loss of effectiveness, outage, and etc. Study of control systems which offers a solution to this problem has received considerable attention in recent years. The control system, in this instance, must be reliable and have the capability to tolerate faults or total failure effects. Instead of using a simple feedback control scheme, a fault tolerant control (FTC) design must be considered. There are wide varieties of control methods in FTC and an extensive research is still conducted. However the lack of a systematical approach is still an open problem. Besides, the performance of controlled system depends on many factors such as:

- Reconfigurable controller design
- Actuator hardware/analytical redundancy
- Parameter estimation of closed-loop system for uncertainties and actuator failure cases
- Stability analysis, stability robustness
- Graceful performance degradation

- Application to nonlinear systems
- Real-time application issues

With the motivation of above open problems and considering system safety and reliability demands, it is aimed to design an adaptive robust control system which preserve the stability of the system and meet the performance specifications in the presence of actuator failures that can occur at any instance of time. Simulations and real time experiments results are used to exhibit overall system performance.

1.2 A Review of Literature

The design of FTC systems is currently an active research topic and draws a great deal of interest [7-17]. In FTC systems that compensate system uncertainties and actuator faults, reachable system performance depends on component analytic and hardware redundancies [18]. FTC systems can be classified as active or passive depending on the type of redundancy and controller structure [19]. These two approaches have different methodologies for the same control objective. For instance, in the case of an actuator fault, passive approach considers some presumed faults in the design stage of controller and it has a simple constant structure. Robust control methods such as H_∞, linear quadratic regulator (LQR), sliding mode control are some methods that are considered in this class [20-25]. On the other hand, active FTC has a variable structure and includes reconfiguration mechanism. Different from the passive approach, it needs a fault detection and diagnosis (FDD) unit that estimates the magnitude of fault and where it occurs. Model predictive control, parametric eigenstructure assignment, and model following, multiple model and adaptive control are some design approaches that can be included in this class [26-28]. Active FTC has the capability of reacting to any type of actuator faults thanks to its variable structure while passive FTC considers a list of potential malfunctions in the design stage. There is an extensive literature on FTC of nonlinear processes [29-35]. Mhaskar, Gani and Christofides [33] considered the problem of controlling nonlinear processes subjected to input constraints and actuator failures. An active FTC that chooses one of available control configurations in the case of a failure in primary control is designed by considering performance and robustness criteria. Robust hybrid predictive controllers for each control configuration are used with the help of a supervisor. The method is applied to a nonlinear single input chemical process which has the ability of accommodating total actuator failures thanks to its structural actuator redundancy. Mhaskar et al [34] considered the control of nonlinear process in the case actuator failures. A fault detection (FD) mechanism with FTC is proposed. In the presence of failure, control loop reconfiguration is provided by orchestrating a family of controllers that the each one is for redundant actuators having the same mission. In a further extension of above work, Mhaskar et al. in [35], consider a nonlinear multi input chemical process and draw attention to absence of fault detection and isolation (FDI) may fail to preserve closed-loop stability due to the fact that totally failed actuator may also be a member of remained back-up control configurations. Therefore an FDI filter is used together with a similar FTC idea given above.

Due to their adaptation ability in the case of system parameter changes, adaptive control methods are suitable for active FTC. These methods could be called "self-reconfigurable" since they do not require reconfiguration mechanism and FDD components. They can be used as main controller of FTC design or placed as an auxiliary control to compensate faults and system uncertainties [36-39]. Jin et al. [38] presented FTC for a linear time-invariant (LTI) system subjected to partial faults and actuator saturations. An auxiliary system-based controller and adaptive adjustment mechanism are added to nominal controller for dealing with loss of effectiveness type fault and actuator saturation. In another study, Jin et al. [39] proposed a robust fault tolerant consensus control strategy for a class of nonlinear second-order leader-following multi-agent systems against actuator faults and time-varying system uncertainties. Partial loss of effectiveness and additive bias-actuator faults are considered. A distributed controller that comprises of two parts is designed. The first part of controller is used to ensure the stability of the system while the second part is designed to compensate actuator faults and system uncertainties by using a varying gain which depends on adaptive law. Chattering that stems from adaptation law is solved by using a boundary condition in stability based design.

Model reference adaptive control (MRAC) method with some robustness modification can be a good solution to fault tolerance problem [40-43]. Besides, it gives the opportunity to deal with interaction effects of faults in multivariable processes with coupling due to their decoupled model following property if it is considered as main control scheme of FTC. In addition, it does not need an FDD unit just as the above mentioned adaptive approaches. However adaptive control estimation algorithms generally need the system parameters to change slowly enough for a good tracking. As a result, they need some modification to react to actuator faults that may cause abrupt and dramatic changes in system parameters. A simple way of achieving fast adaptation is to increase adaptive learning rates. Even though it seems feasible, an update subject to high learning rates may result in high frequency oscillations in the control signal and excite unmodelled dynamics of the plant [44-46]. In order to suppress oscillations and improve transient of MRAC, some recent studies that modify the adaptive controller are available. A robust error feedback compensator is designed without modifying the reference model and integrated into adaptive control, which leads to less oscillatory behavior in the presence of high adaptive gains [47, 48]. Nguyen et al. [49] proposed a fast MRAC that is based on the minimization of the squares of the tracking error which is formulated as an optimal control and derive the adaptive law by using the gradient method. Sun et al. [50] proposed a MRAC with external filter, which can attain the same performance without using a high-static adaptation gain. Yucelen and Gruenwald [51] proposed an adaptive control architecture which involved added terms in the update law entitled artificial basis functions by using gradient optimization procedure. Annaswamy et al. [52-54] used Luenberger observer-based adaptive control scheme to improve transient performance by modifying the reference model with a state error feedback.

Industrial processes are inherently nonlinear and generally multi-input multi-output (MIMO) systems. Therefore a centralized FTC system structure may be advantageous since dynamic input-output interactions are more significant if an actuator malfunction occurs. In addition, if a multivariable MRAC is chosen for fault tolerance, the framework of adaptive control is an important issue because application of state feedback state tracking control design is difficult due to the matching condition in some typical situations [55]. On the other hand, plant-model matching conditions for adaptive output tracking control schemes require less plant information. As a result, they are much less restrictive. However, multivariable adaptive control brings new issues related with the system high frequency gain (HFG) matrix, which may include the search for less restrictive conditions of such a matrix, reducing the need for the knowledge of the system interactor matrix, and how to deal with system faults [56]. Therefore, a designer who aims to construct an adaptive FTC for a multivariable system must find solutions to these technical issues. In particular, a multivariable MRAC design requires maximal plant uncertainty parameterization and a stable parameter adaptation to recover the system performance gracefully in the presence of actuator faults. These faults are difficult to predict and can be abrupt, incipient or intermittent. Abrupt faults take place in an immediate way mostly as a result of hardware damage. Incipient faults, such as component aging, have a slow characteristic and gradually increase with time. In intermittent case, a fault occurs and disappears repeatedly (e.g., bad contact or damaged wiring). In addition to the way of occurrence, fault impact on the system depends on the type of fault since it can be a simple loss of efficiency or may also lead to total system failure. Therefore a generalized parametric actuator fault model that covers all the failure possibilities is important and more practical.

A MIMO quadruple tank process which is first proposed by Johansson [57] is considered. It is a benchmark system developed for process industry. The system under study gives opportunity to find solutions for various application purposes such as actuator and sensor fault tolerance, testing FDD algorithms, centralized and decentralized control structure for multivariable systems, minimum and non-minimum phase system control, and nonlinear control design [58-61].

1.3 Contribution of the Present Work

This thesis work is aimed to constitute a solution to the problem of unpredictable actuator failure in control systems. Stability and performance requirements are met by the control design despite the failure regardless of time and duration. Adaptive robust control strategies constitutes main framework of solution. In the literature, various fault/failure models for actuators are available. These models change depending on the assumptions and structure. In a general fault model, including only a reduction of efficiency is not enough. A comprehensive fault model for valve actuator must contain other cases such as stuck, hard-over and leakage. These actuator faults are encountered frequently in the process control industry. For that purpose, firstly, a generalized actuator fault model is proposed as an alternative to existing models in literature [62-66]. For FTC design, a multivariable output feedback MRAC is chosen and some modifications are added to solve the difficulties in the presence of actuator faults such as relaxing the restrictions of special gain matrix HFG and improving the robustness of controller, control reparametrization for actuator failure and finally designing a novel controller that improves post fault transients by providing fast adaptation using an idea that is applied for the first time for optimization purposes. Applicability of the control method is first tested on the benchmark coupled tank system via simulations. Different from the original system, a valve actuated configuration is considered as well in control simulation part of thesis. In the final stage, real time experiments are conducted on coupled tank system supplied by the research project having the same goal with the thesis.

1.4 Organization of Thesis

The presentation of the thesis is organized as follows: In Chapter 2, the basics of single-input single-output (SISO) adaptive MRAC design and some fundamental theorems are firstly given. Then a quick transition to MIMO counterpart of the design is presented by using the same concept. In Chapter 3, firstly, a unified actuator failure model is given. Then, FTC system design is presented, which constitutes one of the novelties of this work such that it uses advantages of previous designs and besides adds a fast adaptation property without high frequency oscillation so as to obtain an adaptive multivariable MRAC. In Chapter 4, the process model is given. Simulation results are discussed and performance comparison of controllers is presented. In Chapter 5, real time experiment results are presented in graphical form. In Chapter 6, the thesis concluding remarks and recommendations are given.

CHAPTER II

OUTPUT FEEDBACK MRAC DESIGN FOR OUTPUT TRACKING

2.1 Direct MRAC for SISO Plants with Unnormalized Adaptive Laws

In this part, we start with giving a formulation of adaptive control problem for a class of LTI SISO plants. By assuming that plant parameters are known exactly, a control structure can be determined. This assumption provides the structure of the control law which is aimed to combine with an adaptation law to form final MRAC scheme for the plant with unknown parameters.

Consider the SISO LTI plant system representation:

$$\left.\begin{aligned} \dot{\mathbf{x}} &= \mathbf{A}_p \mathbf{x}_p + \mathbf{b}_p u_p \\ \mathbf{x}_p(0) &= \mathbf{x}_0 \\ y_p &= \mathbf{c_p x_p} \end{aligned}\right\} \tag{2.1}$$

where $\mathbf{x}_p \in \mathbf{R}^\mathbf{n}$; $y_p, u_p \in R$. The plant is assumed to be stabilizable and detectable. The transfer function of the dynamical system is as follows:

$$y_p = G_p(s) u_p \tag{2.2}$$

with $G_p(s)$ is given as follows:

$$G_p(s) = k_p \frac{Z_p(s)}{R_p(s)} \tag{2.3}$$

where $Z_p(s)$, $R_p(s)$ are monic polynomials and k_p is high-frequency gain. For the desired plant behavior, a reference model that is chosen by designer can be expressed as follows:

$$\dot{\mathbf{x}} = \mathbf{A}_m \mathbf{x}_m + \mathbf{b}_m r, \quad \mathbf{x}_m(0) = \mathbf{x}_{m0},$$

$$y_m = W_m(s)r \tag{2.4}$$

where $\mathbf{x}_m \in \mathbf{R}^{\mathbf{p}_m}$ for some integer p_m; $y_m, r \in R$; and r is uniformly bounded piecewise continuous function of time. The transfer function of reference model is:

$$W_m(s) = k_m \frac{Z_m(s)}{R_m(s)} \tag{2.5}$$

where $Z_m(s)$, $R_m(s)$ are monic polynomials and k_m is a constant. The model reference control objective with exactly known parameters is to find a control input u_p so that all signals are bounded and y_p tracks reference model output y_m with smallest possible error for any reference input *r(t)*. In order to meet control objective with a control law that is free of differentiators and uses measurable signals, following assumptions must hold:

Assumption 2.1: The following assumptions are considered for the plant model

- Z_p is a monic Hurwitz polynomial.
- An upper bound of n of degree n_p of R_p is known.
- The relative degree $n^*=n_p-m_p$ of $G_p(s)$ is known, where m_p is the degree of Z_p.
- The sign of the high frequency gain k_p is known.

Assumption 2.2: The following assumptions are considered for the reference model

- $Z_m(s)$, $R_m(s)$ are monic Hurwitz polynomials of degree q_m, p_m, respectively where $p_m \leq n$.
- The relative degree $n_m^* = p_m - q_m$ of $W_m(s)$ is the same as that of $G_p(s)$.

By considering all the coefficients of $G_p(s)$ is known and with the condition that reference model must is strictly positive real (SPR) to obtain a stable controller, one can propose a stable feedback control law:

$$u_p = \boldsymbol{\theta}_1^{*T} \frac{\boldsymbol{\alpha}(s)}{\Lambda(s)} u + \boldsymbol{\theta}_2^{*T} \frac{\boldsymbol{\alpha}(s)}{\Lambda(s)} y_p + \theta_3^{*T} y_p + c_0^* r \tag{2.6}$$

where $\alpha(s)=[s^{n-2},s^{n-3},...s,1]^T$ for $n\geq 2$, $\alpha(s)=0$ for n=1, $c^*_0,\theta^*_3\in R$; $\boldsymbol{\theta}_1^{*T},\boldsymbol{\theta}_2^{*T}\in R^{n-1}$ and $\Lambda(s)$ is an arbitrary monic Hurwitz polynomial of degree n-1 that contains $Z_m(s)$ as a factor such that:

$$\Lambda(s)=\Lambda_0(s)Z_m(s) \tag{2.7}$$

Let us now define the control law in a compact form as follows:

$$u_p=\boldsymbol{\theta}^{*T}\boldsymbol{\omega} \tag{2.8}$$

where $\boldsymbol{\theta}^*=\left[\boldsymbol{\theta}_1^{*T}\quad \boldsymbol{\theta}_2^{*T}\quad \theta_3\quad c^*_0\right]^T\in R^{2n}$ is parameter vector that is chosen so that transfer function from r to y_p is equal to $W_m(s)$ and $\boldsymbol{\omega}=\left[\boldsymbol{\omega}_1^T\quad \boldsymbol{\omega}_2^T\quad y^T\quad r^T\right]^T$ is vector of known signals with $\boldsymbol{\omega}_1=\dfrac{\boldsymbol{\alpha}(s)}{\Lambda(s)}u$, $\boldsymbol{\omega}_2=\dfrac{\boldsymbol{\alpha}(s)}{\Lambda(s)}y$. The closed loop system transfer function:

$$y_p=G_c(s)r \tag{2.9}$$

where

$$G_c(s)=\frac{c_0^*k_pZ_p(s)\Lambda^2(s)}{\Lambda(s)[(\Lambda(s)-\boldsymbol{\theta}_1^{*T}\boldsymbol{\alpha}(s))R_p(s)-k_pZ_p(s)(\boldsymbol{\theta}_2^{*T}\boldsymbol{\alpha}(s)+\theta_3^*\Lambda(s))]} \tag{2.10}$$

Since it is assumed that control parameters are exactly known, the closed-loop transfer function $G_c(s)=W_m(s)$ such that:

$$\frac{c_0^*k_pZ_p\Lambda^2}{\Lambda(s)[(\Lambda-\boldsymbol{\theta}_1^{*T}\boldsymbol{\alpha})R_p-k_pZ_p(\boldsymbol{\theta}_2^{*T}\boldsymbol{\alpha}+\theta_3^*\Lambda)]}=k_m\frac{Z_m(s)}{R_m(s)} \tag{2.11}$$

Choosing $c^*_0=\dfrac{k_m}{k_p}$ and using equation (2.7), the matching condition (2.11) becomes

$$(\Lambda-\boldsymbol{\theta}_1^{*T}\boldsymbol{\alpha})R_p-k_pZ_p(\boldsymbol{\theta}_2^{*T}\boldsymbol{\alpha}+\theta_3^*\Lambda)=Z_p\Lambda_0R_m \tag{2.12}$$

Equating the coefficients of powers of s on both sides of (2.12), the algebraic equation can be expressed as:

$$S\overline{\boldsymbol{\theta}}^* = p \tag{2.13}$$

where $\overline{\boldsymbol{\theta}}^* = [\boldsymbol{\theta}_1^{*T}, \boldsymbol{\theta}_2^{*T}, \theta_3]^T$; S is an (n + n_p-1) x (2n - 1) matrix that depends on the coefficients of R_p, k_pZ_p and Λ; p is an n + n_p - 1 vector with the coefficients of $\Lambda R_p - Z_p \Lambda R_m$.

Lemma 2.1: Let the degrees of R_p, Z_p, Λ, Λ_0 and R_m be as specified in equation (2.6) then the solution $\overline{\boldsymbol{\theta}}^*$ of (2.13) always exists. In addition if R_p and Z_p are coprime and $n = n_p$, the solution $\overline{\boldsymbol{\theta}}^*$ is unique.

The proof of the lemma is given in [67].

The control law (2.6) is the important part of MRAC schemes to be designed in the following part to deal with the unknown plant parameters. Let us start with defining the parameter error when unknown parameters exist in the plant such that:

$$\tilde{\boldsymbol{\theta}} = \boldsymbol{\theta}(\mathbf{t}) - \boldsymbol{\theta}^* \Rightarrow \boldsymbol{\theta}(\mathbf{t}) = \tilde{\boldsymbol{\theta}} + \boldsymbol{\theta}^* \tag{2.14}$$

here $\boldsymbol{\theta}(\mathbf{t})$ is the estimation of known plant parameter vector $\boldsymbol{\theta}^*$. By using equation (2.14), equation (2.8) can be written as:

$$u_p = \tilde{\boldsymbol{\theta}}^{\mathbf{T}} \boldsymbol{\omega} + \boldsymbol{\theta}^{*\mathbf{T}} \boldsymbol{\omega} \tag{2.15}$$

In order to choose an adaptation law, we have to first find out how the tracking error is related to the parameter error. The control law can be expressed as an external signal of model reference controlled system block diagram as given in Figure 2.1.

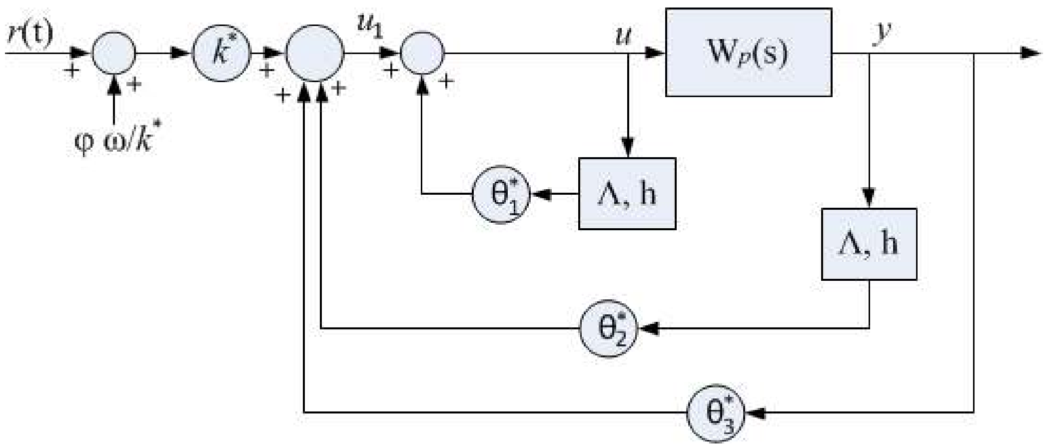

Figure 2.1 Equivalent control system block diagram for time-varying gains

To find the tracking error equation:

$$y(t) = W_m(s)r + W_m(s)(\rho^* \tilde{\boldsymbol{\theta}}^{\mathbf{T}} \boldsymbol{\omega}) \tag{2.16}$$

where $\rho^* = \dfrac{1}{c_0^*}$. Remembering $y_m(t) = W_m(s)r$, the tracking error equation in this case can be given as follows:

$$e(t) = y(t) - y_m(t) = W_m(s)(\rho^* \tilde{\boldsymbol{\theta}}^{\mathbf{T}} \boldsymbol{\omega}) \tag{2.17}$$

For the purpose of finding an adaptation law that uses error equation in (2.17), some stability tools for linear systems are needed. For an SPR transfer function of a system there is an important lemma associated with its state-space representation.

Lemma 2.2 (Kalman-Yakubovich) Consider a controllable LTI system

$$\left.\begin{aligned} \dot{\mathbf{x}} &= \mathbf{A}\mathbf{x} + \mathbf{b}u \\ y &= \mathbf{c}^T \mathbf{x} \end{aligned}\right\} \tag{2.18}$$

The transfer function

$$h(s) = \mathbf{c}^T [s\mathbf{I} - \mathbf{A}]^{-1} \mathbf{b} \tag{2.19}$$

is strictly positive real if, and only if, there exist positive definite matrices **P** and **Q** such that

$$\begin{aligned} &\mathbf{A}^{\mathrm{T}}\mathbf{P} + \mathbf{P}\mathbf{A} = -\mathbf{Q} \\ &\mathbf{P}\mathbf{b} = \mathbf{c} \end{aligned} \tag{2.20}$$

The proof of the above lemma can be found in the literature [68-Slotine]

Corollary 2.1: Consider two signal e and $\boldsymbol{\eta}$ related by the following dynamic equation

$$e(t) = H(s)[k\boldsymbol{\eta}^{\mathrm{T}} v(t)] \tag{2.21}$$

where *e(t)* is scalar output signal, *H(s)* is a strictly positive real transfer function, *k* is and unknown constant with known sign, $\boldsymbol{\eta}$ is a *m*x1 vector function of time, and **v(t)** is a measurable *m*x1 vector. If the vector $\boldsymbol{\eta}$ varies according to

$$\dot{\boldsymbol{\phi}}(t) = -\mathrm{sgn}(\mathrm{k})\gamma e(t)\mathbf{v}(t) \tag{2.22}$$

with γ being a positive constant, then *e(t)* and η(t) are globally bounded. Furthermore, if **v** is bounded, then *e(t)*→0 as *t*→0

Proof: Let the state space representation of (2.21) be

$$\left.\begin{aligned} \dot{\mathbf{x}} &= \mathbf{A}\mathbf{x} + \mathbf{b}[k\boldsymbol{\eta}\mathbf{v}] \\ \mathbf{e} &= \mathbf{c}^T\mathbf{x} \end{aligned}\right\} \tag{2.23}$$

Since *H(s)* is SPR, following the Kalman-Yakubovich lemma, a positive definite function *V* can be defined as:

$$V(\mathbf{x}, \boldsymbol{\phi}) = \mathbf{x}^T\mathbf{P}\mathbf{x} + \frac{|k|}{\gamma}\boldsymbol{\eta}^T\boldsymbol{\eta} \tag{2.24}$$

Considering the system in (2.23) and vector dynamics given in (2.22), time derivative of the Lyapunov function in (2.24) can be written as:

$$\begin{aligned} \dot{V} &= \mathbf{x}^T(\mathbf{PA} + \mathbf{A}^T\mathbf{P})\mathbf{x} + 2\mathbf{x}^T\mathbf{P}(k\boldsymbol{\eta}^T\mathbf{v}) - 2\boldsymbol{\eta}^T(ke\mathbf{v}) \\ &\text{-}\mathbf{x}^T\mathbf{Q}\mathbf{x} \le 0 \end{aligned} \tag{2.25}$$

In the view above result we can conclude that the system defined by (2.21) and (2.22) is globally stable. The equations (2.24) and (2.25) also imply that e, $\boldsymbol{\eta} \in L^\infty$. □

Lemma 2.3 (Barbalat)

i. If *f:* $\mathrm{R}^+ \to \mathrm{R}$ is uniformly continuous for $t \ge 0$

ii. And if $\lim_{t\to\infty} \int_0^t |f(\mathrm{T})|\, dT$ exists and finite

Then $\lim_{t\to\infty} f(t) = 0$

Corollary 2.2: If $g \in L^2 \cap L^\infty$, and $\dot{g}$ is bounded (implies *g* is uniformly continuous), then $\lim_{t\to\infty} g(t) = 0$.

If the signal *v(t)* is bounded, $\dot{\mathbf{x}}$ is bounded, and above corollary in this case implies the uniform continuity of $\dot{V}$, since its derivative

$$\ddot{V} = -2\mathbf{x}\mathbf{Q}\dot{\mathbf{x}} \leq \infty \tag{2.25}$$

Application of Barbalat's lemma and considering the system equation (2.23) indicates that $e(t) \in L^2 \cap L^\infty$ and as a result $e(t)$ converges to zero. □

Since error equation (2.17) is identical with dynamical system equation 2.21 in Lemma 2.2, the adaptation law given below can be chosen:

$$\dot{\boldsymbol{\theta}}(t) = -\boldsymbol{\Gamma} e \boldsymbol{\omega} \operatorname{sgn}(k_p) \tag{2.26}$$

where $\boldsymbol{\Gamma}$ is a positive scalar matrix representing the adaptation gain and since we assume that k_m is positive, we can only consider the sign of k_p. Based on the result given in Lemma 2.1.2 and the corollary, one can show that the tracking error in the above adaptive control system converges to zero asymptotically.

2.1.1 Relative Degree n^*=2

In the design procedure of previous controller, we assume that system has relative degree n^*= 1 which gives the opportunity to design reference model as SPR. For the case that the reference model has relative degree n^*= 2, $W_m(s)$ can no longer be SPR. We can solve this problem by using the fact that $(s+p_0)(s+p_0)^{-1}$ is identity for some $p_0 > 0$ and rewrite the error equation (2.17):

$$e = W_m(s)(s+p_0)\rho^*(u_f - \boldsymbol{\theta}^{*T}\boldsymbol{\phi}) \tag{2.27}$$

where $u_f = \dfrac{1}{s+p_0}u_p$, $\boldsymbol{\phi} = \dfrac{1}{s+p_0}\boldsymbol{\omega}$, and $W_m(s)$, $p_0 \geq 0$ are chosen so that $W_m(s)(s+p_0)$ is SPR. Then control input can be written in the following form:

$$u_p = \boldsymbol{\theta}^T\boldsymbol{\omega} + \dot{\boldsymbol{\theta}}^T\boldsymbol{\phi} \tag{2.28}$$

Since $\dot{\boldsymbol{\theta}}$ can be acquired by the adaptive law, the control input (2.28) can be implemented without use of differentiators and the adaptive law for generating $\boldsymbol{\theta}$ is designed by using Lemma 2.1.2 as in the case of n^*= 1. Finally the adaptation law takes the following form:

$$\dot{\boldsymbol{\theta}}(t) = -\boldsymbol{\Gamma} e \boldsymbol{\phi} \operatorname{sgn}(k_p) \tag{2.29}$$

In the view of the Lemma 2.1.2 and 2.1.3, above adaptation algorithm guarantees that all closed loop signals are bounded and the tracking error converges to zero asymptotically.

2.2 Direct MRAC for SISO Plants with Normalized Adaptive Laws

In this section, a different MRAC approach that dominates the literature of adaptive control due to the simplicity of their design. The design is based on certainty equivalence (CE) approach that combines a control law that is originates from known parameter case, just as previous section, with an adaptive law based on bilinear static parametric model (B-SPM) and as well as gradient algorithm.

2.2.1 B-SPM for Parameter Identification

In some applications, the unknown parameters may not fit the form of the linear in the parameters models. In these cases, it may not possible to show the global convergence of the parametric model. However there exists a nonlinear in the parameters models with possible convergence results if the unknown parameters may be expressed in a special bilinear form such that:

$$z = \rho^* (\boldsymbol{\theta}^{*T} \boldsymbol{\phi} + z_0) \tag{2.30}$$

where z, z_0 are known scalar signals, ρ^* is a scalar parameter and $\boldsymbol{\theta}^*$, $\boldsymbol{\phi}$ are vectors of unknown parameters. For this parametric model parameter identification problem can be stated as follows: given the measurements z, z_0 and $\boldsymbol{\phi}$, generate the estimates $\rho(t)$, $\boldsymbol{\theta}(t)$ of ρ^*, $\boldsymbol{\theta}^*$, respectively at each time t.

2.2.2 Gradient Based Parameter Identification for B-SPM

Let us consider again the bilinear SPM given in equation (2.30). Parameter estimator and the estimation error are generated as follows:

$$\hat{z} = \rho(\boldsymbol{\theta}^{\mathrm{T}} \boldsymbol{\phi} + z_0) \tag{2.31}$$

$$\varepsilon = \frac{z - \hat{z}}{m^2} \tag{2.32}$$

where m_s is designed to bound ϕ, z_0 from above, for instance, $m^2 = 1 + \phi\phi^2 + z_0{}^2$. A cost function to be minimized can be considered as:

$$J(\rho, \theta) = \frac{\varepsilon^2 m^2}{2} = \frac{(z - \rho^* \theta^T \phi - \rho\xi + \rho^* \xi - \rho^* z_0)^2}{2m^2} \tag{2.33}$$

where $\xi = (\theta^T \phi + z_0)$ is available for measurement. Applying the gradient method, one can obtain the following equations:

$$\dot{\theta} = -\Gamma \nabla J_\theta = \Gamma_1 \rho^* \varepsilon \phi \tag{2.34.a}$$

$$\dot{\rho} = -\gamma \nabla J_\rho = \gamma_1 \varepsilon \xi \tag{2.34.b}$$

where $\Gamma_1 = \Gamma_1^T > 0$, $\gamma > 0$ are the adaptive gains. Since ρ^* is unknown, adaptation for θ is not feasible. We can solve this issue by using the following equation:

$$\Gamma \rho^* = \Gamma_1 \left|\rho^*\right| \operatorname{sgn}(\rho^*) = \Gamma \operatorname{sgn}(\rho^*) \tag{2.35}$$

where $\Gamma = \Gamma_1 \left|\rho^*\right|$. Since Γ_1 is arbitrary, $\Gamma = \Gamma^T > 0$ can be selected without knowledge of $\left|\rho^*\right|$. Final form of adaptation law can be written as:

$$\left.\begin{array}{c} \dot{\theta} = -\Gamma \varepsilon \phi \operatorname{sgn}(\rho^*) \\ \dot{\rho} = \gamma \varepsilon \xi, \\ \varepsilon = \dfrac{z - \rho\xi}{m_s^2},\ \xi = (\theta^T \phi + z_0) \end{array}\right\} \tag{2.36}$$

Theorem 2.2.1 The adaptive law (2.36) guarantees that

i. $\theta,\ \rho \in \cap L^\infty$

ii. $\varepsilon,\ \varepsilon m_s,\ \dot{\theta},\ \dot{\rho} \in L^2 \cap L^\infty$ which implies estimation error converges.

Proof: Consider the Lyapunov-like function

$$V = \tilde{\theta}^T \Gamma^{-1} \tilde{\theta} \left|\rho^*\right| + \frac{\tilde{\rho}}{2\gamma} \tag{2.37}$$

Then

$$\dot{V} = \tilde{\boldsymbol{\theta}}^T \boldsymbol{\phi} \varepsilon \left|\rho^*\right| \operatorname{sgn}(\rho^*) + \tilde{\rho} \boldsymbol{\varepsilon} \xi \tag{2.38}$$

Using $\left|\rho^*\right| \operatorname{sgn}(\rho^*) = \rho^*$ and the expression

$$\begin{aligned} \varepsilon m_s &= \rho^* \boldsymbol{\theta}^{*T} \boldsymbol{\phi} + \rho^* z_0 - \rho^* \boldsymbol{\theta} \boldsymbol{\phi} - \rho^* z_0 \\ &= \tilde{\rho} z_0 - \rho^* \boldsymbol{\theta}^{*T} \boldsymbol{\phi} - \rho \boldsymbol{\theta}^T \boldsymbol{\phi} + \rho^* \boldsymbol{\theta}^{*T} \boldsymbol{\phi} - \rho^* \boldsymbol{\theta}^T \boldsymbol{\phi} \\ &= \tilde{\rho}(\mathrm{z}_0 + \boldsymbol{\theta}^T \boldsymbol{\phi}) - \rho^* \tilde{\boldsymbol{\theta}}^T \boldsymbol{\phi} = -\tilde{\rho} \boldsymbol{\xi} - \rho^* \tilde{\boldsymbol{\theta}}^T \boldsymbol{\phi} \end{aligned}$$

We have

$$\dot{V} = \varepsilon(\rho^* \tilde{\boldsymbol{\theta}}^T \boldsymbol{\phi} + \tilde{\rho} \xi) = -\varepsilon^2 m_s^2 \leq 0 \tag{2.39}$$

which results with $V \in L^\infty$ and this implies $\theta,\ \rho \in L^\infty$. Note that $\int_0^t \dot{V}(T) dT = V(T) - V(0)$ and since V is non-increasing and positive definite, $V(0) - V(t) \leq V(0)$. This gives; $-\int_0^t \dot{V}(T) dT \leq V(0)$. Substituting this result in equation (2.39):

$$m_s^2 \int_0^t \varepsilon^2 \leq V(0) \tag{2.40}$$

which is equivalent to:

$$m_s^2 \int_0^t \left\| \varepsilon(T) \right\|^2 d(T) \leq V(0) \leq \infty \tag{2.41}$$

Using the result in equation (2.41) and considering Lemma 2.1.3, we can conclude that $\varepsilon,\ \varepsilon m_s \in L^2 \cap L^\infty$.

We can express error equation (2.17) in the form of B-SPM as:

$$e(t) = \rho^* (\boldsymbol{\theta}^{*\mathbf{T}} \boldsymbol{\phi} + u_f) \tag{2.42}$$

where $\boldsymbol{\phi} = W_m(s) \boldsymbol{\omega}$, $u_f = W_m(s) u_p$. One can relate the equation (2.42) to B-SPM by defining $z = e(t)$, $z_0 = u_f$. Using the adaptation law for B-SPM given in equation

(2.36) with Theorem 2.2.1, we can write adaptation law for normalized direct MRAC as follows:

$$\dot{\boldsymbol{\theta}} = \boldsymbol{\Gamma} \varepsilon \boldsymbol{\phi} \, \mathrm{sgn}(\frac{k_p}{k_m}) \tag{2.43.a}$$

$$\dot{\rho} = \gamma \varepsilon \xi \tag{2.43.b}$$

where $\varepsilon = \dfrac{e - \rho\xi}{m_s^2}$, $\xi = (\boldsymbol{\theta}^{\mathrm{T}}\boldsymbol{\phi} + u_f)$, $m_s^2 = 1 + \boldsymbol{\phi}^{\mathrm{T}}\boldsymbol{\phi} + u_f^2$, $\boldsymbol{\phi} = -W_m(s)\omega$, $u_f = W(s)u_p$ □

The adaptation law (2.43) guarantees that all signals are uniformly bounded and estimation error converges to zero asymptotically [67].

2.3 Multivariable MRAC for MIMO Systems

Adaptive control of multi-input, multi-output (MIMO) systems is an important research area presenting both theoretical and practical significance (e.g., aircraft control systems and process control systems), with unique technical issues [56]. An important issue in multivariable adaptive control is to deal with dynamic interactions between system inputs and outputs. In addition, as in the SISO case, dealing with parametric, structural and environmental uncertainties is inevitable for MIMO systems. In this section, we start with giving the basic MRAC scheme that is widely used in the literature of adaptive control [67, 69]. The system under study may be considered as a linear time-invariant plant with **m**-inputs and **m**-outputs for output feedback control in a more generalized fashion such that $\dot{\mathbf{x}} = \mathbf{A}\mathbf{x} + \mathbf{B}\mathbf{u}$ $\mathbf{y} = \mathbf{C}\mathbf{x}$, with $\mathbf{A} \in \mathbf{R}^{\mathbf{n \times n}}$ and $\mathbf{C} \in \mathbf{R}^{\mathbf{m \times n}}$. For control design, transfer matrix of the system $\mathbf{G}(s) = \mathbf{C}(s\mathbf{I} - \mathbf{A})^{-1}\mathbf{B}$ is considered. In normal operation mode without any failure, one may describe the closed-loop system as:

$$\mathbf{y}(t) = \mathbf{G}(s)\mathbf{u}(t) \tag{2.44}$$

where $\mathbf{G}(s)$ $\mathbf{m} \times \mathbf{m}$ transfer matrix of the plant and $\mathbf{u(t)} \in \mathbf{R}^{\mathbf{m}}$ is the plant input vector. The control goal is to find multivariable adaptive output feedback control

$\mathbf{u(t)} = [u_1(t),\dots,u_m(t)]^T$ such that the plant output vector $\mathbf{y(t)} \in \mathbf{R^m}$ asymptotically tracks a reference output $\mathbf{y}_m\mathbf{(t)}$ despite the system uncertainties.

$$\mathbf{y}_m = \mathbf{W}_m\mathbf{(s)r(t)}, \quad \mathbf{W}_m\mathbf{(s)} = \xi_m^{\mathbf{-1}} \tag{2.45}$$

where $\mathbf{W}_m$ is an $\mathbf{m}\times\mathbf{m}$ stable transfer matrix, $\mathbf{r(t)} \in \mathbf{R^m}$ is a bounded reference input vector and ξ_m is modified interactor matrix. The interactor matrix that is crucial in multivariable adaptive control design since its inverse is used as reference transfer matrix (inverse of it must be stable). In addition, if modified interactor matrix of $\mathbf{G(s)}$ is diagonal then the chosen reference model implies feedback dynamical coupling [56].

Lemma 2.3.1 For any $\mathbf{m}\times\mathbf{m}$ strictly proper rational full rank transfer matrix, $\mathbf{G(s)}$ there exists a (non-unique) lower triangular polynomial matrix $\xi_m(s)$, defined as the modified left interactor (MLI) matrix of $\mathbf{G(s)}$ of the form

$$\xi_m(s) = \begin{bmatrix} d_1(s) & 0 & \dots & 0 & 0 \\ h_{12} & d_2(s) & 0 & \dots & 0 \\ \vdots & & & \ddots & 0 \\ h_{N1}(s) & \dots & \dots & h_{N(1-N)}(s) & d_N(s) \end{bmatrix} \tag{2.46}$$

where $h_{ij}(s),\ j=1,\dots,N-1,\ i=2,\dots,N$ are some polynomials and $d_i(s)$, $i=1,\dots,N$, are arbitrary monic Hurwitz polynomials of certain degree $l_i > 0$, such that $\lim_{s\to\infty} \xi_{\mathbf{m}}(s)\mathbf{G}(s) = \mathbf{K}_p$, the high frequency-gain matrix of $\mathbf{G(s)}$, is finite and non-singular.

The basic design assumptions for an output feedback MIMO adaptive controller can be given as:

1. System high frequency gain matrix $\mathbf{K}_p = \lim_{s\to\infty} \xi_m\mathbf{(s)G(s)}$ is nonsingular and finite
2. $\xi_m\mathbf{(s)}$ of $\mathbf{G(s)}$ is known and its inverse is stable
3. All zeros of $\mathbf{G(s)}$ are stable and **A**, **B**, **C** is stabilizable and detectable

4. All leading principal minors of the high frequency gain matrix $\mathbf{K}_p$ are nonzero, with known signs
5. The observability index v of $\mathbf{G(s)}$ is known

Let us start with giving the basic MRAC scheme that is widely used in the literature of adaptive control [67, 69]. An output feedback direct model reference controller structure with known parameters can be written as:

$$\mathbf{u} = \mathbf{\Theta}_1^{*T} \frac{\mathbf{A(s)}}{\lambda(s)} \mathbf{u} + \mathbf{\Theta}_2^{*T} \frac{\mathbf{A(s)}}{\lambda(s)} \mathbf{y} + \mathbf{\Theta}_3^{*T} \mathbf{y} + \mathbf{\Theta}_4^{*T} \mathbf{r} \tag{2.47}$$

where the parameters of controller are $\mathbf{\Theta}_1 = \begin{bmatrix} \mathbf{\Theta}_{11} & \cdots & \mathbf{\Theta}_{1v-1} \end{bmatrix}^T$, $\mathbf{\Theta}_2 = \begin{bmatrix} \mathbf{\Theta}_{21} & \cdots & \mathbf{\Theta}_{2v-1} \end{bmatrix}^T$ with $\mathbf{\Theta}_{ij} \in \mathbf{R}^{\mathbf{m \times m}}$, $\mathbf{\Theta_3} \in \mathbf{R}^{\mathbf{m \times m}}$, $\mathbf{\Theta_4} \in \mathbf{R}^{\mathbf{m \times m}}$, $i = 1, 2$, j=1,...,$v-1$ with v being observability index of plant $\mathbf{G(s)}$ and the regressor vector $\boldsymbol{\omega} = \begin{bmatrix} \boldsymbol{\omega}_1^T & \boldsymbol{\omega}_2^T & \mathbf{y}^T & \mathbf{r}^T \end{bmatrix}^T$ contains reference inputs, plant outputs and inputs/outputs of the plant with the following filters:

$$\boldsymbol{\omega}_\mathbf{1} = \frac{\mathbf{A(s)}}{\lambda(s)} \mathbf{u}, \quad \boldsymbol{\omega}_\mathbf{2} = \frac{\mathbf{A(s)}}{\lambda(s)} \mathbf{y} \tag{2.48}$$

where $\mathbf{A(s)} = \begin{bmatrix} \mathbf{I_m} & s\mathbf{I_m} & \dots & s^{v-2}\mathbf{I_m} \end{bmatrix}^T$ and $\lambda(s)$ is a monic stable polynomial of degree $v-1$. Direct MRAC given in equation (2.47) is based on certainty equivalence (CE) approach that combines; a control law derived from a known parameter case with an adaptive law generated using an appropriate parameterization. The adaptation is driven by the normalized estimation error and is based on bilinear static parametric model (B-SPM) of the plant that involves unknown controller parameters [70]. It can be shown that the closed loop transfer matrix from **y** to **r** is equal to $\mathbf{W}_m\mathbf{(s)}$ provided $\boldsymbol{\theta}_\mathbf{4}^* = \mathbf{K}_p$ and $\mathbf{\Theta}_\mathbf{1}^*, \mathbf{\Theta}_\mathbf{2}^*, \mathbf{\Theta}_\mathbf{3}^*$ are chosen to satisfy the matching condition:

$$\mathbf{\Theta}_\mathbf{4}^{*\mathbf{T}} \mathbf{W}_m^{-1} \mathbf{G(s)} = \mathbf{I} - \mathbf{\Theta}_\mathbf{1}^{*\mathbf{T}} \frac{\mathbf{A(s)}}{\lambda(s)} \mathbf{u} - \mathbf{\Theta}_\mathbf{2}^{*\mathbf{T}} \frac{\mathbf{A(s)}}{\lambda(s)} \mathbf{G(s)} - \mathbf{\Theta}_\mathbf{3}^{*\mathbf{T}} \mathbf{G(s)} \tag{2.49}$$

Since the parameters of normal plant $\mathbf{G(s)}$ are unknown it is possible to write the control law given in (2.47) as follows:

$$\mathbf{u} = \mathbf{\Theta}^{\mathbf{T}}\mathbf{\omega} \tag{2.50}$$

where $\mathbf{\Theta}^{\mathbf{T}}$ is the estimation of the matrix $\mathbf{\Theta}^{*}$ to be generated by adaptive law. From the plant and matching (2.47) and (2.49), one can obtain:

$$\mathbf{u} - \mathbf{\Theta}_{1}^{*\mathbf{T}}\mathbf{\omega}_{1} - \mathbf{\Theta}_{2}^{*\mathbf{T}}\mathbf{\omega}_{2} - \mathbf{\Theta}_{3}^{*\mathbf{T}}\mathbf{y} = \mathbf{\Theta}_{4}^{*}\mathbf{W}_{m}^{-1}\mathbf{y} \tag{2.51}$$

Adding and subtracting the term $\mathbf{\Theta}_{4}^{*}\mathbf{W}_{m}^{-1}\mathbf{y}_{m}$ yields:

$$\mathbf{u} - \mathbf{\Theta}_{1}^{*\mathbf{T}}\mathbf{\omega}_{1} - \mathbf{\Theta}_{2}^{*\mathbf{T}}\mathbf{\omega}_{2} - \mathbf{\Theta}_{3}^{*\mathbf{T}}\mathbf{y} - \mathbf{\Theta}_{4}^{*\mathbf{T}}\mathbf{r} = \mathbf{\Theta}_{4}^{*}\mathbf{W}_{m}^{-1}\mathbf{y} - \mathbf{\Theta}_{4}^{*}\mathbf{W}_{m}^{-1}\mathbf{y}_{m} \tag{2.52}$$

Defining output tracking error $\mathbf{e}_{1} = \mathbf{y} - \mathbf{y}_{m}$ using the compact form of the controller given in (2.50), the matching condition finally yields:

$$\mathbf{\Theta}_{4}^{*\mathbf{T}}(\mathbf{u} - \mathbf{\Theta}^{*\mathbf{T}}\mathbf{\omega}) = \mathbf{W}_{m}^{-1}(\mathbf{y} - \mathbf{y}_{m}) = \xi_{m}(s)\mathbf{e}_{1} \tag{2.53}$$

The relation given in (2.53) allows expressing the closed-loop system in terms of the tracking error e_1 and parameter error $\tilde{\mathbf{\Theta}}(t) = \mathbf{\Theta}(t) - \mathbf{\Theta}^{*}$ such that letting d_m be the maximum degree of $\xi_{m}(s)$ and choosing Hurwitz polynomial $f(s)$ of degree d_m to filter each side of (2.53), the following B-SPM is obtained:

$$\mathbf{z} = \mathbf{\Psi}^{*}\left[\mathbf{\Theta}^{*T}\mathbf{\varphi} + \mathbf{z}_{0}\right] \tag{2.54}$$

where $\mathbf{z} = -\dfrac{\xi_{m}(s)}{f(s)}\mathbf{e}_{1}$, $\mathbf{\Psi}^{*} = \mathbf{\Theta}_{4}^{*-1} = \mathbf{K}_{p}$, $\mathbf{\varphi} = \dfrac{1}{f(s)}\mathbf{\omega}$, $\mathbf{z}_{0} = -\dfrac{1}{f(s)}\mathbf{u}$, $\mathbf{\xi} = \mathbf{\Theta}^{\mathbf{T}}\mathbf{\varphi} + \mathbf{z}_{0}$. By using the equation (2.32), one can define normalized estimation error of controller adaptation law. In this case bilinear parametric form of estimator is $\hat{\mathbf{z}} = \mathbf{\Psi}\left[\mathbf{\Theta}^{\mathbf{T}}\mathbf{\varphi} + \mathbf{z}_{0}\right]$. It can be verified that the estimation error can be expressed as:

$$\mathbf{\varepsilon} = -\frac{\tilde{\mathbf{\Psi}}\xi + \mathbf{\Psi}^{*}\tilde{\mathbf{\Theta}}^{\mathbf{T}}\mathbf{\varphi}}{m^{2}} \tag{2.55}$$

where $\tilde{\mathbf{\Theta}} = \mathbf{\Theta}(t) - \mathbf{\Theta}^{*}$, $\tilde{\mathbf{\Psi}} = \mathbf{\Psi}(t) - \mathbf{\Psi}^{*}$ and $m^{2} = 1 + |\xi|^{2} + |\mathbf{\varphi}|^{2}$. Here, boundedness of parameters implies a bounded estimation error. Let us now consider the following cost function:

$$J = m^{2}\mathbf{\varepsilon}\mathbf{\varepsilon}^{T} \tag{2.56}$$

Considering (2.56) and using steepest-descent method to reach a minimum of cost function J with respect to $\mathbf{\Theta}$ and $\mathbf{\Psi}$, the following result is obtained:

$$\dot{\mathbf{\Theta}}^{\mathbf{T}} = -\mathbf{\Gamma}_p^{-T} \nabla J_\theta, \;\; \dot{\mathbf{\Psi}} = -\mathbf{\Gamma} \nabla J_\psi \tag{2.57}$$

Then one can obtain the following update law for controller parameter estimation:

$$\dot{\mathbf{\Theta}}^T = -\mathbf{\Gamma}_p^{-T} \boldsymbol{\varepsilon\varphi}^T, \;\; \dot{\mathbf{\Psi}} = -\mathbf{\Gamma}\boldsymbol{\varepsilon\xi}^T \tag{2.58}$$

Defining gain matrix $\mathbf{\Gamma}_p = \mathbf{K}_{pa}^T \mathbf{S}_p^{-1}$, (2.58) can be written as:

$$\dot{\mathbf{\Theta}}^T = -\mathbf{S}_p \boldsymbol{\varepsilon\varphi}^T, \;\; \dot{\mathbf{\Psi}} = -\mathbf{\Gamma}\boldsymbol{\varepsilon\xi}^T \tag{2.59}$$

Stability proof of the controller can be done by using the following Lyapunov-like equation:

$$V(\tilde{\mathbf{\Theta}}, \tilde{\mathbf{\Psi}}) = \frac{1}{2} tr\left[\tilde{\mathbf{\Theta}}^{\mathbf{T}} \mathbf{\Gamma}_P \tilde{\mathbf{\Theta}}\right] + \frac{1}{2} tr\left[\tilde{\mathbf{\Psi}}^T \mathbf{\Gamma}^{-1} \tilde{\mathbf{\Psi}}\right] \tag{2.60}$$

Since this is a basic control system stability proof which can be found in literature, calculations are not given in details and at the end, the following time derivative of (2.60) is obtained:

$$\dot{V} = -\boldsymbol{\varepsilon}^T \boldsymbol{\varepsilon} m^2 \le 0 \tag{2.61}$$

Theorem 3.1 The adaptive controller (2.50) with the adaptive law (2.57), applied to the plant (2.44), guarantees that

i. $V(\tilde{\mathbf{\Theta}}, \tilde{\mathbf{\Psi}}) \in L^\infty$ which implies that, $\mathbf{\Theta}, \mathbf{\Psi} \in L^\infty$,

ii. $\boldsymbol{\varepsilon}(\mathbf{t}) m(t) \in L^2 \cap L^\infty$.

iii. In view of the fact that $\boldsymbol{\varepsilon}(\mathbf{t}) m(t) \in L^2 \cap L^\infty$ and $m^2 = 1 + |\boldsymbol{\xi}|^2 + |\boldsymbol{\varphi}|^2$;

$\dot{\mathbf{\Theta}}(t), \; \dot{\mathbf{\Psi}}(t) \in L^2 \cap L^\infty$.

Proof: A detailed proof is available in books related with the subject [70, 71].

CHAPTER III

ADAPTIVE FAULT TOLERANT CONTROL DESIGN

3.1 Actuator Fault Model

In the literature, various fault/failure models for actuators are available. These models change depending on the assumptions and structure. In a general fault model, including only a reduction of efficiency is not enough. A comprehensive fault model for valve actuator must contain other cases such as stuck, hard-over and leakage. These actuator faults are encountered frequently in the process control industry. To represent valve actuator faults, for the system considered, we use the following mathematical model:

$$u_{fi} = \rho_i u_i(t) + \sigma_i(t)(u_{si} - \rho_i u_i(t)) + \delta_i(t) \tag{3.1}$$

where $u_{fi} \in R,\ i = 1,...,m$ represents system control inputs and $\sigma_i(t) = \{1,0\}$ implies that a total fault (i.e. a complete failure) of *i-th* actuator of system, ρ_i is a multiplier that represent the loss of effectiveness of actuator, u_{si} is a bounded generally constant signal that corresponds to hard-over and stuck type uncontrollable failures and $\delta_i(t)$ is again a bounded signal and can be considered as input disturbance such as valve liquid leakage faults.

3.2 Design I: Modification of Controller for Actuator Failure Case

Previous control design approach is able to tolerate parameter uncertainties and partial actuator faults such as loss of effectiveness, however in the case of total failure of one actuator, adverse effect of failure on system outputs becomes significant. To overcome such problems, some modifications on MIMO model reference adaptive control design are needed. Firstly, a parameterization of possible total failures must be obtained. Considering (3.1) with $\sigma_i(t)=1$, one can obtain:

$$u_{fj}(t)=u_{sj},\ t\geq t_j,\ j\in\{1,2,\ldots\mathrm{m}\} \tag{3.2}$$

Here we assume that at time *t* there are totally *p* failed actuators such that $0\leq p_j<\mathrm{m}$,$\sum_{j=1,\ldots,\mathrm{m}} p_j = p$. In this case, the plant described in (2.44) needs to be updated as follows:

$$\mathbf{y(t)}=\mathbf{G}_f\mathbf{(s)u}_f\mathbf{(t)}+\bar{\mathbf{y}}_{\delta(t)} \tag{3.3}$$

where $\mathbf{G}_f=G_{ij},\ j\neq p_j$ is the **m** x **m** transfer matrix associated with the unfailed actuators and bounded uncontrollable failure effect at the output is given as:

$$\bar{\mathbf{y}}_{\delta(t)}=G_{ij}u_{sj},\ j=p_j \tag{3.4}$$

To achieve the control goal, firstly, it is required to establish plant-model output matching conditions such that all system parameters and actuator fault/failure parameters are known. A basic assumption here is that in the case of total failure of one actuator, the remaining actuators are still functional and adverse effect of failure on system outputs is tolerated by designed controller. It is assumed that $\mathbf{G}_f\mathbf{(s)}$ is strictly proper and has full rank for each failure possibility and the following assumptions must also hold [67]:

1. An upper bound of observability index $\bar{v}_0$ of all possible $\mathbf{G}_f\mathbf{(s)}$ is known.
2. Zero structure at infinity of $\mathbf{G}_f\mathbf{(s)}$ is known and does not depend on actuator failures (and has a stable inverse). In other words, there is a known modified interactor matrix for all failures such that

$$\lim_{t\to\infty}\xi_m(s)\mathbf{G}_f\mathbf{(s)}=\mathbf{K}_{pf} \tag{3.5}$$

and HFG matrix $\mathbf{K}_{pf}$ is finite and nonsingular.

3. All zeros of $\mathbf{G}_f\mathbf{(s)}$ are stable.

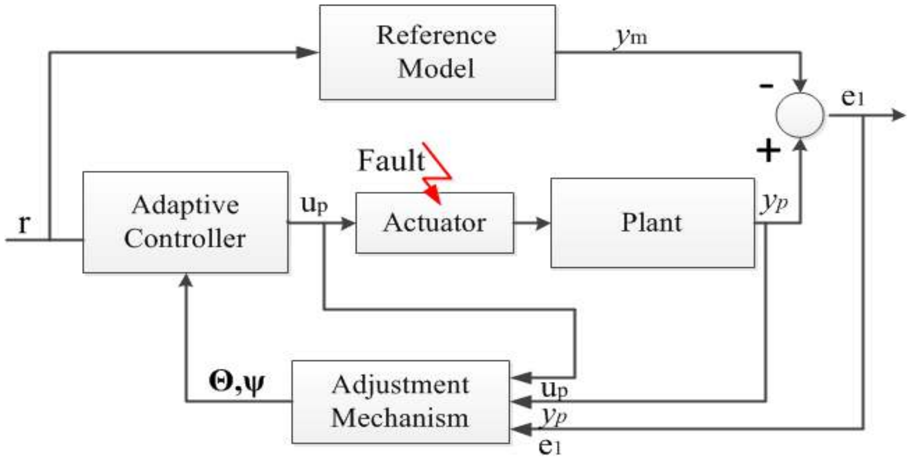

Figure 3.1 General MIMO MRAC block structure with fault consideration

The nominal control input and controller structure can be proposed in a similar way given in [71]:

$$\mathbf{u}_f = \mathbf{u}_f^* = \mathbf{\Theta}_1^{*T} \frac{\mathbf{A}(s)}{\lambda(s)} \mathbf{u} + \mathbf{\Theta}_2^{*T} \frac{\mathbf{A}(s)}{\lambda(s)} \mathbf{y} + \mathbf{\Theta}_3^{*T} \mathbf{y} + \mathbf{\Theta}_4^{*T} \mathbf{r} + \mathbf{\Theta}_5^{*} \tag{3.6}$$

Let us write the control design in a compact form:

$$\mathbf{\Theta}^* = \begin{bmatrix} \mathbf{\Theta}_1^{*T} & \mathbf{\Theta}_2^{*T} & \mathbf{\Theta}_3^{*T} & \mathbf{\Theta}_4^{*T} & \mathbf{\theta}_5^{*T} \end{bmatrix}^T \tag{3.7}$$

$$\mathbf{\omega(t)} = \begin{bmatrix} \mathbf{\omega}_1^T\mathbf{(t)} & \mathbf{\omega}_2^T\mathbf{(t)} & \mathbf{y(t)}^T & \mathbf{r}^T\mathbf{(t)} & 1 \end{bmatrix}^T \tag{3.8}$$

$$\mathbf{u}_f^* = \mathbf{\Theta}^{*T} \mathbf{\omega}(t) \tag{3.9}$$

Since the actual controller uses estimation values of the above real parameters with the superscript of asterisk, the adaptive control can be described in compact form as:

$$\mathbf{u}_f = \mathbf{\Theta}(t)^T \mathbf{\omega}(t) \tag{3.10}$$

The structure of the controller is the same with conventional one except additional term $\mathbf{\theta_5}^* \in \mathbf{R^m}$ which is used to compensate the effect of actuator failure. For update law of control parameters, (2.59) is used. It is obvious that $\mathbf{\theta_5}^* = 0$ should be used for normal operation case. The matching condition, error equation details is given in[69] and parameter convergence can be concluded as given in Theorem 3.1.

Remark 3.1: The knowledge of HFG matrix is crucial for multivariable MRAC scheme. In order to design relatively simpler adaptive controllers as given above, one needs to impose some conditions on HFG matrix. However these conditions are nongeneric and may be very fragile in the presence of certain failures. Besides, in (2.59), update gain $\mathbf{S}_p$ which depends on HFG matrix constraints improvement of transient response. To this end, some modifications on controller are needed to relax assumptions on $\mathbf{K}_{pf}$ and obtain a robust control mechanism.

3.3 Design II: Adaptive Multivariable Control without Gain Symmetry

This modification uses a multiplier in the update law to guarantee stability properties for the closed loop system such that a nominal HFG matrix $\mathbf{K}_{pnom}$ is known and all leading minors of it are nonzero. In addition, the multiplier $\bar{\mathbf{L}}$ must be chosen such that $\bar{\mathbf{L}}\mathbf{K}_p$ is positive diagonal Jordan (PDJ). Then, a factorization given below is always valid [72]:

$$\mathbf{K}_p = \mathbf{L}_p \mathbf{D}_P \mathbf{U}_P \tag{3.11}$$

where $\mathbf{L}_p$ is unit lower triangular, $\mathbf{D}_p$ is diagonal and $\mathbf{U}_P$ is unit upper triangular.

Let $\mathbf{D}_0$ be a diagonal matrix with positive and distinct elements. Then, the following multiplier $\bar{\mathbf{L}}$ for the nominal $\mathbf{K}_p$ can be obtained:

$$\bar{\mathbf{L}} = \mathbf{D}_0 (\mathbf{L}_p \mathbf{D}_p)^{-1} \tag{3.12}$$

Using the multiplier that is given in (3.12), it is possible to redesign the adaptation law:

$$\dot{\mathbf{\Theta}}^T = -\bar{\mathbf{L}}\boldsymbol{\varepsilon}\phi^T \mathbf{\Gamma}_1, \quad \dot{\mathbf{\Psi}} = -\boldsymbol{\varepsilon}\boldsymbol{\xi}^T \mathbf{\Gamma}_2 \tag{3.13}$$

where $\mathbf{\Gamma}_1$ and $\mathbf{\Gamma}_2$ are free symmetric positive definite matrices, while in conventional design, the gain $\mathbf{S}_p$ requires the symmetrization of $\mathbf{K}_p \mathbf{S}_p$. To prove boundedness of parameters, a Lyapunov function can be chosen as follows:

$$V(\tilde{\mathbf{\Theta}}, \tilde{\mathbf{\Psi}}) = \frac{1}{2} tr\left[\mathbf{S}_1 \tilde{\mathbf{\Theta}}^T \mathbf{\Gamma}_1^{-1} \tilde{\Theta} \mathbf{S}_1^{\ T}\right] + \frac{1}{2} tr\left[\mathbf{S}_2 \bar{\mathbf{L}} \tilde{\mathbf{\Psi}}^T \mathbf{\Gamma}_2^{-1} \tilde{\mathbf{\Psi}}^T \bar{\mathbf{L}}^T \mathbf{S}_2^{\ T}\right] \tag{3.14}$$

It yields the following time derivative of (3.13):

$$\dot{V} = -m^2\left[\boldsymbol{\varepsilon}^T\bar{\mathbf{L}}^T\mathbf{W}_2\bar{\mathbf{L}}\boldsymbol{\varepsilon}\right] \le 0 \tag{3.15}$$

where $\mathbf{W}_2 = \mathbf{S}_2{}^T\mathbf{S}_2$, $\mathbf{S}_2 \in \mathbf{R}^{m\times m}$ is a symmetric positive definite matrix included for only stability proof. A detailed proof can be found in literature.[71]

Remark 3.2: Design modification in (3.13) gives us the opportunity to change learning rate freely by using $\boldsymbol{\Gamma}_1$ and $\boldsymbol{\Gamma}_2$. Besides, the controller structure is simpler than the other matrix factorization based controllers since there is no need to the augmented control reparametrization. Increasing adaptation gain freely may be an important advantage for structural and actuator damage cases which may cause large uncertainties. By doing so, tracking performance and post-fault transients can be improved. However, there is a trade-off between stability and fast adaptation. It is well known that fast adaptation leads to a control signal with high-frequency oscillations and excite unmodelled dynamics that may adversely affect stability of adaptive control law. Here a solution in order to increase the range of learning rate that leads to improve the speed of convergence without causing high frequency oscillations in control signal in proposed.

3.4 Design III: New Adaptive FTC with Performance Improvement

In this part, starting point is the idea of dynamical inertial system (DIN), of which theory is given by Alvarez et al. [73] Unlike the steepest descent method that is given in (2.53), a second order dissipative dynamical system with Hessian-driven damping can be used for optimization purposes such that:

$$\ddot{\boldsymbol{\theta}}(t) + \alpha\dot{\boldsymbol{\theta}}(t) + \eta\nabla^2 J(\boldsymbol{\theta}(t))\dot{\boldsymbol{\theta}}(t) + \nabla J(\boldsymbol{\theta}(t)) = 0 \tag{3.16}$$

where α and η are positive parameters. Equation (3.16) can be seen as a second order extension of steepest descent method with some additional properties such as the acceleration term $\ddot{\boldsymbol{\theta}}$ makes DIN a well-posed dynamical system, two damping terms $\eta\nabla^2 J(\boldsymbol{\theta})\dot{\boldsymbol{\theta}}$ and $\alpha\dot{\boldsymbol{\theta}}$ have the ability to suppress transversal and longitudinal oscillations of a minimizer parameter to the valley axis of a convex function. A remarkable property of DIN, that is also crucial for this study, is that an equivalent system which is first-order in time can be produced without occurrence of the Hessian of cost function $J(\boldsymbol{\theta}(t))$. This first order system can be represented as follows:[72]

$$\dot{\boldsymbol{\theta}}(t) + c\nabla J(\boldsymbol{\theta}(t)) + a\boldsymbol{\theta}(t) + b\boldsymbol{\varsigma}(t) = 0 \qquad (3.17.a)$$

$$\dot{\mathbf{y}}(t) + a\boldsymbol{\theta}(t) + b\boldsymbol{\varsigma}(t) = 0 \qquad (3.17.b)$$

where *a*, *b* and *c* are positive constants. The first order system given in (3.17) is named as generalized DIN or g-DIN. If *J* is convex and $a = \alpha - 1/c,\ b = 1/c$ conditions hold, the systems DIN and g-DIN are equivalent. In other words, $\boldsymbol{\theta}$ is a solution of DIN if and only if there exists $\boldsymbol{\varsigma} \in \mathbf{C}^2([0,+\infty],\mathrm{H})$ such that $(\boldsymbol{\theta},\boldsymbol{\varsigma})$ is a solution of g-DIN. In addition to above conditions, if $\arg\min J \neq \varnothing$ then for any solution of g-DIN converges to minimizer of *J* as time goes to infinity. The proof of boundedness and convergence is given by Alvarez et al. [73]

Theorem 3.4.1 Consider adaptive controller in the parametric form given by (2.54) with estimation error and cost function defined in (2.55) and (2.56), respectively. By using the same structure given in g-DIN optimization equations, it is possible to find a new parameter estimation rule that contains extra variable **Z** for oscillation refinement with suitable gain matrices. In this case, one can use the following update law for a novel adaptive multivariable fault tolerant control [74]:

$$\left.\begin{aligned} \dot{\boldsymbol{\Theta}}^T &= -\bar{\mathbf{L}}\boldsymbol{\Gamma}_1\boldsymbol{\varepsilon}\boldsymbol{\varphi}^T - \boldsymbol{\Theta}^T\mathbf{A}_1 - \mathbf{Z}_\theta^T\mathbf{B}_1 \\ \dot{\mathbf{Z}}_\theta^T &= -\boldsymbol{\Theta}^T\mathbf{A}_1 - \mathbf{Z}_\theta^T\mathbf{B}_1 \end{aligned}\right\} \qquad (3.18.a)$$

$$\left.\begin{aligned} \dot{\boldsymbol{\Psi}} &= -\boldsymbol{\Gamma}_2\boldsymbol{\varepsilon}\boldsymbol{\xi}^T - \mathbf{A}_2\boldsymbol{\Psi} - \mathbf{B}_2\mathbf{Z}_\psi \\ \dot{\mathbf{Z}}_\psi &= -\mathbf{A}_2\boldsymbol{\Psi} - \mathbf{B}_2\mathbf{Z}_\psi \end{aligned}\right\} \qquad (3.18.b)$$

where $\boldsymbol{\Gamma}_1$ and $\boldsymbol{\Gamma}_2$ are diagonal **m** x **m** free gain matrices and $\mathbf{A_1}$, $\mathbf{A_2}$, $\mathbf{B_1}$, $\mathbf{B_2}$ are positive diagonal gain matrices to tolerate oscillation in parameter estimation. The update law given by (3.18) guarantees that closed loop system is stable and tracking error asymptotically converges to zero.

Proof: By considering equations (3.6) and (3.10), gradient based update law can be reformulated as a g-DIN problem such that:

$$\left.\begin{aligned}\dot{\mathbf{\Theta}}^T &= -\mathbf{N}_1\nabla J_{\mathbf{\Theta}}(\mathbf{\Theta},\mathbf{\Psi}) - \mathbf{A}_1\mathbf{\Theta}^T - \mathbf{B}_1\mathbf{Z}_{\mathbf{\Theta}}^T \\ \dot{\mathbf{Z}}_\theta^T &= -\mathbf{A}_1\Theta^T - \mathbf{B}_1\mathbf{Z}_{\mathbf{\Theta}}^T\end{aligned}\right\} \tag{3.19}$$

$$\left.\begin{aligned}\dot{\mathbf{\Psi}} &= -\mathbf{N}_2\nabla J_{\mathbf{\Psi}}(\mathbf{\Theta},\mathbf{\Psi}) - \mathbf{A}_2\mathbf{\Psi} - \mathbf{B}_2\mathbf{Z}_{\mathbf{\Psi}} \\ \dot{\mathbf{Z}}_{\mathbf{\Psi}} &= -\mathbf{A}_2\mathbf{\Psi} - \mathbf{B}_2\mathbf{Z}_{\mathbf{\Psi}}\end{aligned}\right\} \tag{3.20}$$

where $\mathbf{A}_i$, $\mathbf{B}_i$ and $\mathbf{N}_i$, i=1,2 are positive scalar matrices (i.e. n×**I**, n>0) with appropriate dimensions and additional dynamic terms can always be stated alternatively as $\dot{\mathbf{Z}}_{\mathbf{\Theta}}{}^T = \dot{\mathbf{\Theta}}^T + \mathbf{N}_1\nabla J(\mathbf{\Theta},\mathbf{\Psi})$, $\dot{\mathbf{Z}}_{\mathbf{\Psi}}{}^T = \dot{\mathbf{\Psi}}^T + \mathbf{N}_2\nabla J(\mathbf{\Theta},\mathbf{\Psi})$. A Lyapunov-like function candidate is proposed by using the factorizations similar with [66] such that $\mathbf{W}_1 = \mathbf{S}_1^T\mathbf{S}_1$, $\mathbf{S}_1 \in \mathbf{R}^{m\times m}$ nonsingular, $\mathbf{W}_2 = \mathbf{S}_2^T\mathbf{S}_2$, $\mathbf{S}_2 \in \mathbf{R}^{m\times m}$ nonsingular; $\bar{\mathbf{\Gamma}}_1 = \mathbf{A}_1\mathbf{\Gamma}_1\mathbf{B}_1$ and $\bar{\mathbf{\Gamma}}_2 = \mathbf{A}_2\mathbf{\Gamma}_2\mathbf{B}_2$ with $\mathbf{A}_i$, $\mathbf{B}_i$ and $\mathbf{\Gamma}_i$, i=1,2 are all positive diagonal matrices of appropriate dimensions:

$$\begin{aligned}V(\tilde{\mathbf{\Theta}},\mathbf{Z}_\Theta,\tilde{\mathbf{\Psi}},\mathbf{Z}_\Psi) &= \frac{1}{2}tr\left[\mathbf{S}_1\tilde{\mathbf{\Theta}}^{\mathbf{T}}\mathbf{\Gamma}_1^{-1}\tilde{\mathbf{\Theta}}\mathbf{S}_1^{\mathbf{T}}\right] + \frac{1}{2}tr\left[\mathbf{S}_1(\mathbf{A}_1\tilde{\Theta} + \dot{\mathbf{Z}}_\Theta)\bar{\mathbf{\Gamma}}_1^{-1}(\mathbf{A}_1\tilde{\mathbf{\Theta}} + \dot{\mathbf{Z}}_\Theta)^T\mathbf{S}_1^{\mathbf{T}}\right] \\ &+ \frac{1}{2}tr\left[\mathbf{S}_2\bar{\mathbf{L}}\tilde{\mathbf{\Psi}}\mathbf{\Gamma}_2^{-1}\tilde{\mathbf{\Psi}}^{\mathbf{T}}\bar{\mathbf{L}}^{\mathbf{T}}\mathbf{S}_2^{\mathbf{T}}\right] + \frac{1}{2}tr\left[\mathbf{S}_2\bar{\mathbf{L}}(\mathbf{A}_2\tilde{\mathbf{\Psi}} + \dot{\mathbf{Z}}_\Psi)\bar{\mathbf{\Gamma}}_2^{-1}(\mathbf{A}_2\tilde{\mathbf{\Psi}} + \dot{\mathbf{Z}}_\Psi)^T\bar{\mathbf{L}}^{\mathbf{T}}\mathbf{S}_2^{\mathbf{T}}\right]\end{aligned} \tag{3.21}$$

For the sake of simplicity, time derivative of above equation may be divided into two parts with respect to control parameters **Θ** and **Ψ**:

$$\dot{V} = \dot{V}_{\mathbf{\Theta}} + \dot{V}_{\mathbf{\Psi}} \tag{3.22}$$

For the first part of time derivative:

$$\dot{V}_{\mathbf{\Theta}} = tr\left[\mathbf{S}_1\dot{\tilde{\mathbf{\Theta}}}^T\mathbf{\Gamma}_1^{-1}\tilde{\mathbf{\Theta}}\mathbf{S}_1^T\right] + tr\left[\mathbf{S}_1(\mathbf{A}_1\dot{\tilde{\mathbf{\Theta}}} + \ddot{\mathbf{Z}}_{\mathbf{\Theta}})^T\bar{\mathbf{\Gamma}}_1^{-1}(\mathbf{A}_1\tilde{\mathbf{\Theta}} + \dot{\mathbf{Z}}_{\mathbf{\Theta}})\mathbf{S}_1^T\right] \tag{3.23}$$

Using the second line of (46):

$$\dot{V}_{\mathbf{\Theta}} = tr\left[\mathbf{S}_1\dot{\tilde{\mathbf{\Theta}}}^{\mathbf{T}}\mathbf{\Gamma}_1^{-1}\tilde{\mathbf{\Theta}}\mathbf{S}_1^{\mathbf{T}}\right] + tr\left[\mathbf{S}_1(\mathbf{A}_1\dot{\tilde{\mathbf{\Theta}}} - \mathbf{A}_1\dot{\mathbf{\Theta}} - \mathbf{B}_1\dot{\mathbf{Z}})^{\mathbf{T}}\bar{\mathbf{\Gamma}}_1^{-1}(\mathbf{A}_1\tilde{\mathbf{\Theta}} + \dot{\mathbf{Z}}_\theta)\mathbf{S}_1^{\mathbf{T}}\right] \tag{3.24}$$

Considering the facts that $\dot{\tilde{\mathbf{\Theta}}} = \dot{\mathbf{\Theta}} - \dot{\mathbf{\Theta}}^* = \dot{\mathbf{\Theta}}$ (due to $\mathbf{\Theta}^*$ being constant) and $\dot{\mathbf{Z}}_\theta{}^T = \dot{\mathbf{\Theta}}^T + \mathbf{N}_1\nabla J_{\mathbf{\Theta}}(\mathbf{\Theta},\mathbf{\Psi})$ with a condition that $\mathbf{N}_1 = \bar{\mathbf{L}}\mathbf{\Gamma}_1$, $\mathbf{\Gamma}_1 = \gamma\mathbf{I}$.

$$\dot{V}_{\mathbf{\Theta}} = tr\left[\mathbf{S}_1\dot{\tilde{\mathbf{\Theta}}}^T\mathbf{\Gamma}_1^{-1}\tilde{\mathbf{\Theta}}\mathbf{S}_1^{\mathbf{T}}\right] + tr\left[\mathbf{S}_1(-\mathbf{B}_1\dot{\mathbf{Z}})^T\bar{\mathbf{\Gamma}}_1^{-1}(\mathbf{A}_1\tilde{\mathbf{\Theta}} + \dot{\mathbf{Z}}_\theta)\mathbf{S}_1^T\right] \tag{3.25}$$

$$= tr\left[\mathbf{S_1}\dot{\tilde{\mathbf{\Theta}}}^T\Gamma_1^{-1}\tilde{\mathbf{\Theta}}\mathbf{S_1^T}\right] - tr\left[\mathbf{S}_1(\dot{\mathbf{\Theta}}^T + \mathbf{N_1}\nabla J_{\mathbf{\Theta}}(\mathbf{\Theta},\mathbf{\Psi}))^T\bar{\mathbf{\Gamma}}_1^{-1}(\mathbf{A_1}\tilde{\mathbf{\Theta}} + \dot{\mathbf{Z}}_\theta)\mathbf{S}_1^T\right]$$

$$= tr\left[\mathbf{S_1}\dot{\tilde{\mathbf{\Theta}}}^T\mathbf{\Gamma_1^{-1}}\tilde{\mathbf{\Theta}}\mathbf{S}_1^T\right] - tr\left[\mathbf{S_1}(\dot{\mathbf{\Theta}}^T + \mathbf{N}_1\nabla J_{\mathbf{\Theta}}(\mathbf{\Theta},\mathbf{\Psi}))^T\mathbf{B_1}\bar{\mathbf{\Gamma}}_1^{-1}\mathbf{A}_1\tilde{\mathbf{\Theta}}\mathbf{S}_1^T\right] - tr\left[\mathbf{S}_1\dot{\mathbf{Z}}_{\mathbf{\Theta}}{}^T\mathbf{B}_1\bar{\mathbf{\Gamma}}_1^{-1}\dot{\mathbf{Z}}_{\mathbf{\Theta}}\mathbf{S}_1^T\right]$$

$$= tr\left[\mathbf{S}_1\dot{\tilde{\mathbf{\Theta}}}^T\mathbf{\Gamma}_1^{-1}\tilde{\mathbf{\Theta}}\mathbf{S}_1^T\right] - tr\left[\mathbf{S}_1\dot{\tilde{\mathbf{\Theta}}}^{\mathbf{T}}\mathbf{\Gamma}_1^{-1}\tilde{\mathbf{\Theta}}\mathbf{S}_1^T\right] - tr\left[\mathbf{S}_1\bar{\mathbf{L}}\boldsymbol{\varepsilon}\boldsymbol{\varphi}^T\tilde{\mathbf{\Theta}}\mathbf{S}_1^T\right] - tr\left[\mathbf{S}_1\dot{\mathbf{Z}}_{\mathbf{\Theta}}{}^T\mathbf{B}_1\bar{\mathbf{\Gamma}}_1^{-1}\dot{\mathbf{Z}}_{\mathbf{\Theta}}\mathbf{S}_1^T\right]$$

$$\dot{V}_{\mathbf{\Theta}} = -tr\left[\mathbf{S_1}\bar{\mathbf{L}}\boldsymbol{\varepsilon}\boldsymbol{\varphi}^T\tilde{\mathbf{\Theta}}\mathbf{S_1}^T\right] - tr\left[\mathbf{S}_1\dot{\mathbf{Z}}_{\mathbf{\Theta}}{}^T\mathbf{B}_1\bar{\mathbf{\Gamma}}_1^{-1}\dot{\mathbf{Z}}_{\mathbf{\Theta}}\mathbf{S}_1^T\right] \quad (3.26)$$

For the second part of time derivative of Lyapunov function:

$$\dot{V}_{\mathbf{\Psi}} = tr\left[\mathbf{S}_2\bar{\mathbf{L}}\dot{\tilde{\mathbf{\Psi}}}\mathbf{\Gamma}_2^{-1}\tilde{\mathbf{\Psi}}^T\bar{\mathbf{L}}^T\mathbf{S}_2^T\right] + tr\left[\mathbf{S}_2\bar{\mathbf{L}}(\mathbf{A}_2\dot{\tilde{\mathbf{\Psi}}} + \ddot{\mathbf{Z}}_{\mathbf{\Psi}})\bar{\mathbf{\Gamma}}_2^{-1}(\mathbf{A}_2\tilde{\mathbf{\Psi}} + \dot{\mathbf{Z}}_{\mathbf{\Psi}})^T\bar{\mathbf{L}}^T\mathbf{S}_2^T\right] \quad (3.27)$$

Using the facts that $\dot{\tilde{\mathbf{\Psi}}} = \dot{\mathbf{\Psi}} - \dot{\mathbf{\Psi}}^* = \dot{\mathbf{\Psi}}$ and $\dot{\mathbf{Z}}_{\mathbf{\Psi}}{}^T = \dot{\boldsymbol{\theta}}^T + \mathbf{N}_2\nabla J_{\mathbf{\Psi}}(\mathbf{\Theta},\mathbf{\Psi})$ with a condition that $\mathbf{A_2}$, $\mathbf{B_2}$ and $\mathbf{\Gamma}_2$ are scalar matrices and can be used commutatively:

$$\dot{V}_{\mathbf{\Psi}} = tr\left[\mathbf{S_2}\bar{\mathbf{L}}\dot{\mathbf{\Psi}}\mathbf{\Gamma}_2^{-1}\tilde{\mathbf{\Psi}}^T\bar{\mathbf{L}}^T\mathbf{S}_2^T\right] + tr\left[\mathbf{S}_2\bar{\mathbf{L}}(\mathbf{A}_2\dot{\tilde{\mathbf{\Psi}}} - \mathbf{A}_2\dot{\mathbf{\Psi}} - \mathbf{B}_2\dot{\mathbf{Z}}_\Psi)\bar{\mathbf{\Gamma}}_2^{-1}(\mathbf{A}_2\tilde{\mathbf{\Psi}} + \dot{\mathbf{Z}}_\Psi)^T\bar{\mathbf{L}}^T\mathbf{S}_2^T\right] \quad (3.28)$$

$$= tr\left[\mathbf{S_2}\bar{\mathbf{L}}\dot{\mathbf{\Psi}}\mathbf{\Gamma}_2^{-1}\tilde{\mathbf{\Psi}}^T\bar{\mathbf{L}}^T\mathbf{S}_2^T\right] + tr\left[\mathbf{S}_2\bar{\mathbf{L}}(-\mathbf{B}_2\dot{\mathbf{Z}}_{\mathbf{\Psi}})\bar{\mathbf{\Gamma}}_2^{-1}(\mathbf{A}_2\tilde{\mathbf{\Psi}} + \dot{\mathbf{Z}}_{\mathbf{\Psi}})^T\bar{\mathbf{L}}^T\mathbf{S}_2^T\right]$$

$$= tr\left[\mathbf{S}_2\bar{\mathbf{L}}\dot{\mathbf{\Psi}}\mathbf{\Gamma}_2^{-1}\tilde{\mathbf{\Psi}}^T\bar{\mathbf{L}}^T\mathbf{S}_2^T\right] - tr\left[\mathbf{S}_2\bar{\mathbf{L}}\dot{\mathbf{Z}}_{\mathbf{\Psi}}\mathbf{B}_2\bar{\mathbf{\Gamma}}_2^{-1}\mathbf{A}_2\tilde{\mathbf{\Psi}}\bar{\mathbf{L}}^T\mathbf{S}_2^T\right] - tr\left[\mathbf{S}_2\bar{\mathbf{L}}\dot{\mathbf{Z}}_{\mathbf{\Psi}}{}^T\mathbf{\Gamma}_2^{-1}\mathbf{A}_2\dot{\mathbf{Z}}_{\mathbf{\Psi}}\bar{\mathbf{L}}^T\mathbf{S}_2^T\right]$$

$$= tr\left[\mathbf{S_2}\bar{\mathbf{L}}\dot{\mathbf{\Psi}}\mathbf{\Gamma}_2^{-1}\tilde{\mathbf{\Psi}}^T\bar{\mathbf{L}}^T\mathbf{S}_2^T\right] - tr\left[\mathbf{S_2}\bar{\mathbf{L}}(\dot{\mathbf{\Psi}} + \mathbf{N}_2\nabla J_{\mathbf{\Psi}}(\mathbf{\Theta},\mathbf{\Psi})\mathbf{\Gamma}_2^{-1}\tilde{\mathbf{\Psi}}\bar{\mathbf{L}}^T\mathbf{S}_2^T\right] - tr\left[\mathbf{S_2}\bar{\mathbf{L}}\dot{\mathbf{Z}}_{\mathbf{\Psi}}{}^T\mathbf{\Gamma}_2^{-1}\mathbf{A_2}\dot{\mathbf{Z}}_{\mathbf{\Psi}}\bar{\mathbf{L}}^T\mathbf{S}_2^T\right]$$

$$\begin{aligned}&= tr\left[\mathbf{S_2}\bar{\mathbf{L}}\dot{\mathbf{\Psi}}\mathbf{\Gamma}_2^{-1}\tilde{\mathbf{\Psi}}^T\bar{\mathbf{L}}^T\mathbf{S}_2^T\right] - tr\left[\mathbf{S_2}\bar{\mathbf{L}}\dot{\mathbf{\Psi}}\mathbf{\Gamma}_2^{-1}\tilde{\mathbf{\Psi}}^T\bar{\mathbf{L}}^T\mathbf{S}_2^T\right] - tr\left[\mathbf{S}_2\bar{\mathbf{L}}(\boldsymbol{\varepsilon}\boldsymbol{\xi}^T\mathbf{\Gamma}_2)\mathbf{\Gamma}_2^{-1}\tilde{\mathbf{\Psi}}\bar{\mathbf{L}}^T\mathbf{S}_2^T\right]\\ &-tr\left[\mathbf{S}_2\bar{\mathbf{L}}\dot{\mathbf{Z}}_{\mathbf{\Psi}}{}^T\mathbf{\Gamma}_2^{-1}\mathbf{A}_2\dot{\mathbf{Z}}_{\mathbf{\Psi}}\bar{\mathbf{L}}^T\mathbf{S}_2^T\right]\end{aligned}$$

$$\dot{V}_\psi = -tr\left[\mathbf{S_2}\bar{\mathbf{L}}\boldsymbol{\varepsilon}\boldsymbol{\xi}^T\tilde{\mathbf{\Psi}}\bar{\mathbf{L}}^T\mathbf{S}_2^T\right] - tr\left[\mathbf{S_2}\bar{\mathbf{L}}\dot{\mathbf{Z}}_{\mathbf{\Psi}}{}^T\mathbf{\Gamma}_2^{-1}\mathbf{A_2}\dot{\mathbf{Z}}_{\mathbf{\Psi}}\bar{\mathbf{L}}^T\mathbf{S}_2^T\right] \quad (3.29)$$

Finally, combining two parts of time derivative of total Lyapunov equation:

$$\begin{aligned}\dot{V} = &-tr\left[\mathbf{S_1}\bar{\mathbf{L}}\boldsymbol{\varepsilon}\boldsymbol{\varphi}^T\tilde{\mathbf{\Theta}}\mathbf{S}_1^T\right] - tr\left[\mathbf{S_2}\bar{\mathbf{L}}\boldsymbol{\varepsilon}\boldsymbol{\xi}^T\tilde{\mathbf{\Psi}}\bar{\mathbf{L}}^T\mathbf{S}_2^T\right] - tr\left[\mathbf{S}_1\dot{\mathbf{Z}}_{\mathbf{\Theta}}{}^T\mathbf{\Gamma}_1^{-1}\mathbf{A}_1\dot{\mathbf{Z}}_{\mathbf{\Theta}}\mathbf{S}_1^T\right]\\ &-tr\left[\mathbf{S_2}\bar{\mathbf{L}}\dot{\mathbf{Z}}_\Psi{}^T\mathbf{\Gamma}_2^{-1}\mathbf{A_2}\dot{\mathbf{Z}}_{\mathbf{\Psi}}\bar{\mathbf{L}}^T\mathbf{S}_2^T\right]\end{aligned} \quad (3.30)$$

By using the fact that $tr(\mathrm{x}\mathrm{y}^T) = \mathrm{y}^T x$ for the first two term of (3.30) and considering matrices $\mathbf{W}_1$ and $\mathbf{W}_2$:

$$\begin{aligned}\dot{V} &= -(\boldsymbol{\varphi}^T\tilde{\boldsymbol{\Theta}}\mathbf{W}_1 + \xi^T\tilde{\boldsymbol{\Psi}}^T\bar{\mathbf{L}}^T\mathbf{W}_2)\bar{\mathbf{L}}\boldsymbol{\varepsilon} - tr\left[\mathbf{S}_1\dot{\mathbf{Z}}_{\boldsymbol{\Theta}}{}^T\boldsymbol{\Gamma}_1^{-1}\mathbf{A}_1\dot{\mathbf{Z}}_{\boldsymbol{\Theta}}\mathbf{S}_1^T\right] \\ &-tr\left[\mathbf{S}_2\bar{\mathbf{L}}\dot{\mathbf{Z}}_{\boldsymbol{\Psi}}{}^T\boldsymbol{\Gamma}_2^{-1}\mathbf{A}_2\dot{\mathbf{Z}}_{\boldsymbol{\Psi}}\bar{\mathbf{L}}^T\mathbf{S}_2^T\right]\end{aligned} \tag{3.31}$$

Defining $\mathbf{W_1} = \mathbf{W_2}\bar{\mathbf{L}}\mathbf{K}_P$ such that $\mathbf{W}_2^{-1}\mathbf{W}_1 = \bar{\mathbf{L}}\mathbf{K}_P$, which requires $\bar{\mathbf{L}}\mathbf{K}_P$ has real positive eigen-values and diagonal Jordan form (PDJ), using the parameter estimation error definition given in (2.55), time derivative of Lyapunov function becomes:

$$\dot{V} = -m^2(\boldsymbol{\varepsilon}^T\bar{\mathbf{L}}^T\mathbf{W}_2\bar{\mathbf{L}}\boldsymbol{\varepsilon}) - tr\left[\mathbf{S}_1\dot{\mathbf{Z}}_{\boldsymbol{\Theta}}{}^T\boldsymbol{\Gamma}_1^{-1}\mathbf{A}_1\dot{\mathbf{Z}}_{\boldsymbol{\Theta}}\mathbf{S}_1^T\right] - tr\left[\mathbf{S}_2\bar{\mathbf{L}}\dot{\mathbf{Z}}_{\Psi}{}^T\boldsymbol{\Gamma}_2^{-1}\mathbf{A}_2\dot{\mathbf{Z}}_{\boldsymbol{\Psi}}\bar{\mathbf{L}}^T\mathbf{S}_2^T\right] \le 0 \tag{3.32}$$

which implies that $V(\tilde{\boldsymbol{\Theta}}, \mathbf{Z}_{\boldsymbol{\Theta}}, \tilde{\boldsymbol{\Psi}}, \mathbf{Z}_{\boldsymbol{\Psi}}) \in L^\infty$ and hence $\boldsymbol{\varepsilon}(t), \boldsymbol{\Theta}(t), \boldsymbol{\Psi}(t), \dot{\mathbf{Z}}_{\boldsymbol{\Theta}}, \dot{\mathbf{Z}}_{\boldsymbol{\Psi}} \in L^\infty$, integrating both sides of (3.30) and recalling the boundedness of V, one can conclude that $\boldsymbol{\varepsilon}m \in L^2 \cap L^\infty$ and $\dot{\mathbf{Z}}_{\boldsymbol{\Theta}}, \dot{\mathbf{Z}}_{\boldsymbol{\Psi}} \in L^2 \cap L^\infty$. From (3.18) and normalized error definition given in (2.55), in the view of the fact that $\boldsymbol{\varepsilon}m \in L^2 \cap L^\infty$, one can obtain $\dot{\boldsymbol{\Theta}}(t)$, $\dot{\boldsymbol{\Psi}}(t) \in L^2 \cap L^\infty$. Based on these properties, update law given in (3.18) guarantees that all closed-loop signals are bounded and tracking error goes to zero as time goes to infinity □.

CHAPTER IV

PHYSICAL MODEL AND SIMULATIONS

In this chapter, the prototype we utilize for fault tolerant applications is modeled and simulated. The designed controllers are tested on the benchmark system that consist of nonlinear MIMO interconnected liquid tanks. The system under study is a MIMO nonlinear 4-tank system which is an experimental facility developed for research purposes for the processing and aerospace industries. Since our aim is to develop robust adaptive controllers that compensate actuator faults, before application step, we need to understand the physical system properties well in the case of structural changes of benchmark process. For that purpose, firstly, the system mathematical model is obtained and simulated.

4.1 System Modeling

The quadruple tank process first introduced by Johansson [57] is a coupled tank process that comprises four interconnected water tanks and two submersible pumps. Since a valve-actuated version is considered, the system inputs are voltages to the two valve actuators and the outputs are the liquid levels in the lower tanks. The system is depicted in Figure 4.1.

In the original system which is actuated by water pumps the control objective is generally to regulate the level of Tank1 and Tank2. The output of each pump is split into two using three-way valves. In quadruple-tank system given in Figure 4.1, water is pumped into each tank at the top through the pumps and at the bottom of tank the water flows out through a pipe. According to Bernoulli equation, the rate of flow of water through the pipe is given by:

$$q_{out_i} = a_i \sqrt{2gh_i} \tag{4.1}$$

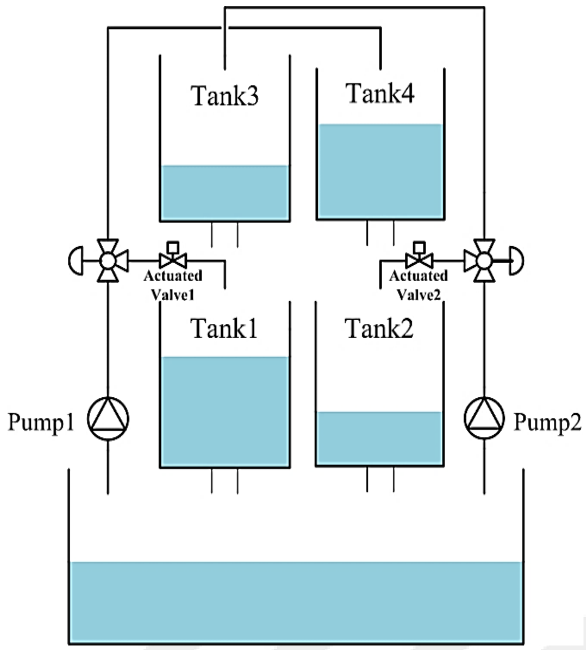

Figure 4.1 Illustrative diagram of the quadruple-tank process

where h_i, i=1..4 is the level of the tank, a_i is the out pipe cross-section area of i^{th} tank and g is the acceleration of gravity. Conservation of mass yields the equation:

$$A_i \frac{dh_i}{dt} = q_{in_i} - q_{out_i} \tag{4.2}$$

where A_i is the bottom area of the i^{th} tank , q_{in_i} is the inflow through the pipe. Each pump i=1, 2 gives a flow proportional to the control signal as follows:

$$q_{in_i} = k_i v_i \tag{4.3}$$

where k_i is the pump constant. Considering the inflow and outflow of all tanks at the same time, the non-linear dynamics of the coupled tank process is given by:

$$\left.\begin{aligned} A_1 \frac{dh_1}{dt} &= -a_1\sqrt{2gh_1} + a_3\sqrt{2gh_3} + \gamma_1 k_1 v_1 \\ A_2 \frac{dh_2}{dt} &= -a_2\sqrt{2gh_2} + a_4\sqrt{2gh_4} + \gamma_2 k_2 v_2 \\ A_3 \frac{dh_3}{dt} &= -a_3\sqrt{2gh_3} + (1-\gamma_2) k_2 v_2 \\ A_4 \frac{dh_4}{dt} &= -a_4\sqrt{2gh_4} + (1-\gamma_1) k_1 v_1 \end{aligned}\right\} \tag{4.4}$$

The parameters γ_1, $\gamma_2 \in (0,1)$ are determined from how valves are set prior to an experiment. The flow to Tank 1 is $\gamma_1 k_1 v_1$ and the flow to Tank 4 is $(1-\gamma_1)k_1 v_1$ and similarly for Tank 2 and Tank 3. The measured level signals are $k_c h_1$ and $k_c h_2$. The above mass balance and Bernoulli's law can be rewritten as:

$$\left.\begin{aligned}
\frac{dh_1}{dt} &= -\frac{a_1}{A_1}\sqrt{2gh_1} + \frac{a_3}{A_1}\sqrt{2gh_3} + \frac{\gamma_1 k_1}{A_1} v_1 \\
\frac{dh_2}{dt} &= -\frac{a_2}{A_2}\sqrt{2gh_2} + \frac{a_4}{A_2}\sqrt{2gh_4} + \frac{\gamma_2 k_2}{A_2} v_2 \\
\frac{dh_3}{dt} &= -\frac{a_3}{A_3}\sqrt{2gh_3} + \frac{(1-\gamma_2)}{A_3} k_2 v_2 \\
\frac{dh_4}{dt} &= -\frac{a_4}{A_4}\sqrt{2gh_4} + \frac{(1-\gamma_1)}{A_4} k_1 v_1
\end{aligned}\right\} \tag{4.5}$$

We need linearized system model to test various linear controllers. The linearization procedure to be presented in equation (4.6) is based on the expansion of nonlinear function into a Taylor series about the operating point and higher order terms are neglected:

$$f(h_i, v_j) = f(h_{io}, v_{jo}) + \frac{\partial f}{\partial h_i}\Big|_{h_{io}, v_{io}} (h_1 - h_{io}) + \frac{\partial f}{\partial v_j}\Big|_{h_{io}, v_{io}} (v_1 - v_{jo}) \tag{4.6}$$

By introducing the variables $x_i := h_i - h_{io}$ and $u_i := v_i - v_{io}$, the system can be represented in state space form as follows:

$$\left.\begin{aligned}
\dot{x}_1 &= -\frac{a_1}{A_1}\sqrt{\frac{g}{2h_{1o}}} x_1 + \frac{a_3}{A_1}\sqrt{\frac{g}{2h_{2o}}} x_1 + \frac{\gamma_1 k_1}{A_1} u_1 \\
\dot{x}_2 &= -\frac{a_2}{A_2}\sqrt{\frac{g}{2h_{2o}}} x_2 + \frac{a_4}{A_2}\sqrt{\frac{g}{2h_{2o}}} x_1 + \frac{\gamma_2 k_2}{A_2} u_2 \\
\dot{x}_3 &= -\frac{a_3}{A_3}\sqrt{\frac{g}{2h_{3o}}} x_3 + \frac{(1-\gamma_2)}{A_3} k_2 u_2 \\
\dot{x}_4 &= -\frac{a_4}{A_4}\sqrt{\frac{g}{2h_{4o}}} x_4 + \frac{(1-\gamma_1)}{A_4} k_1 u_1
\end{aligned}\right\} \tag{4.7}$$

Putting in a compact form linear state space model:

$$\left.\begin{aligned}
\frac{d\mathbf{x}}{dt} &= \begin{bmatrix} -\frac{1}{T_1} & 0 & \frac{A_3}{A_1T_3} & 0 \\ 0 & -\frac{1}{T_2} & 0 & \frac{A_4}{A_2T_4} \\ 0 & 0 & -\frac{1}{T_3} & 0 \\ 0 & 0 & 0 & -\frac{1}{T_4} \end{bmatrix}\mathbf{x} + \begin{bmatrix} \frac{\gamma_1 k_1}{A_1} & 0 \\ 0 & \frac{\gamma_1 k_1}{A_1} \\ 0 & \frac{(1-\gamma_2)k_2}{A_3} \\ \frac{(1-\gamma_1)k_1}{A_4} & 0 \end{bmatrix}\mathbf{u} \\
\mathbf{y} &= \begin{bmatrix} k_c & 0 & 0 & 0 \\ 0 & k_c & 0 & 0 \end{bmatrix}\mathbf{x}
\end{aligned}\right\} \tag{4.8}$$

where the time constants are $T_i = \frac{A_i}{a_i}\sqrt{\frac{2h_{io}}{g}}$, i=1,...,4, and h_{io} is water level of each tank at operating point. Transfer function matrix of the linearized system can be written as:

$$\mathbf{G(s)} = \begin{bmatrix} \frac{\gamma_1 c_1}{1+T_1 s} & \frac{(1-\gamma_2)\mathrm{c}_1}{(1+T_3 s)(1+sT_1)} \\ \frac{(1-\gamma_1)\mathrm{c}_2}{(1+sT_4)(1+sT_2)} & \frac{\gamma_2 c_2}{1+sT_2} \end{bmatrix} \tag{4.9}$$

where $c_1 = T_1 k_1 k_c / A_1$ and $c_2 = T_2 k_2 k_c / A_2$.

System transfer matrix given in equation (4.9) has two finite transmission zeros for γ_1, $\gamma_2 \in (0,1)$. A transmission zero can be defined as a pole of the inverse plant (for square matrix). The other interpretation is that transmission zeros are the values that input-output matrix loses rank. In the case of existence of a right half plane zero, if a multivariable controller is designed to calculate the control signal by using inverse of the system transfer matrix then the system may well be unstable. The transfer matrix of the process has a transmission zero in the left-half plane of s-domain while the other one can be located either in the left or the right half-plane by changing the valve positions. In our applications, we adjust the valve settings so that $1 < \gamma_1 + \gamma_2 \leq 2$. This implies that two transmission zeros are always in the left-half plane and the system is minimum phase.

4.2 Simulations

In order to construct system simulation, parameters of a real system that are frequently used in the literature are chosen. The real system parameters are given in Table 4.1. Since in the presented case flows to the tanks are supplied by a servo valve actuator, the valve dynamics must be added to transfer matrix. The valves are frequently represented by a first order transfer function between controller output $U(s)$ and system input $M(s)$:

$$G_v = \frac{M(s)}{U(s)} = \frac{K_v}{T_v s + 1} \tag{4.10}$$

Table 4.1 Process parameters

Parameter	Value	Unit
Height of tanks, h_{max}	20	cm
Bottom area, Tank1, Tank3, A_1, A_3	28	cm^2
Bottom area, Tank2, Tank4, A_2, A_4	32	cm^2
Out pipe cross-sections, a_1, a_3	0.071	cm^2
Out pipe cross-sections, a_2, a_4	0.057	cm^2
Level measurement device constant, k_c	0.500	V/cm
Gravity g	981	cm/s^2

The system inputs are v_1 and v_2 (input voltages to water pumps (0-10V)) and the system outputs y_1 and y_2 (output voltages form measurement devices (0-10V)). Process linear model is studied at an operating point that makes the system minimum-phase. The operating point parameters of the process are given in Table 4.2.

Table 4.2 System operating point

Parameters	Values	Unit
h_{1o}, h_{2o}	12.26, 12.78	cm
h_{3o}, h_{4o}	1.63, 1.41	cm
v_1, v_2	3.00	V
k_1, k_2	3.33, 3.35	cm^3/Vs
γ_1, γ_2	0.70, 0.60	-

Valve actuator parameters are chosen as $K_v = 1$ and $T_v = 0.1$. The transfer matrix of the plant with valve dynamics:

$$\mathbf{G(s)} = \begin{bmatrix} \dfrac{1.56}{(1+62.3s)(1+0.1s)} & \dfrac{0.89}{(1+22.8s)(1+62.3)(1+0.1s)} \\ \dfrac{0.85}{(1+30s)(1+90.6s)(1+0.1s)} & \dfrac{1.70}{(1+90.6s)(1+0.1s)} \end{bmatrix} \quad (4.11)$$

All control system designs in this thesis consider the linear model of the plant however experimental results are acquired from the nonlinear process simulation. In order to show that linearized system model is valid for control applications, data from linear model and nonlinear plant outputs are compared. The operating point parameters given in Table 4.1 are used and two inputs are applied to open-loop linear and nonlinear models of the plant. Square wave signals $v_1(t) = 4\,\mathrm{sgn}[\sin(0.05\mathrm{t}-\pi)]$, $v_2(t) = 2\,\mathrm{sgn}[\sin(0.03\mathrm{t}-\pi)]$ are considered as inputs of the plants. The total simulation time is 500s. The results are shown in Figure 4.2.

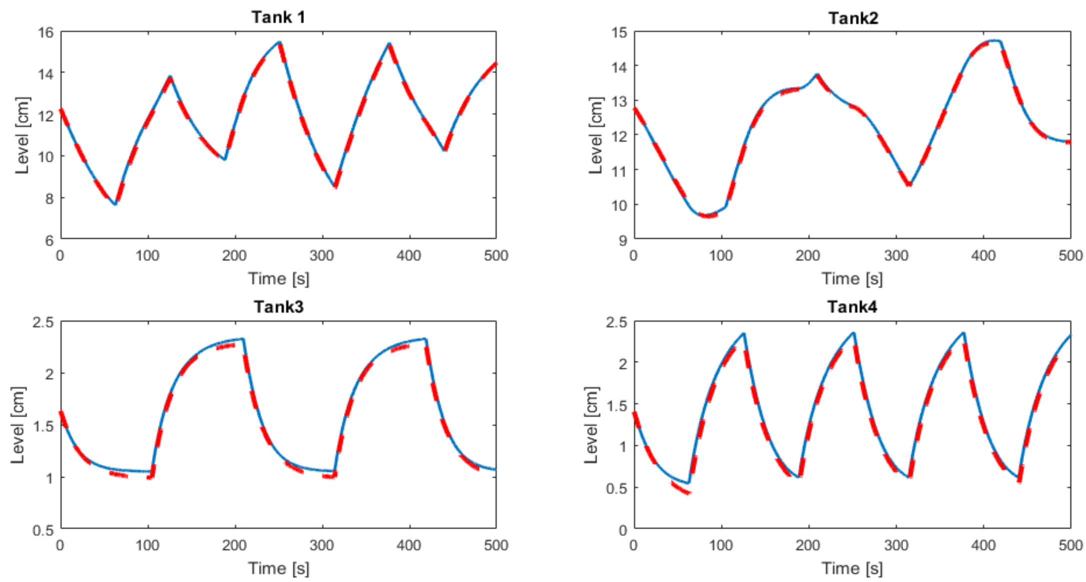

Figure 4.2 Outputs from the nonlinear process (solid) together with the outputs from linear model (dashed)

It is clear from Figure 4.2 that linear model outputs agree well with the responses of the nonlinear process. Table 4.3 shows integral squared error (ISE) index of system outputs. In the view of the results with the fact that linear model is validated by using a real system data in the literature [57], we can conclude that the linearization of nonlinear process works properly for control applications.

Table 4.3 Comparison of nonlinear process and linear model using ISE index.

	Tank1	Tank2	Tank3	Tank4
ISE factor	38.45	10.58	7.45	20.42

In this section, multivariable adaptive control methods that are presented in Chapter 3 are applied to the nonlinear quadruple tank system simulation to observe the system performance and compare the results. For that purpose, firstly, the plant reference model is selected as inverse of a diagonal interactor matrix provided that HFG matrix $\mathbf{K}_p$ is finite and nonsingular. In this case, a modified interactor matrix is given in the following form:

$$\boldsymbol{\xi}_m = \begin{bmatrix} (\tau s+1)^2 & 0 \\ 0 & (\tau s+1)^2 \end{bmatrix} = \begin{bmatrix} (10s+1)^2 & 0 \\ 0 & (10s+1)^2 \end{bmatrix} \tag{4.12}$$

Reference model which possesses dynamical decoupling property can be given as follows:

$$\mathbf{W}_m = \begin{bmatrix} \dfrac{1}{(10s+1)^2} & 0 \\ 0 & \dfrac{1}{(10s+1)^2} \end{bmatrix} \tag{4.13}$$

By using the interactor matrix, a nominal HFG matrix for fault free plant is calculated as follows:

$$\mathbf{K}_{pnom} = \begin{bmatrix} 25.04 & 0 \\ 0 & 18.76 \end{bmatrix} \tag{4.14}$$

The common control parameters that constitute the basic of all designs are selected as $\lambda(s) = s+10,\ \mathbf{A(s)} = I_{2x2},\ \boldsymbol{\Theta}_1, \boldsymbol{\Theta}_2, \boldsymbol{\Theta}_3, \boldsymbol{\Theta}_4 \in \mathbf{R}^{2\times 2}$ and for the controllers mentioned in Design II and Design III, additional failure tolerance parameter is $\boldsymbol{\theta}_5 \in \mathbf{R}^{2\times 2}$. A Hurwitz polynomial $f(s) = 1/(20s+1)^2$ which has the maximum degree of $\boldsymbol{\xi}_m$ is chosen and used to filter each side of bilinear parametric form given in (2.54). For the stabilizing multiplier method which is mentioned in Design I, the multiplier matrix is chosen as:

$$\bar{\mathbf{L}} = \begin{bmatrix} \mu_1 & 0 \\ 0 & \mu_2 \end{bmatrix} \begin{bmatrix} 25.04 & 0 \\ 0 & 18.76 \end{bmatrix} \tag{4.15}$$

Here μ_1 and μ_2 are arbitrary design parameters. In addition, choosing a large μ_1 parameter compared with μ_2 can increase the allowable range of uncertainty in the HFG matrix [71]. Therefore, in simulations, the parameters are selected as $\mu_1 = 50$ and $\mu_2 = 1$. For the proposed fault tolerant control design (Design III), additional parameters $\mathbf{A_1}$, $\mathbf{A_2}$, $\mathbf{B_1}$ and $\mathbf{B_2}$ must be chosen such that they are large enough to suppress oscillations. However, very high values of these parameters may worsen the performance again. Monte Carlo simulations are used to find nominal values of the parameters for the system under study. The chosen parameters are $\mathbf{A_1} = 250\mathbf{I_{2\times2}}$, $\mathbf{A_2} = 100\mathbf{I_{2\times2}}$, $\mathbf{B_1} = 10\mathbf{I_{2\times2}}$, $\mathbf{B_2} = 0.02\mathbf{I_{2\times2}}$.

Simulations are started with comparing the oscillation suppression property of proposed fault tolerant control scheme given in Design II and the one given in Design III. A step change at reference input of Tank1 is applied at 50^{th} second of simulation time while Tank2 output is regulated at its initial level. It is clear from the Figures 4.3-4.5 that proposed novel controller is suppressing the oscillations in two control channels with smooth control signals even when we have further increase in the adaptation gains of two control parameter matrices $\mathbf{\Theta}$ and $\mathbf{\Psi}$. In addition to the aforementioned property, the proposed controller has better dynamical decoupling since it tracks the reference model more accurately.

Figure 4.6 shows reference model tracking error when a step change for Tank1 reference is applied at 50^{th} second of simulation. It can be seen from the figure that proposed new controller increases allowable range of adaptation gain, which yields better reference model tracking and exhibits a better transient performance without causing any high frequency oscillation.

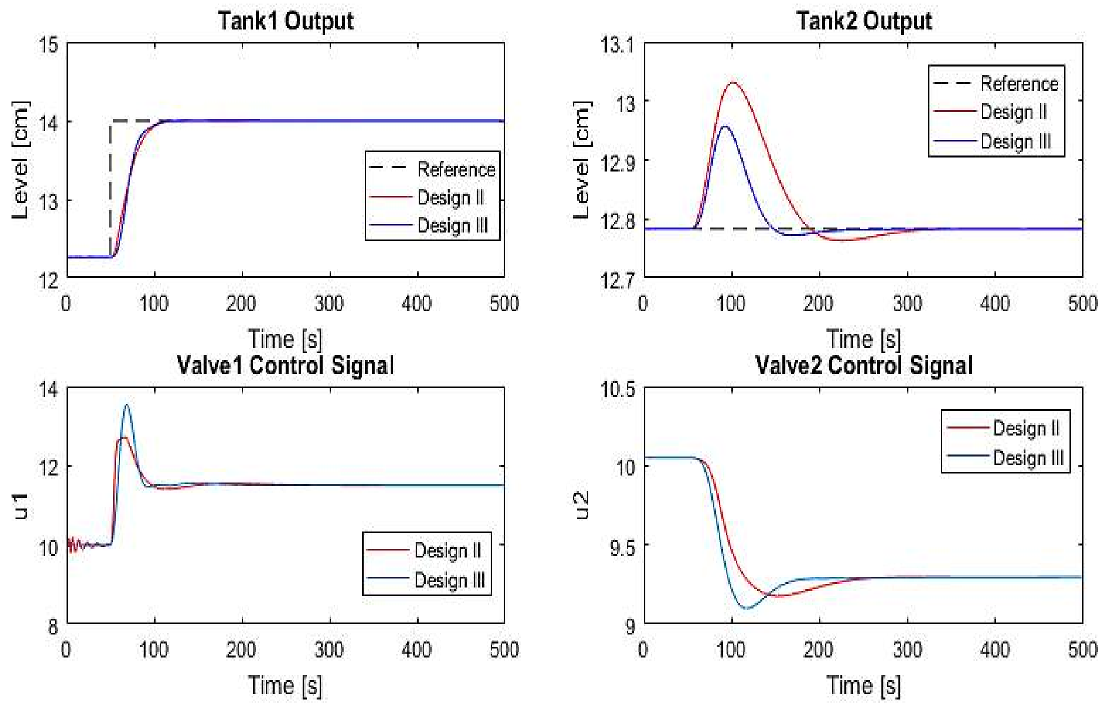

Figure 4.3 Adaptive fault tolerant control performance comparison for adaptation gains $\mathbf{\Gamma}_1 = 50\mathbf{I}_{2\times2}$, $\mathbf{\Gamma}_2 = \mathbf{I}_{2\times2}$

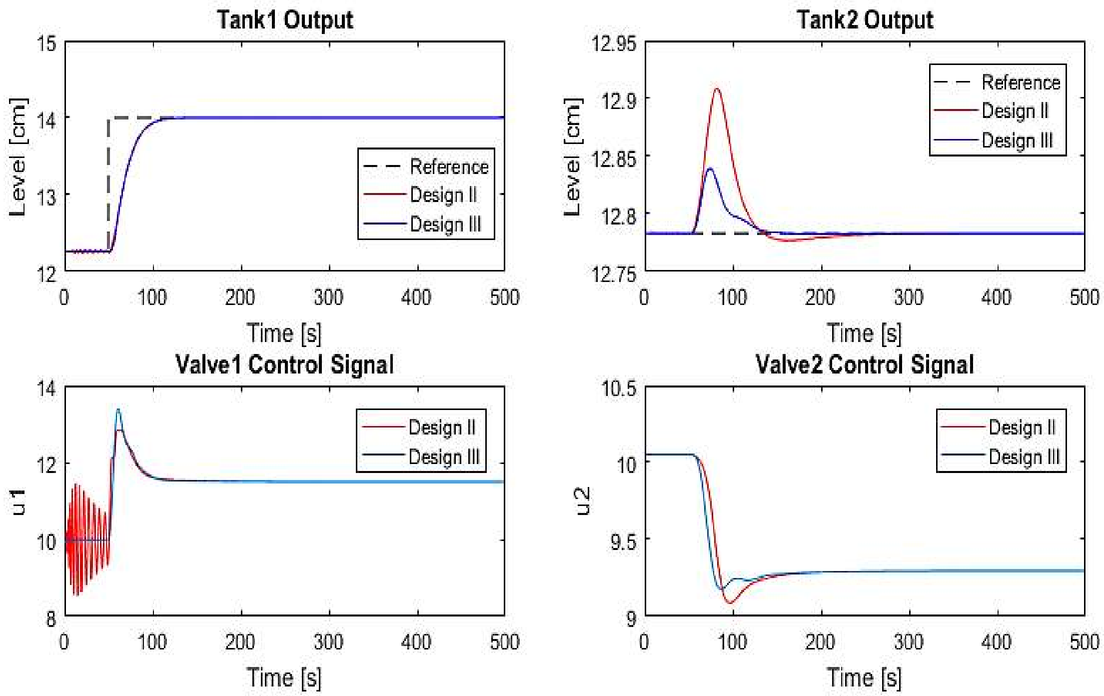

Figure 4.4 Adaptive fault tolerant control performance comparison for adaptation gains $\mathbf{\Gamma}_1 = 200\mathbf{I}_{2\times2}$, $\mathbf{\Gamma}_2 = \mathbf{I}_{2\times2}$

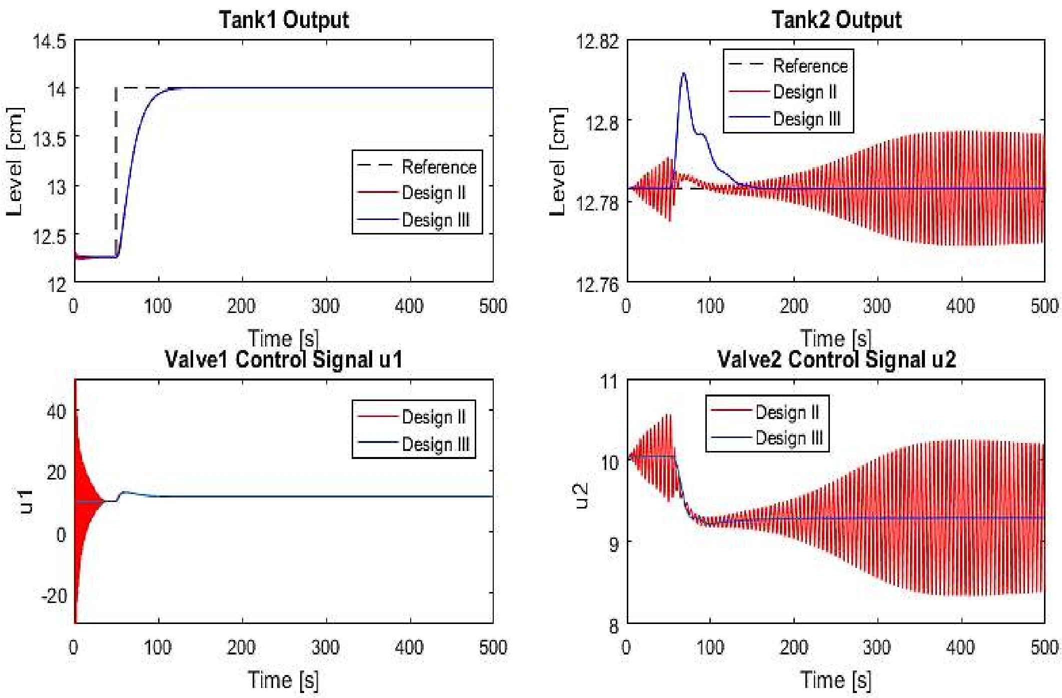

Figure 4.5 Adaptive fault tolerant control performance comparison for adaptation gains $\mathbf{\Gamma}_1 = 400\mathbf{I}_{2\times2}$, $\mathbf{\Gamma}_2 = 50\mathbf{I}_{2\times2}$

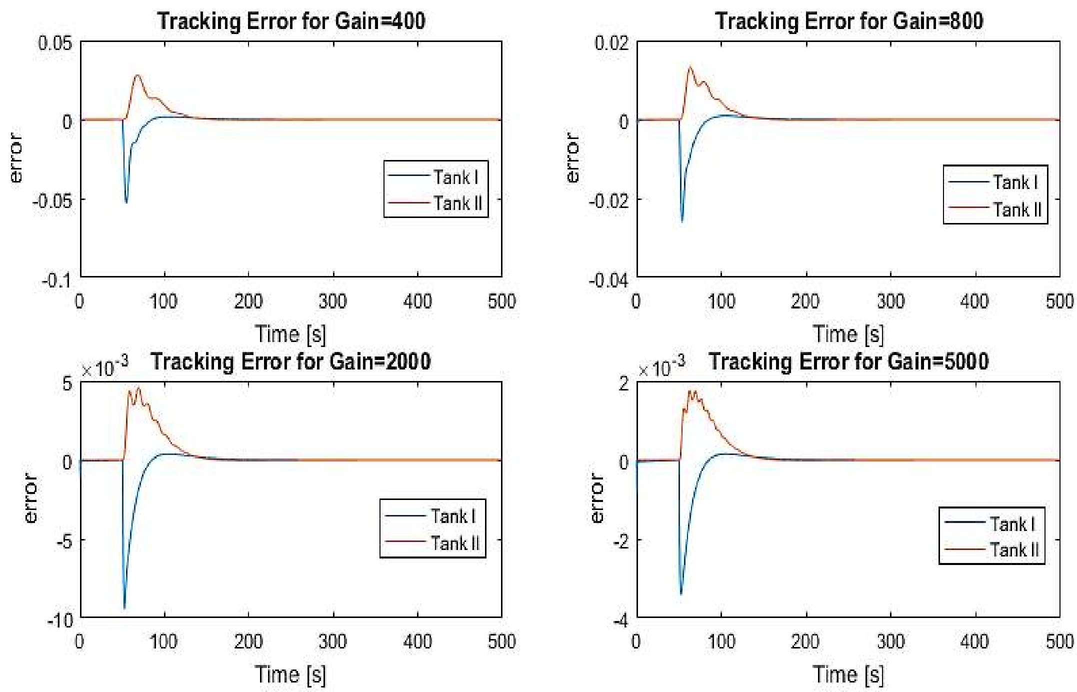

Figure 4.6 Proposed fault tolerant control tracking error degradation for various adaptation gains $\mathbf{\Gamma}_1$

In the second part of simulations, actuator failure tolerance property of three proposed design methods is examined. Here various fault/failure scenarios that can represent real world cases are presented, which can occur in a random time with unknown type and magnitude. It is assumed that valve1 gets stuck at a random time of simulation and stays at that position until the simulation stops. Figure 4.7 shows valve1 output signal when a periodical signal is added to the open-loop process input at equilibrium point. The figure illustrates that valve1 actuator immediately jumps to failure mode on 75th second of simulation. In the case of abrupt lock-in-place fault for valve1 actuator, closed-loop plant response is given in Figure 4.9. It is clear from the figure that plant loses its full controllability as it is not possible to control both levels at the same time. However, the novel controller has better fault tolerance and output that corresponds to fault free actuator has the ability of tracking the reference value with graceful performance degradation. Figure 10 shows valve outputs for the same failure scenario. In Table 4.4, performances of the three controllers for lock-in-place failure are compared by using ISE index.

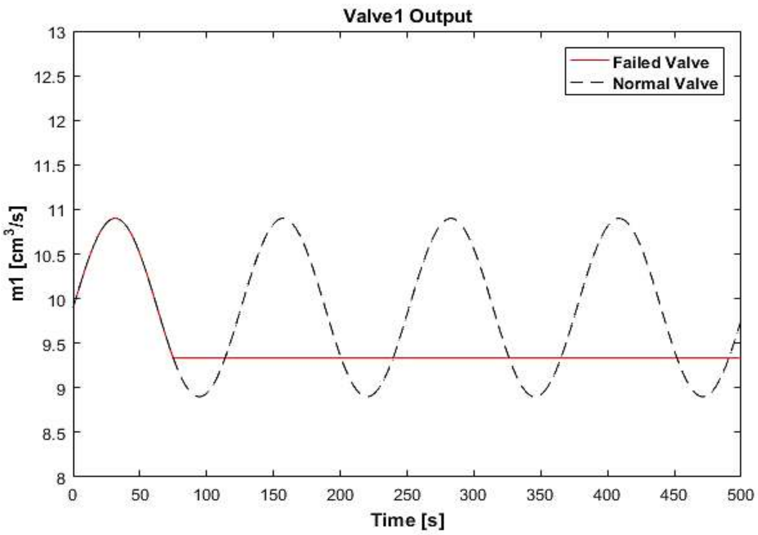

Figure 4.7 Open loop process valve1 output signal for normal/failed modes

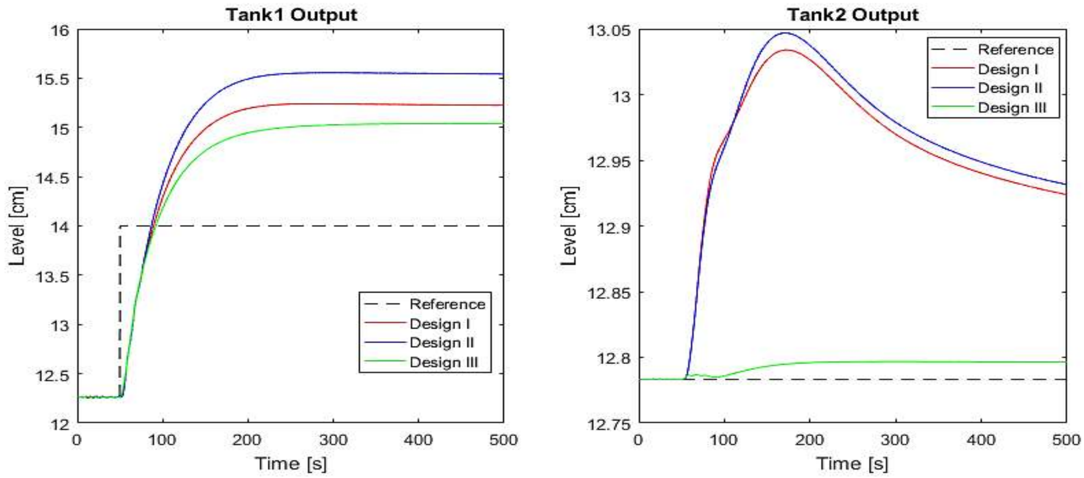

Figure 4.8 Process output responses for abrupt lock-in-place failure at valve1 actuator (on 75th second of simulation)

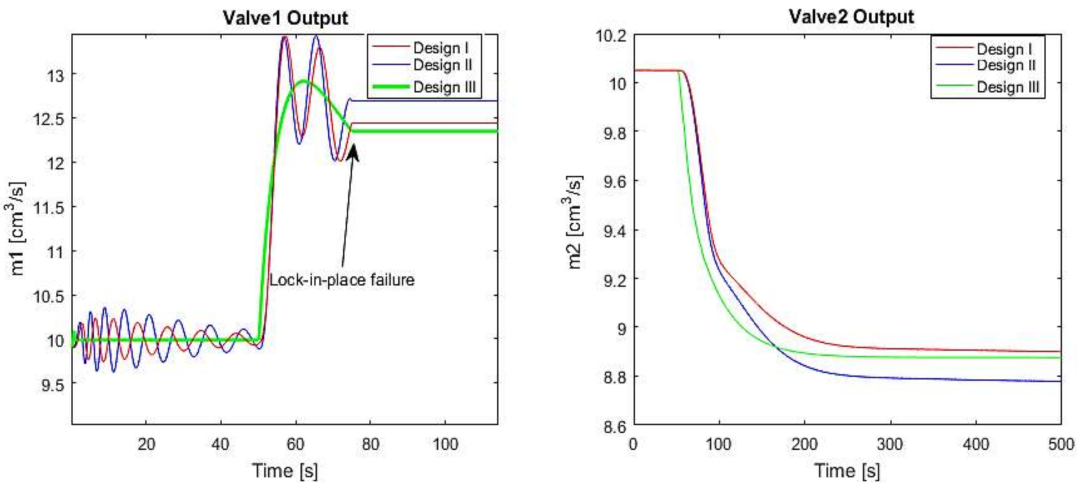

Figure 4.9 Process valve output signals for lock-in-place failure at valve1 actuator (on 75th second of simulation)

Table 4.4 Comparison of controllers by ISE index for abrupt lock-in-place fault

Control Method	Output1 ISE($\times 10^3$)	Output2 ISE
Design I	5.82	158.18
Design II	8.97	171.80
Design III	4.04	0.49

In the case of gain loss faults of actuators, the possibility that both actuators may fail in different times of simulation is considered. Furthermore, these faults can occur in abrupt and incipient ways. Firstly, the gradual gain loss of actuators is taken into account. The gains are reduced by 50% at slow exponential rate from 100s to 200s for valve1 actuator and from 75s to 175s for valve2 actuator. Figure 4.10 shows the actuator gains.

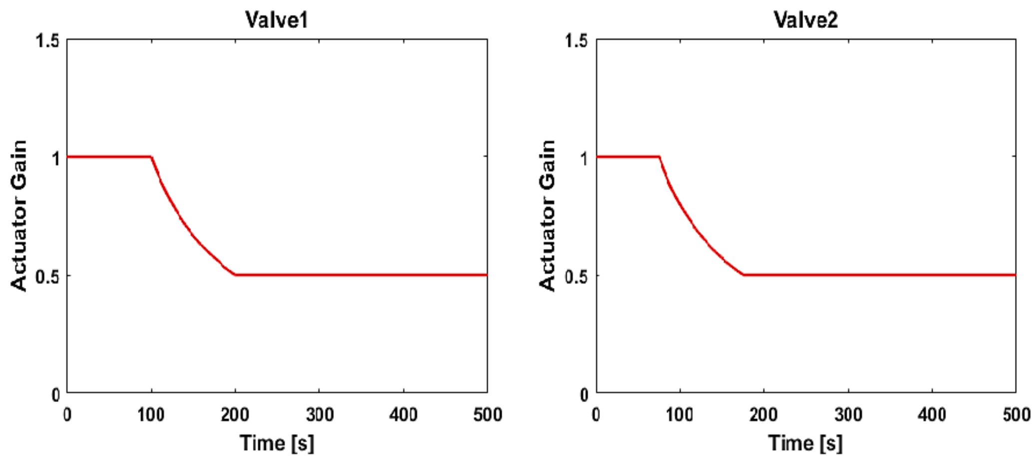

Figure 4.10 Incipient gain loss faults in actuators

Figure 4.11 shows close-up view of plant output transients. It is clear from the figure that the proposed FTC exhibits a better transient response to incipient loss of effectiveness faults. However the system performance is extremely degraded under the control of the other designs. Figure 4.12 shows valve outputs for the same fault case. Performance improvement of the novel controller can also be seen from ISE index quantities given in Table 4.5. It is obvious from the table that, especially for Tank2 level, there is a significant improvement in post-fault transient.

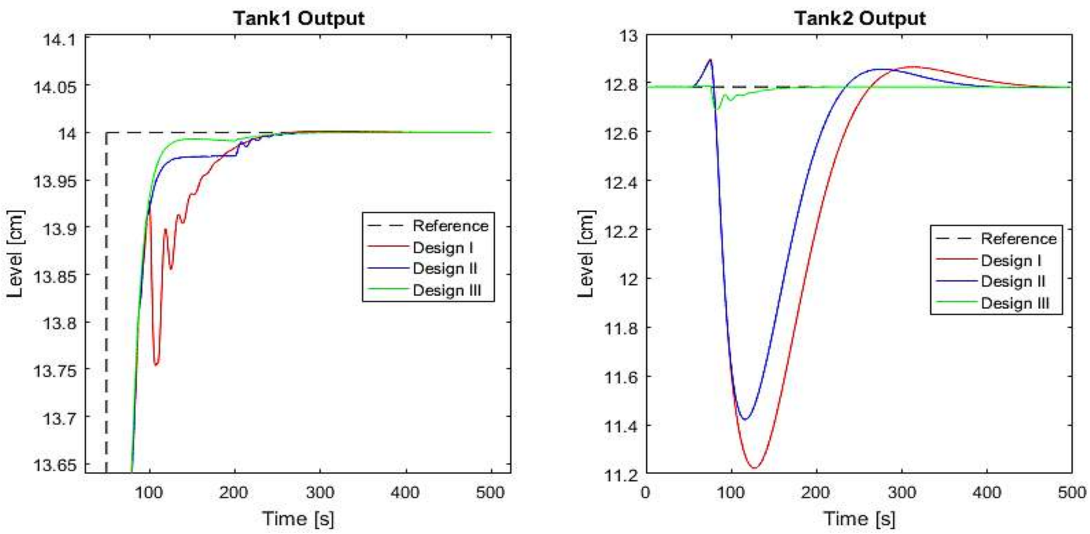

Figure 4.11 Process output responses for incipient gain loss at valve1 actuator (on 100th second of simulation) and valve2 actuator (on 75th second of simulation)

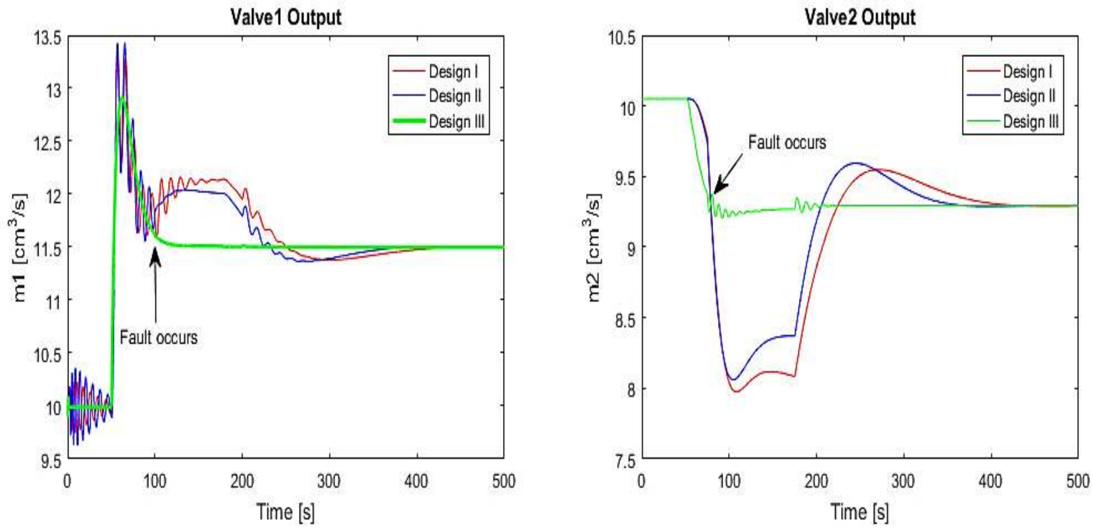

Figure 4.12 Process valve output signals for incipient gain loss at valve1 actuator (on 100th second of simulation) and valve2 actuator (on 75th second of simulation)

Table 4.5 Comparison of controllers by ISE index for incipient gain losses

Control Method	Output1 ISE	Output2 ISE ($\times 10^3$)
Design I	391.59	1.0151
Design II	389.58	0.6418
Design III	379.61	0.0001

Secondly, an abrupt gain loss occurs for both actuators is taken into account in different instants of simulation time. Figure 4.13 illustrates the immediate changes on actuator gains of two valves. Figures 4.14-4.15 display system outputs and valve outputs respectively for the case. It is obvious from Figure 4.14 that adaptive controllers given in Design I and Design II suffer from the slow reaction property since their higher adaptation gains cause high frequency oscillations. Quantitative comparison of controller performances is given in Table 4.6.

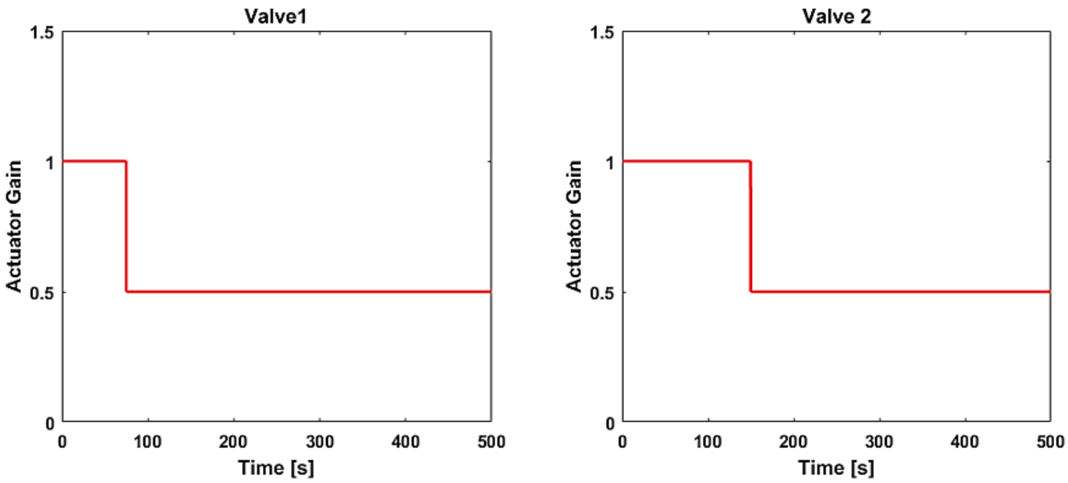

Figure 4.13 Abrupt gain loss faults in actuators

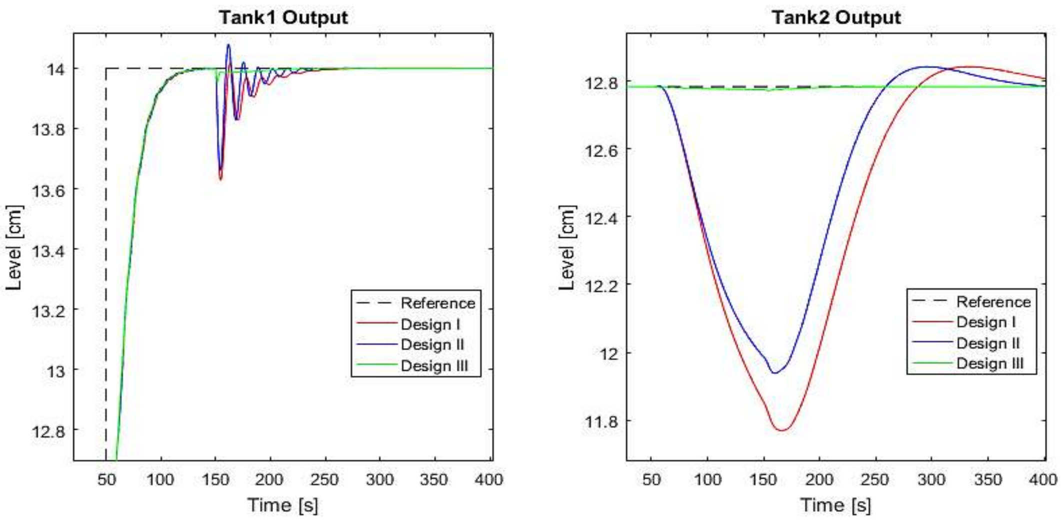

Figure 4.14 Process output responses for abrupt 50% gain loss at valve1 actuator (on 150th second of simulation) and valve2 actuator (on 75th second of simulation)

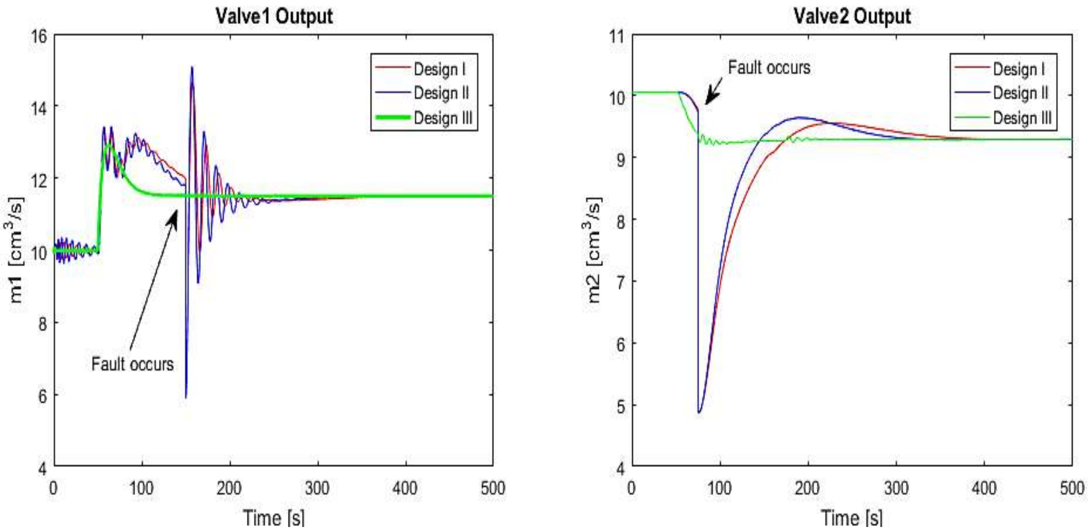

Figure 4.15 Process valve output signals for abrupt 50% gain loss at valve1 actuator (on 150th second of simulation) and valve2 actuator (on 75th second of simulation)

Table 4.6 Comparison of controllers by ISE index for abrupt gain losses

Control Method	Output1 ISE	Output2 ISE ($\times10^3$)
Design I	399.15	1.578
Design II	395.58	1.069
Design III	379.91	0.001

In the leakage scenario, an additive periodical signal is used to mimic extra liquid leakage at the valve output. Figure 4.16 depicts the leakage fault on the control valves of open-loop process at equilibrium point. It shows that both valve actuator jumps to fault mode abruptly in different instants of simulation time and faults result with illustrated valve output changes. The controller with stabilizing multiplier (Design I) and the one with additional control parameter (Design II) exhibit undesired oscillations while the proposed controller maintains the system performance with good transient behavior. The response can be seen from Figure 4.17. Figure 4.18 gives valve outputs for the same fault scenario. It is obvious from ISE index that post-fault transient performance of the proposed controller is superior to other controllers.

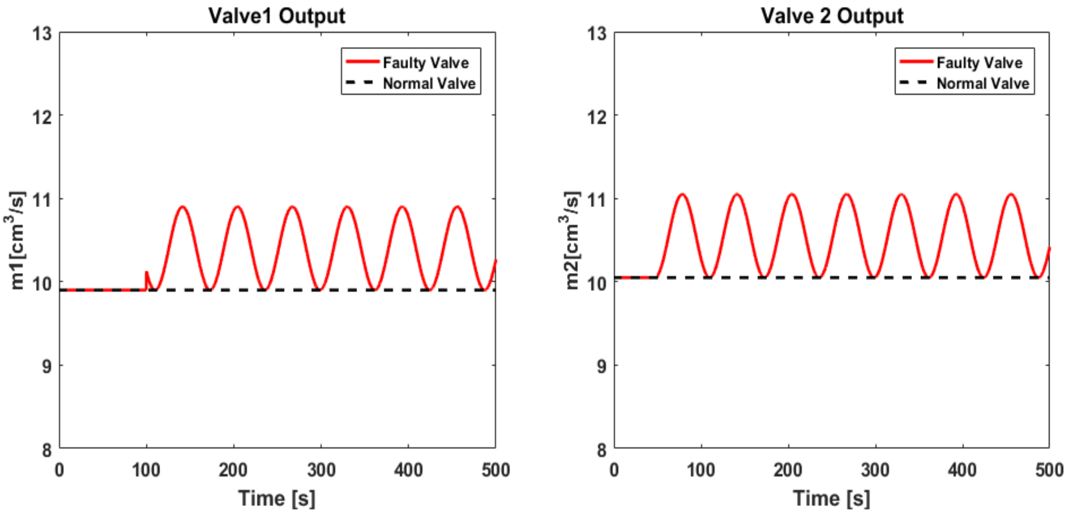

Figure 4.16 Open-loop process valve outputs in normal/faulty mode for a sinusoidal system input

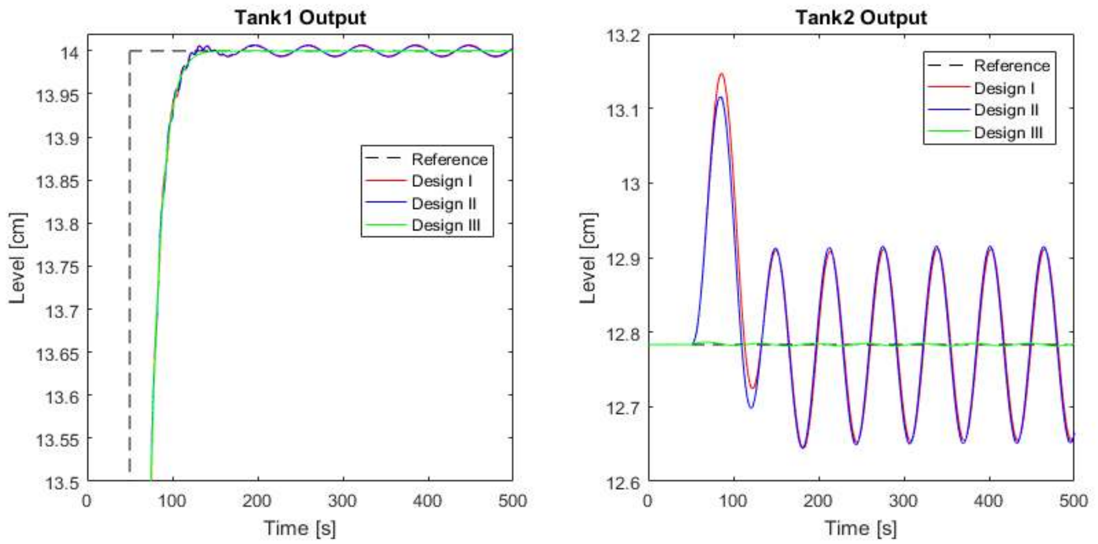

Figure 4.17 Process output responses for abrupt periodical leakage at valve1 (on 100th second of simulation) and valve2 (on 50th second of simulation)

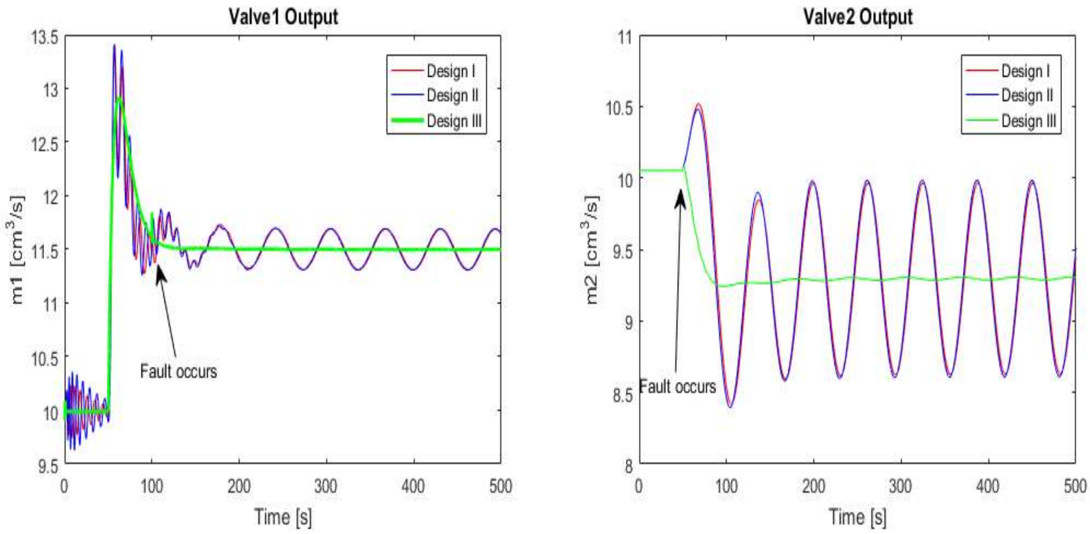

Figure 4.18 Process valve output signals for abrupt periodical leakage at valve1 (on 100th second of simulation) and valve2 (on 50th second of simulation)

Table 4.7 Comparison of controllers by ISE index for abrupt periodical leakage

Control Method	Output1 ISE	Output2 ISE
Design I	389.41	63.85
Design II	388.19	59.54
Design III	379.76	0.01

In normal operating mode without failure/fault consideration, reference tracking performance and tendency of the designs to control signal oscillation under high learning rate gains are examined. We built the final proposed controller given in Design III in such a way that it features all the modified properties of Design I and Design II. In addition, it has the ability of suppressing the high frequency oscillations in control signal for higher adaptation gains which leads to better reference model tracking. The example results in normal operation shows a significant recovery on system performance in comparison with Design II which does not have the mentioned property. In actuator failure/fault cases, three methods are compared by means of simulation results and ISE performance index. All three designs have the failure tolerance property to some extend thanks to the extra term in adaptive control law proposed in Design I. However, for total failure case of one actuator, none of the methods meet the complete control goal because of lack of actuator redundant system configuration. Design II and Design III have extra modification that relaxes the restriction of HFG matrix which may easily change with fault effect. Process simulation results for actuator partial fault cases show that Design II has relatively better post-fault transient performance than Design I and two designs generate similar control signals with some high frequency oscillation. The proposed controller in Design III has distinct improvement in post-fault transient responses with very small reaction time and ISE index values at the cost of more calculation effort and higher system complexity. Besides, it generates smooth control signals despite the fact that it has very high learning rate gains.

CHAPTER V

APPLICATION OF CONTROLLER TO REAL QUADRUPLE TANK PROCESS

In previous chapters, mathematical model of the process, controller design details and computer simulation studies are given and the results are discussed. In this section, it is aimed to prepare the controller to a real-time application and compare acquired results by using benchmark system.

5.1 Coupled Tanks Experiment Setup Description

The Coupled Tanks is a mechanical experimental setup which consists of 4 tanks interconnected tanks. The rig has an extra tank which is placed at the bottom as a reservoir. Inside the reservoir, there are 2 submersible pumps. The liquid is pumped via series pipes and 7 configuration valves. Configuration valves give the opportunity to introduce various coupling between the tanks. The water level measurement for each tank is acquired by using 4 pressure sensors. The Coupled Tanks Setup is organized according to the schematic presented in Figure 5.1.

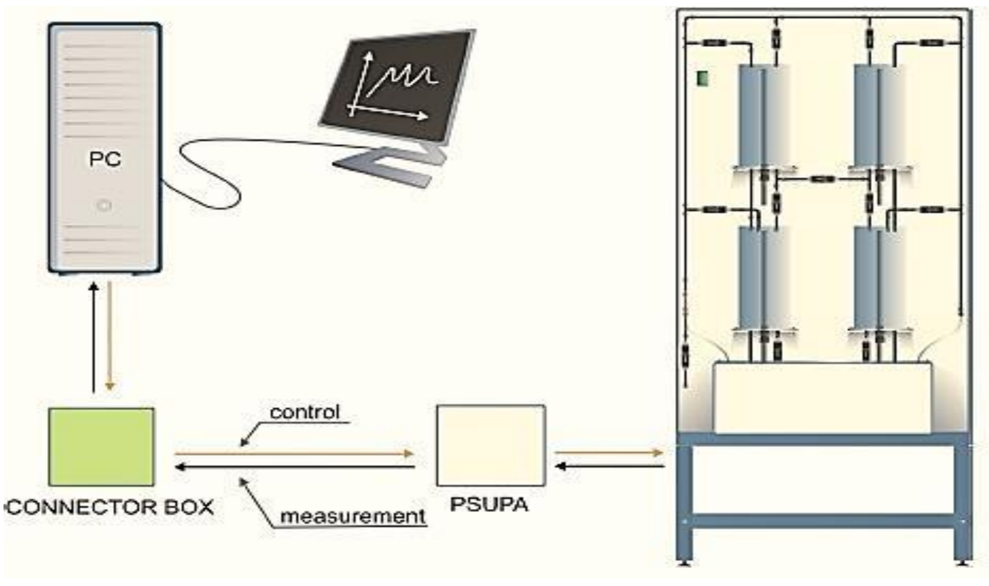

Figure 5.1 Control system schematic [77]

The PC with data acquisition card and Matlab/Simulink environment serve as the main control unit. The control signals, which are voltages between 0V and 5V, are transferred to the power amplifier where they are transformed into 24V DC signals driving the pumps. Real system configuration is illustrated in Figure 5.2.

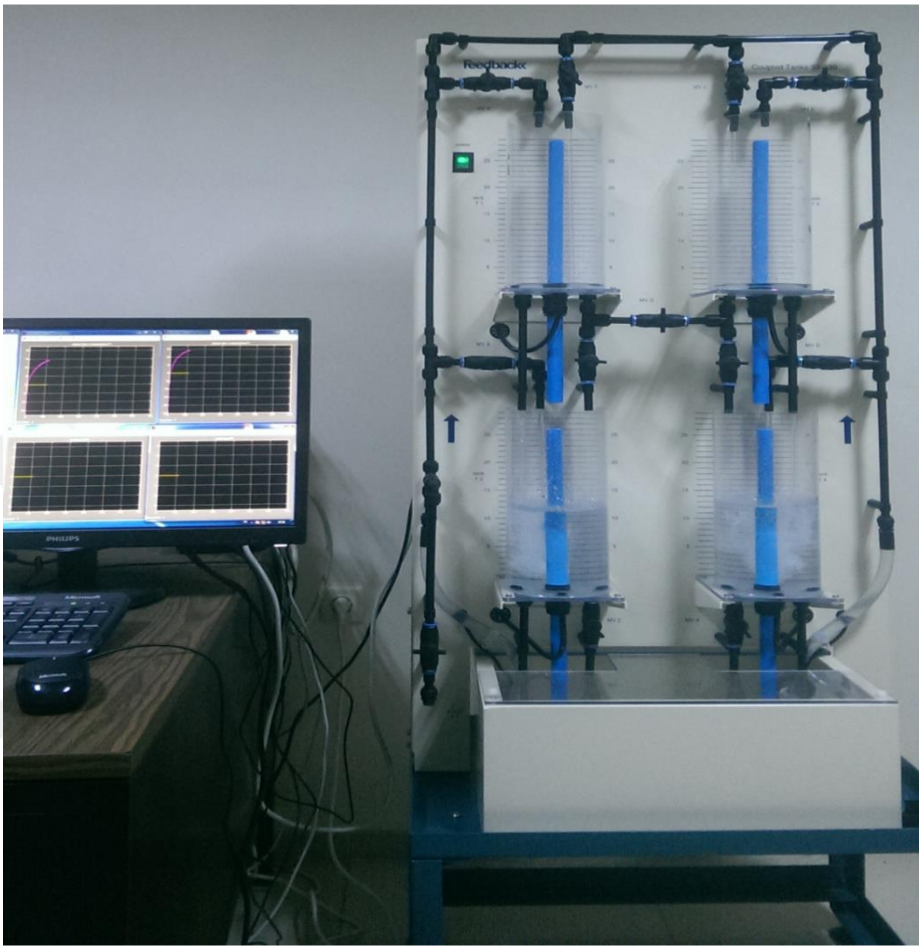

Figure 5.2 Real system setup

The computer part of control system comprises the following main elements:

1. A computer with control algorithm software
2. A/D and D/A converters in order to maintain interface between computer and physical system
3. The benchmark process
4. Actuators
5. Sensors

The control algorithm and the converter units are coordinated by computer with a specific sample time adjusted by the clock. This sampling time is mostly constant for applications. The clock delivers an interrupt called interrupt service routine (ISR).

During ISR routine, A/D converter supply discrete version of acquired sensor information in order that the control algorithm calculates and generate a control signal. At the end of the ISR, the next sample of the control signal value set by the D/A converter to be held for the next sampling interval.

5.2 Preparing Proposed Controller to Real Time Applications

In design phase of adaptive FTC, the process signals are assumed to be free of noises. However this is not the case for real time applications since they may be subjected to sensor/actuator noises. This disruptive practical system difference may well cause the overall system instability which stems from the adaptation law itself since closed loop system is no longer linear and time-invariant. In the presence of noise and bounded disturbance, adaptive system parametric model may be represented with the following form:

$$\mathbf{z} = \mathbf{\Psi}^{*}\left[\mathbf{\Theta}^{*T}\boldsymbol{\varphi} + \mathbf{z}_0\right] + d \tag{5.1}$$

where d represents parametric model error. To solve the sensor noise problem that is main cause of above modeling error for our system, some methods are available such as dead zone modification and dynamic normalization. The system which is subjected to above problems can be made robust and closed loop signal boundedness is guaranteed if a proper filter $f(s)$ is chosen and the following normalization signal is used:

$$m^2 = 1 + m_s,\ \ \dot{m}_s = -\delta_o m_s + |u|^2 + |y|^2,\ \ m_s(0) = 0 \tag{5.2}$$

$\delta_o > 0$ is a design constant and m_s is referred as the dynamic normalizing signal.

In the quadruple tank process experiments, the reference model is chosen as inverse of the diagonal interactor matrix provided that HFG matrix K_{p} is finite and nonsingular. In this case modified interactor matrix is chosen as follows:

$$\xi_m = \begin{bmatrix} (\alpha s+1)^2 & 0 \\ 0 & (\alpha s+1)^2 \end{bmatrix} = \begin{bmatrix} (10s+1)^2 & 0 \\ 0 & (10s+1)^2 \end{bmatrix} \tag{5.3}$$

Reference model with dynamic decoupling property can be written as:

$$W_m = \begin{bmatrix} \frac{1}{(10s+1)^2} & 0 \\ 0 & \frac{1}{(10s+1)^2} \end{bmatrix} \tag{5.4}$$

Experimental set-up parameters and process operating point is given in Table 5.1. By using the system parameters in Table 5.1 and Equation (5.3) a nominal HFG matrix which is independent of actuator faults is calculated as follows:

$$K_{pnom} = \begin{bmatrix} 13.77 & 0 \\ 0 & 0.30 \end{bmatrix} \tag{5.5}$$

Table 5.1 Experiment set-up parameters and operating point

Parameters	**Value**
Tank height, h_{max}	25 cm
Pomp voltage level	0-5 V
Bottom area, Tank1, Tank2, A_1, A_2	0.01389 m^2
Bottom area, Tank3, Tank4, A_3, A_4	0.01389 m^2
Out pipe cross-sectional area, a_1, a_3, a_2, a_4	50.26e-6 m^2
Pomp constant, k	2.2e-3 lt/Vs
Tank1 operating point level h_1^o	8.0 cm
Tank2 operating point level h_2^o	5.0 cm
Tank3 operating point level h_3^o	1.5 cm
Tank4 operating point level h_4^o	1.10 cm
Pump1 voltage level v_1^o	3 V
Pompa2 voltage level v_2^o	3 V

The parametric model filter is chosen as $f(s) = \frac{1}{(50s+1)^2}$ and the stabilizing multiplier is calculated as:

$$\bar{L} = \begin{bmatrix} 50 & 0 \\ 0 & 1 \end{bmatrix} \begin{bmatrix} 13.77 & 0 \\ 0 & 0.30 \end{bmatrix} \tag{5.6}$$

For the final proposed controller (Design III), oscillation suppression constant design matrices are chosen so that $A_1 = 250 I_{2x2}$, $A_2 = 100 I_{2x2}$, $B_1 = diag\{1,10\}$, $B_2 = 0.02 I_{2x2}$.

5.3 Real Time Fault Tolerant Control Experiments

In all experiments, after bringing tank levels to the vicinity of operating point values, it is aimed that a 3cm step change in Tank1 reference level is applied on 70th second of experiment while Tank2 level is regulated at 5cm operating point level. Total experiment time is chosen to be 550 s and sampling time of computer control system is 0.1 s. Firstly, improved fault tolerant controller given in Design III is compared with the controller given in Design II which does not contain modification of first controller. Figure 5.3 shows the response in the mentioned case. Here we investigate the effect of high adaptation gains ($\Gamma_1 = 5000\mathbf{I}_{2x2}, \Gamma_2 = 50\mathbf{I}_{2x2}$) on the system performance.

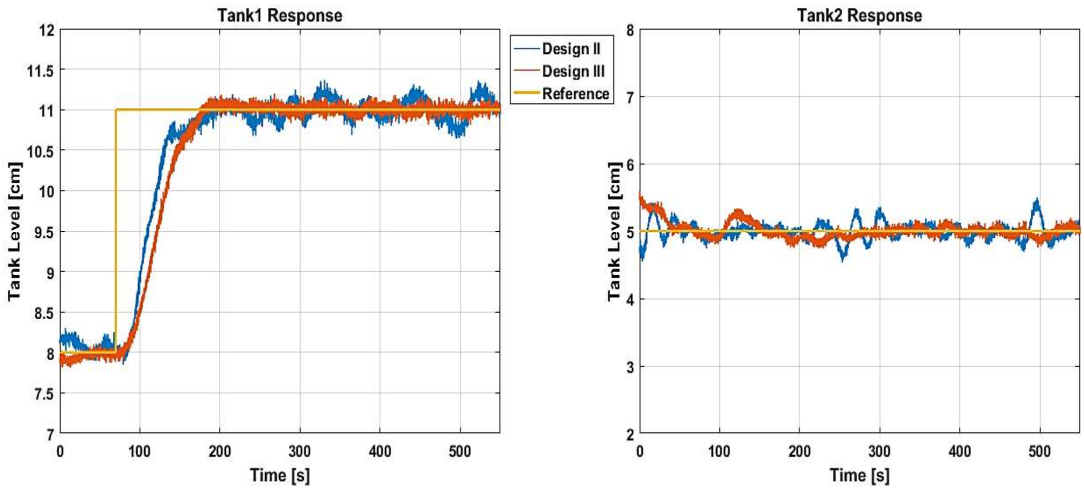

Figure 5.3 Adaptive control performances in normal operation mode

It clear from the figure that Design II controller causes oscillations around reference signals. Control signals generated by adaptive controllers are given in Figure 5.4. The controller in Design II that is free of proposed modifications generates a control signal with high frequency component.

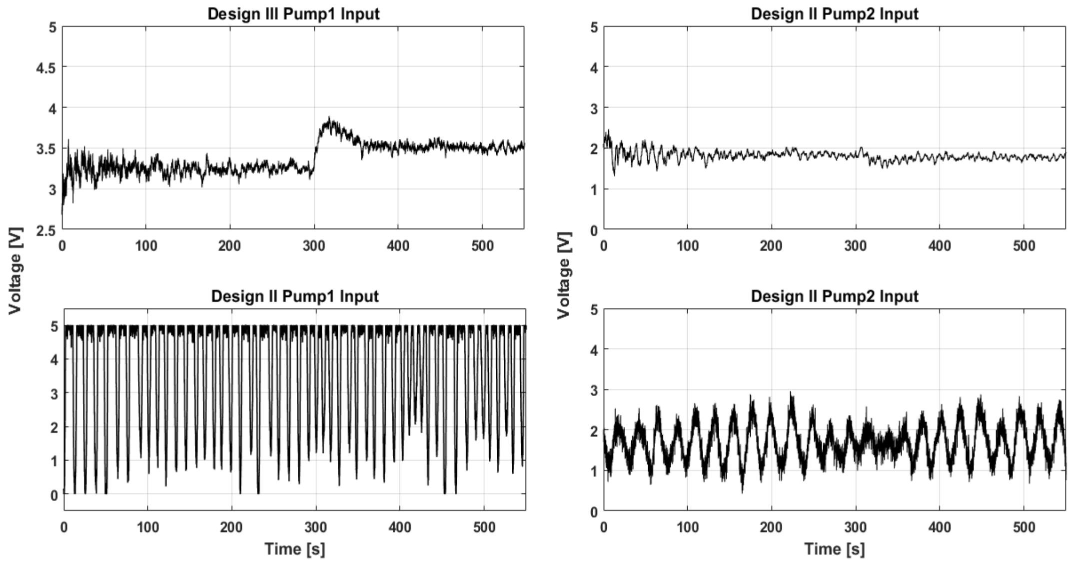

Figure 5.4 Generated actuator input signals in normal operation mode

In the next part of experiments, fault tolerance of controllers is investigated. A similar fault tolerant control approach that is applied to the same benchmark process is also added to the experiment for the purpose of literature comparison and revealing that the proposed controller has a significant refinement in performance or not. The above mentioned controller is a reconfigurable parametric eigenstructure assignment control (PEA) and the design details are available in [27]. Just as simulation experiment, the real time experiments start with stuck type total actuator failure scenario. In this scenario, pump1 actuator is subjected to the failure on 70th second of experiment. Figure 5.5 shows pre-fault and post-fault responses of both output levels.

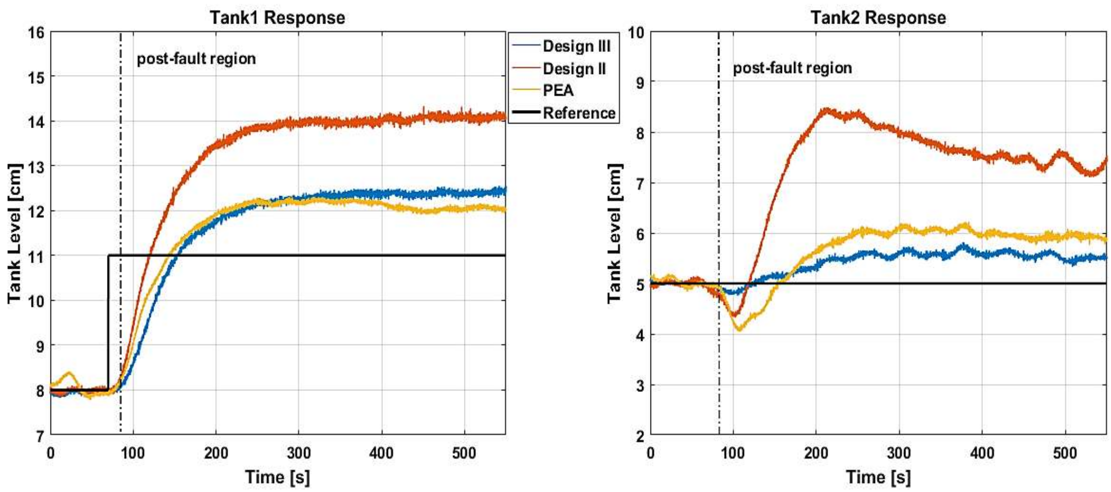

Figure 5.5 Process output responses in the case of stuck type failure on 70th second of experiment

While pump1 controlled Tank1 loose its controllability property as a result of lack of actuator, considering mean square error (MSE) index given in Table 5.2, pump2 in normal operation mode makes possible to control Tank2 level with graceful performance degradation. In that case, final proposed controller in Design III exhibits the best performance.

Table 5.2 Comparison of controllers with MSE index in the case of stuck actuator failure

Control Method	Output1 MSE	Output2 MSE
Design II	6.38	5.57
Design III	1.70	0.21
PEA	1.31	0.66

Figure 5.6 shows actuator input signals in the case of stuck actuator faults in pump1. Experiments continue with considering incipient gain loss up to 20% in pump1. In this scenario, it assumed that actuator fault occurs 320^{th} second of experiment and pump2 actuator is in normal operation mode. Considering Table 5.3 index values and the process response given in Figure 5.7, proposed final control system, Design III, exhibits the best performances with regard to post-fault transients and tank interaction decoupling. Figure 5.8 illustrates actuator input signals for the gain loss fault of pump1. In the light of given input signals, Design III-controlled real system reaches the control goal with less control input effort.

Table 5.3 Comparison of controllers with MSE index in the case of gain loss fault for pump1

Control Method	Output1 MSE	Output2 MSE
Design II	0.70	0.11
Design III	0.39	0.01
PEA	0.75	0.23

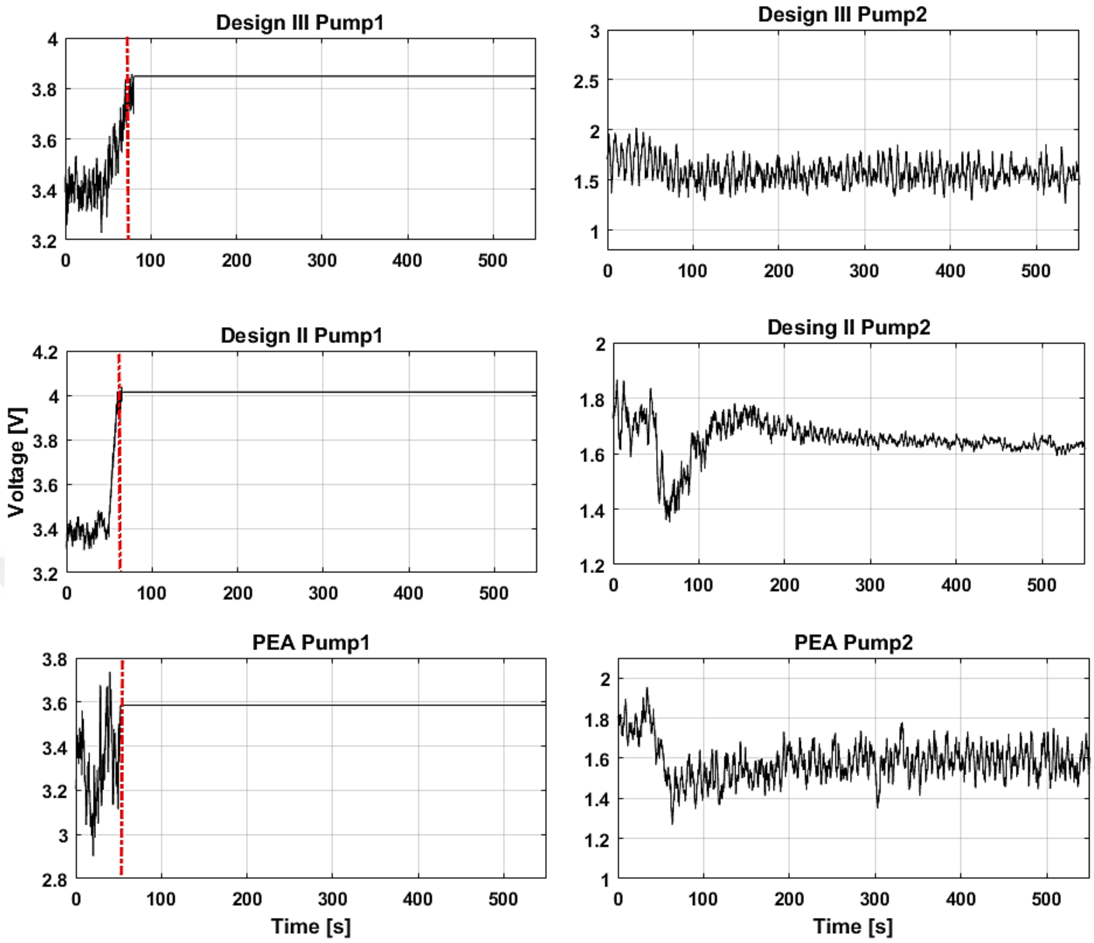

Figure 5.6 Actuator input signals in the case of pump1 actuator stuck failure (red dashed line failure start time)

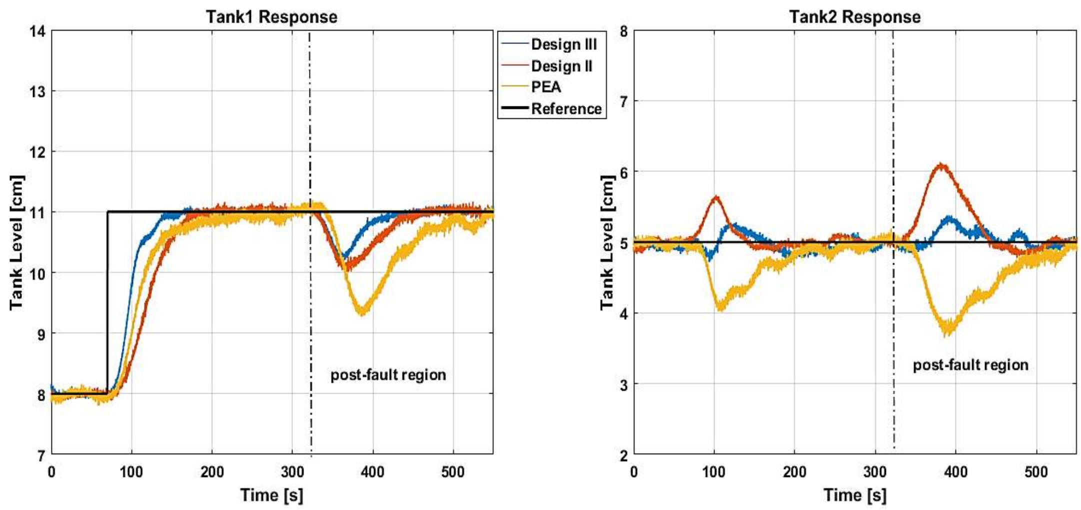

Figure 5.7 System responses when 20% incipient gain loss occurs on 320th second of experiment

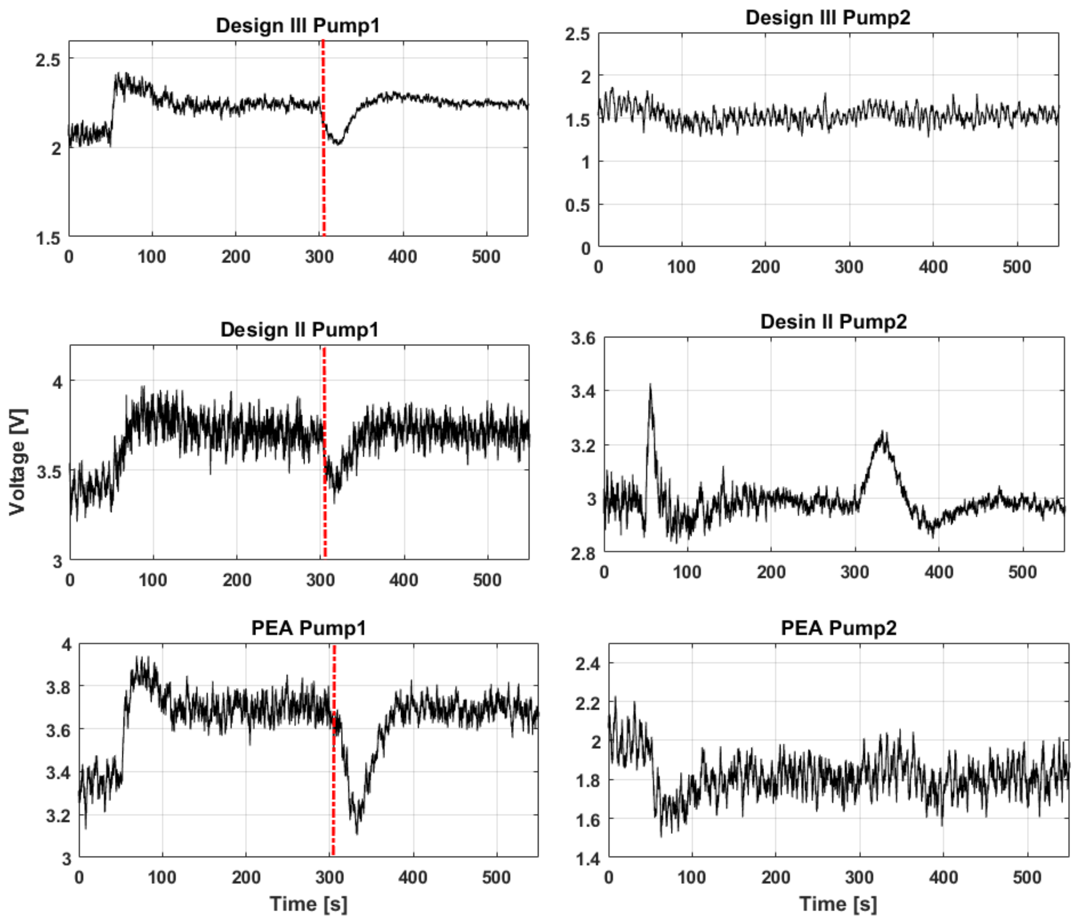

Figure 5.8 Incipient gain loss fault up to 20% in pump1 (red dashed lines imply fault occurs)

In the second scenario of gain loss type actuator faults, it is assumed that an abrupt loss of effectiveness fault of 40% occurs in pump2 only. Figure 5.9 shows normal operating mode and post-fault responses of the process. The fault occurred in pump2 actuator leads Tank1 level to deviate from its reference in different amount for each control method as a result of inter-tank coupling. All the control approaches is able to compensate the fault to some extend however Design III needs smaller time for post-fault transient. The index values of controller performances are given in Table 5.4.

Table 5.4 Control performance comparison in the presence of pump2 gain loss fault

Control Method	Output1 MSE	Output2 MSE
Design II	0.43	0.33
Design III	0.38	0.17
PEA	0.69	0.38

The control signals of actuators that are exposed to the above mentioned fault is given in Figure 5.10. With a significant amount of gain loss, controllers cause the failed actuator to saturate except PEA approach since it uses less actuator voltage for level regulation.

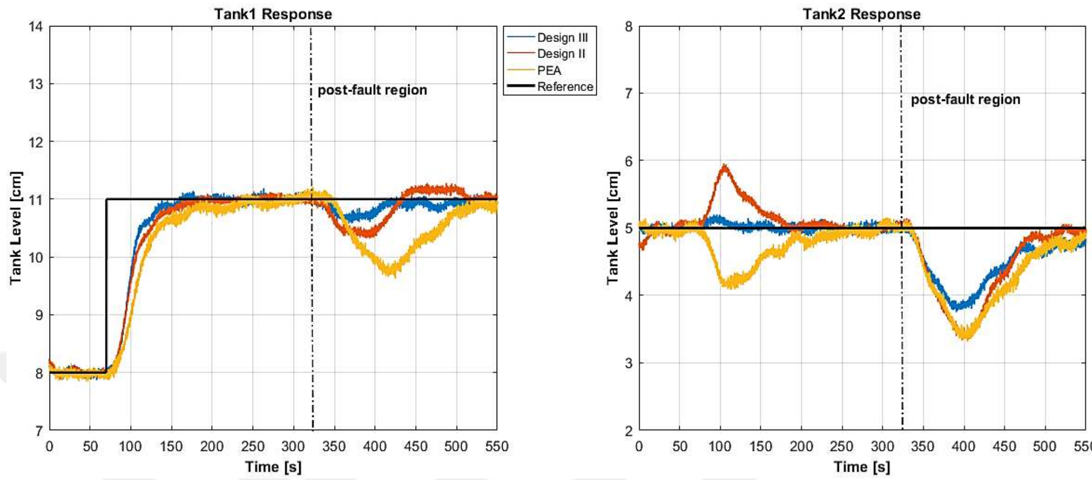

Figure 5.9 Abrupt gain loss fault of 40% occurs in pump2 (dashed line implies fault occurs)

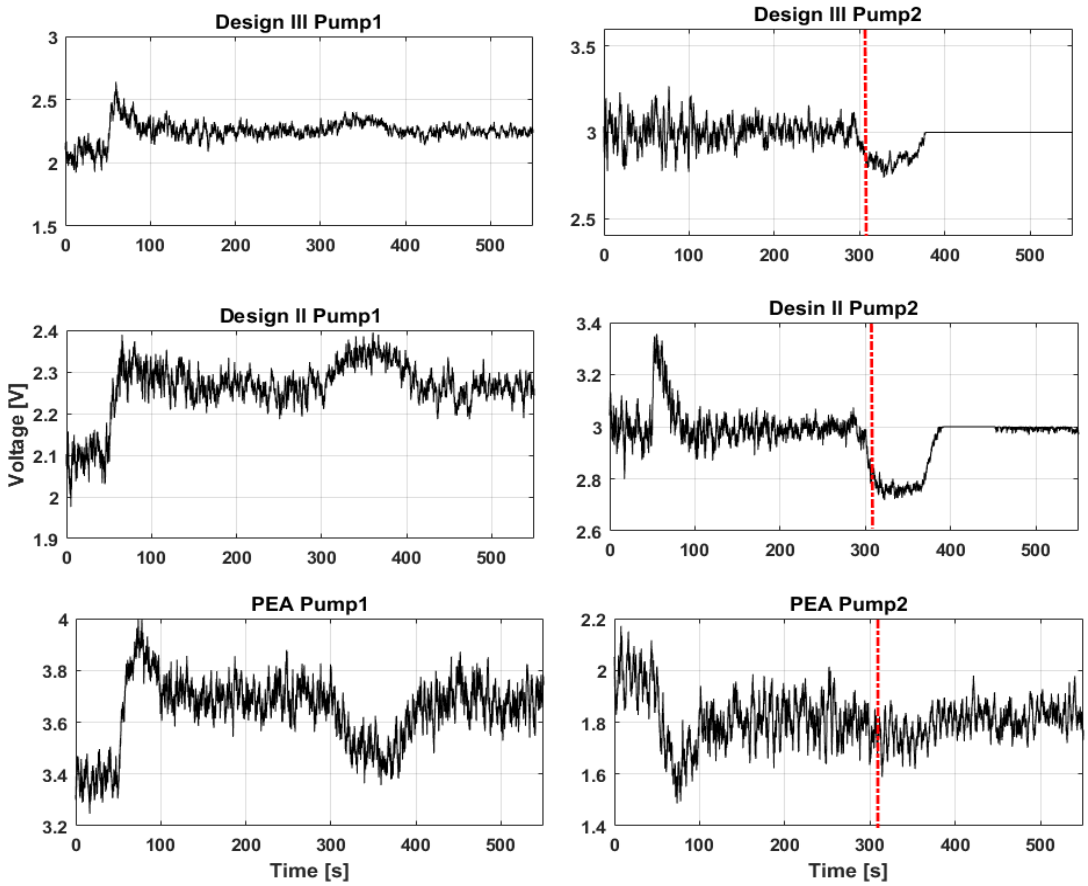

Figure 5.10 Actuator input signals in the presence of abrupt gain loss fault of 40% occurs in pump2

In the last fault scenario, both pump1 and pump2 are assumed to be exposed to gain loss failure in different instants of experimental time. Figure 5.11 shows closed loop system performances. The process enters post-fault region I with 40% gain loss in pump2 occurs on 170th second of experiment. After 150 seconds, system enters post-fault region II with an incipient 20% gain loss occurs in pump1 actuator.

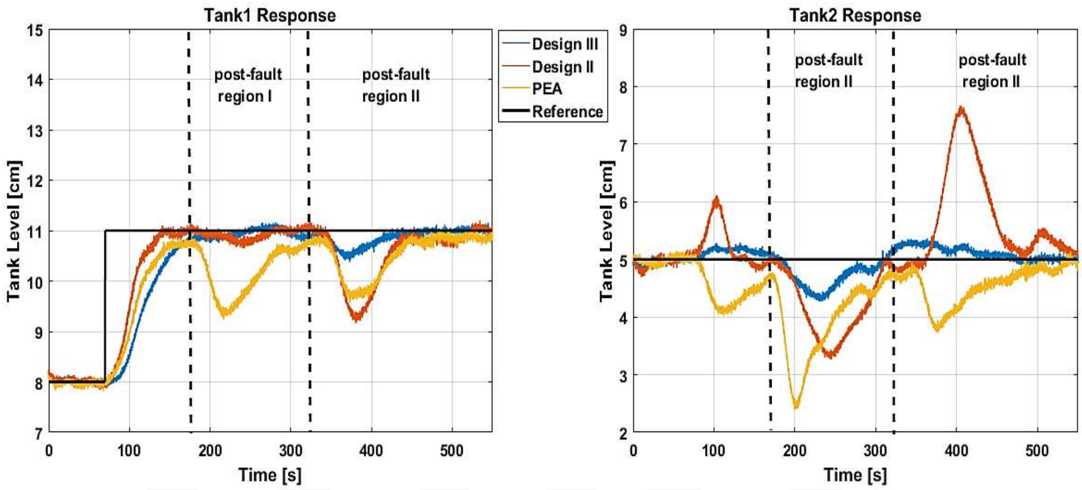

Figure 5.11 System response in the presence of abrupt 40% gain loss in pump2 (first dashed line implies fault occurrence) and incipient gain loss up to 20% in pump1(after second dashed line)

It is clear from the figure that, before entering post-fault region I, once step change in Tank1 reference is applied, Design II-controlled and PAE-controlled processes exhibit large deviations from reference in Tank2 level as a result of coupling between tanks. In region I, the fault occurred in pump2 causes significant performance degradation in Tank1 reference tracking through the coupling effect except the Design III-controlled process. In region II, second fault (incipient gain loss in pump1) occurs and larger deviations in reference tracking of Tank2 is exhibited by Design II and PEA controlled processes. It can also be seen from MSE index of controllers given in Table 5.5. By considering index values and the above given figure one can conclude that proposed controller in Design III has better performance with acceptable reference deviations. Figure 5.12 shows actuator input signals in the case of both actuator fails in different times of experiment.

Table 5.5 MSE performance index of controllers in the case that both actuators fail in different times of experiment

Control Method	Output1 MSE	Output2 MSE
Design II	0.66	0.77
Design III	0.61	0.05
PEA	0.89	0.62

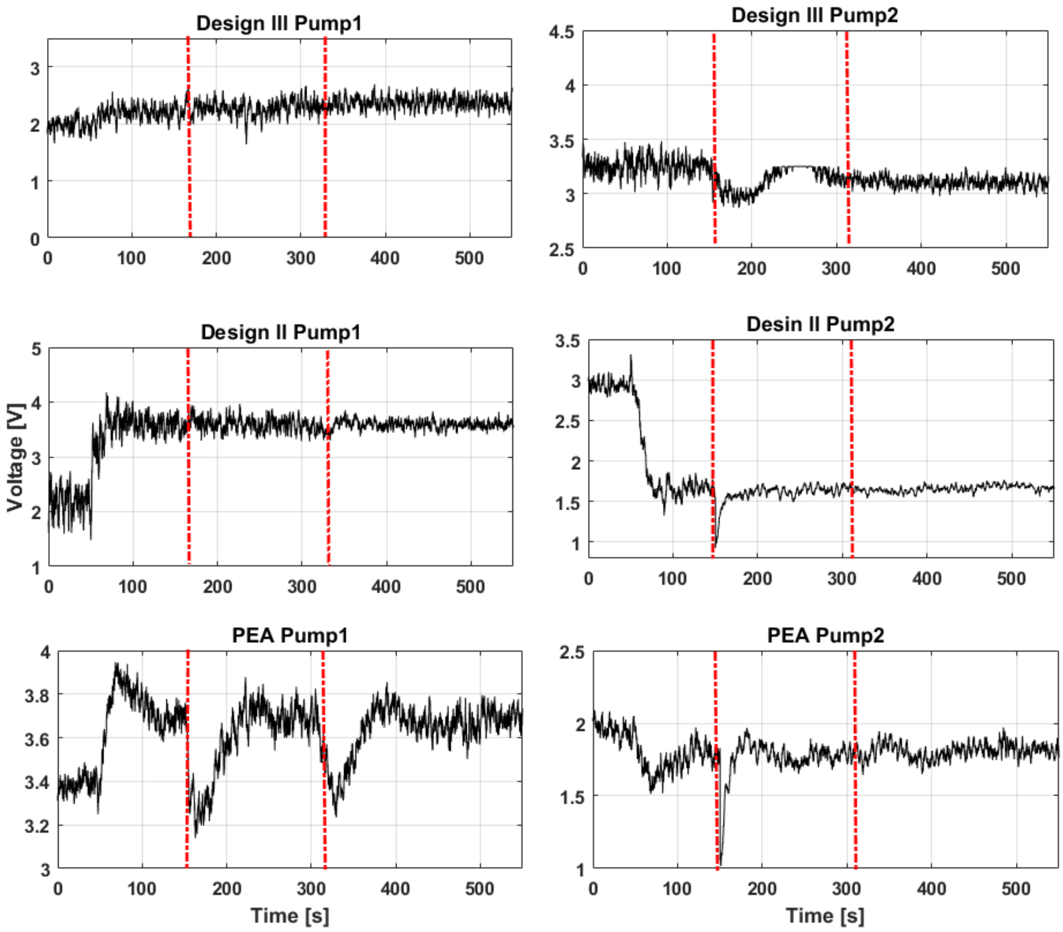

Figure 5.12 Actuator input signals in the presence of abrupt 40% gain loss in pump2 (first dashed line implies fault occurrence) and incipient gain loss up to 20% in pump1(after second dashed line)

CHAPTER VI

CONCLUSION AND RECOMMENDATIONS

This thesis study constitutes a solution to the problem of unpredictable actuator failures in control systems. Stability and performance requirements are met by the control design despite the failure regardless of the time and duration. To this end a modified MRAC is designed. The proposed adaptive approach is applied to a nonlinear process via simulations and real time experiments with some presumed fault/failure scenarios. The contributions of thesis can be summarized as follows:

- A generalized actuator fault model that covers electrical and hydraulic types is given as an alternative to existing models in literature. It unifies hard-over, gain loss, leakage and lock-in-place type failures in order to obtain a mathematical model that helps designer find an analytical solution.

- For FTC design, multivariable output feedback adaptive approaches are reviewed. A MRAC design is chosen and some modifications are added to solve the difficulties in the presence of actuator faults such as relaxing the restrictions of high frequency gain matrix and improving the robustness of controller, control reparametrization for actuator failure and finally designing a novel controller that improves post fault transients by providing fast adaptation using an idea that is applied first for optimization purposes.

- The results are numerically and graphically demonstrated. Although the controllers studied in design and simulation part have the ability of compensating partial failures up to some extent, the results reveal that proposed fault tolerant controller is superior to the counterparts with better post-fault transient response. It is also effective on maintaining the reference tracking for

- the tank with fully functional actuator when total actuator failure occurs in the other control channel.

- A quadruple-tank system which comprises of two liquid pumps and level sensors is used as testbed. In the simulation part, different from the original system, a valve-actuated configuration is considered as well. The final control scheme, with some robustness modification by considering practical issues, is applied to the real process and it is shown that the control system leads to a faster smooth post-fault transient response compared with similar methods. In addition, it generates a smooth control signal without high frequency oscillations making the system less vulnerable to actuator damages.

6.1 Recommendations for Future Work

The result presented in this study is open to further development. Future work of the present study can be the following:

- The proposed controller can be used to solve real industrial control problems especially in coupled tanks processes. The comprehensive design approach of controller allows us to apply it to MIMO systems in wide variety such as robotic applications, chemical processes, water treatment facilities, nuclear plants, paper production etc. It may also be a solution to underactuated systems with actuator redundancy in analytical or hardware class.

- In some cases, faults may well cause structural variations in systems and also considered as bounded disturbances. Besides control system may excite unmodelled system dynamics. Therefore, additional robustness modifications in controller may enhance the control system performance by considering unmodelled dynamics and disturbances in design phase.

- The quadruple-tank system constitutes a benchmark problem system developed for process industry. The system under study gives opportunity to find solutions for various application purposes such as actuator and sensor fault tolerance, testing FDD algorithms, centralized and decentralized control structure for multivariable systems, minimum and non-minimum phase system control, and nonlinear control design. The implementation of advanced robust and adaptive FTC methods to the benchmark will give useful results for practical applications.

REFERENCES

[1] Hur, A., Sajjad, A., Shahid, Q. (2012). Sliding Mode Control for Coupled-tank Liquid Level Control, *10th International Conference on Frontiers of Information Technology*. 325-330.

[2] Srinivas, P., Lakshmi, K. V., Kumar, V. N. (2014). A Comparison of PID Controller Tuning Methods for Three Tank Level Process, *International Journal of Advanced Research in Electrical, Electronics and Instrumentation Engineering*. **3(1)**, 6810-6820.

[3] Iqbal, M., Bhatti, A. I., Butt, Q. R. (2008). Controller Synthesis of an Uncertain Three Tank System Using Polytypic system Approach, *Proceedings of the 17th World Congress, The International Federation of Automatic Control*. 9910-9915.

[4] Graebe, S. F., Goodwin, G. C., Elsley, G. (1995). Control Design and Implementation in Continuous steel Casting, *IEEE, Control Systems*. **15(4)**, 64-71.

[5] Noura, H., Theilliol, D., Sauter, D. (2000). Actuator Fault-Tolerant Control Design: Demonstration on a Three-tank-system. *Int. J. Syst. Sci*. **31**(9), 1143-1155.

[6] Sarailoo, M., Rezaie, B., Rahmani, B. (2014). Fuzzy predictive control of three-tank system based on a modeling framework of hybrid systems. *J. Syst. Control Eng.* **228(6)**, 369-384.

[7] Yin, S. Lao, H., Ding, S.X. (2014). Real-Time Implementation of Fault-Tolerant Control Systems with Performance Optimization, *IEEE Trans. Ind. Electron.* **61(5)**, 2402-2411.

[8] Hijiani, P., Poshtan, J. (2012). Reconfigurable Controller Design for Actuator Faults in a Four-tank System Benchmark, *International Journal of Instrumentation and Control Systems*. **2**(2), 69-76.

[9] Wang, L., Sun, L., Yu, J., Zhang, R.; Gao, F. (2017). Robust Iterative Learning Fault-Tolerant Control for Multiphase Batch Processes with Uncertainties, *Ind. Eng. Chem. Res.* **56**(36), 10099–10109.

[10] Gao, M.; Sheng, L.; Zhou, D.; Gao, F. (**2017**). Iterative Learning Fault-Tolerant Control for Networked Batch Processes with Multirate Sampling and Quantization Effects, *Ind. Eng. Chem. Res.* **56**(9), 2515–2525.

[11] Alanqar, A., Durand, H., Christofides, P. D. (2017**).** Fault-Tolerant Economic Model Predictive Control Using Error-Triggered Online Model Identification, *Ind. Eng. Chem. Res.* **56**(19), 5652–5667.

[12] Luppi, P. A., Basualdo, M. S. (2016). Smart Investment for Redundancies Selection Integrated to Reconfigurable Fault-Tolerant Control Design, *Ind. Eng. Chem. Res.* **55**(35), 9485–9497.

[13] Luppi, P. A., Outbib, R., Basualdo, M. S. (2015). Nominal Controller Design Based on Decentralized Integral Controllability in the Framework of Reconfigurable Fault-Tolerant Structures, *Ind. Eng. Chem. Res.*, **54**(4), 1301–1312.

[14] Fan, H., Liu, B., Wang, W., Wen, C. (2015). Adaptive fault-tolerant stabilization for nonlinear systems with Markovian jumping actuator failures and stochastic noises, *Automatica*, **51**, 200-209.

[15] Li, X. J., Yang, G. H. (2012). Robust adaptive fault-tolerant control for uncertain linear systems with actuator failures, *IET Control Theory & Applications*. **6**(10), 1544-1551.

[16] Hu, J. Liang, J. Chen, D. (2015). Reliable guaranteed-cost control for networked systems with randomly occurring actuator failures and fading performance output, *International Journal of General Systems*. **44**(2), 129–141.

[17] Orani, N., Pisano, A., Usai, E. (2009) Fault detection and reconstruction for a three-tank system via high-order sliding-mode observer, *IEEE Conference on Control Applications and Intelligent Control*. 1714-1719.

[18] Noura, H., Theilliol, D., Sauter, D. (2000). Actuator Fault-Tolerant Control Design: Demonstration on a Three-tank-system. *International Journal of Systems Science*. **31**(9), 1143-1155.

[19] Jiang, J., Yu, X. (2012). Fault-tolerant control systems: A comparative study between active and passive approaches, *Annual Reviews in Control*. **36**(1), 60-72.

[20] Zhao Q., Jiang J. (1998). Reliable state feedback control system design against actuator failures, *Automatica*. **34**, 1267–1272.

[21] Veillette R. J. (1995). Reliable linear-quadratic state-feedback control, *Automatica*. 31, 137–143.

[22] Yang G. H., Wang J. L., Soh, Y. C. (2001). Reliable H1 controller design for linear systems. *Automatica*. **37**, 717–725.

[23] Harkegard O., Glad, S. T. (2005). Resolving actuator redundancy–optimal control vs. control allocation, *Automatica*. **41**, 137–144.

[24] Gu, Z., Liu, J., Peng, C., Tian, E. (2012). Reliable control for interval time-varying delay systems subjected to actuator saturation and stochastic failure, *Optimal Control Applications and Methods*. **33**(6), 739–750.

[25] Niu, Y., Liu, Y., Jia, T. (2013). Reliable Control of Stochastic Systems via a SMC Technique, *Optimal Control Applications and Methods*. **34**(6), 712–727.

[26] Zhang, Y., Jiang, J. 2008. Bibliographical review on reconfigurable fault-tolerant control systems, *Annual Reviews in Control*. **32**(1), 229-252.

[27] Hijiani, P., Poshtan, J. 2014. Abrupt and incipient fault detection and compensation for a 4-tank system benchmark. *Turkish Journal of Electrical Engineering & Computer Sciences*, **22**(5), 1287-1297.

[28] Zhang, R., Lu, R., Xue, A., Gao, F. (2014). Predictive Functional Control for Linear Systems under Partial Actuator Faults and Application on an Injection Molding Batch Process, *Ind. Eng. Chem. Res*. **53**(2), 723–731.

[29] Anand, A., Samavedham, L., Sundaramoorthy, S. (2012). Comparative Performance Analysis of Coordinated Model Predictive Control Schemes in the Presence of Model–Plant Mismatch, *Ind. Eng. Chem. Res.* **51**(24), 8273–8285.

[30] Karra, S., Shaw, R., Patwardhan, S. C., Noronha, S. (2008). Adaptive Model Predictive Control of Multivariable Time-varying Systems, *Ind. Eng. Chem. Res.* **47**(8), 2708–2720.

[31] Wang, Y., Yang, Y., Zhou, D., Gao, F. (2007). Active Fault-Tolerant Control of Nonlinear Batch Processes with Sensor Faults, *Ind. Eng. Chem. Res.* **46**(26), 9158–9169.

[32] Mhaskar, P., Liu, J., Christofides, P. D. (2013). *Fault-Tolerant Process Control: Methods and Applications*; Springer-Verlag: London.

[33] Mhaskar, P., Gani, A., Christofides, P. D. (2006). Fault-Tolerant Control of Nonlinear Processes: Performance-Based Reconfiguration and Robustness, *Int. J. Rob. & Non. Contr*. **16**, 91-111.

[34] Mhaskar, P., Gani, A., El-Farra, N. H., McFall, C., Christofides P. D., Davis, J. F. (2006). Integrated Fault Detection and Fault-Tolerant Control of Process Systems, *AIChE J.* 52, 2129-2148.

[35] Mhaskar, P., McFall, C., Gani, A., Christofides, P. D., Davis, J. F. (2008). Isolation and Handling of Actuator Faults in Nonlinear Systems, *Automatica*, 44, 53-62.

[36] Edwards, C., Lombaerts, T., Smaili, H. (2010). *Fault Tolerant Flight Control: A Benchmark Challenge;* Springer-Verlag: London.

[37] Ye, D., Chen, M.-M., Yang, H.-J. (2018). Distributed Adaptive Event-Triggered Fault-Tolerant Consensus of Multiagent Systems with General Linear Dynamics, *IEEE Transactions on Cybernetics*. 1–11.

[38] Jin, X., Qin, J., Shi, Y., Zheng, W. X. (2017). Auxiliary Fault Tolerant Control with Actuator Amplitude Saturation and Limited Rate, *IEEE Transactions on Systems, Man, and Cybernetics:Systems*. 1–10.

[39] Jin, X., Wang, S., Qin, J., Zheng, W. X., Kang, Y. (2018). Adaptive Fault-Tolerant Consensus for a Class of Uncertain Nonlinear Second-Order Multi-Agent Systems with Circuit Implementation, *IEEE Trans. Circuits Syst. I: Regular Papers*, 1–13.

[40] Chen S., Tao G., Joshi S. M. (2002). On matching conditions for adaptive state tracking control of systems with actuator failures, *IEEE Trans. Autom. Control*. **47**, 473–8.

[41] Tao G., Joshi S. M., Ma X. L. (2001). Adaptive state feedback and tracking control of systems with actuator failures, *IEEE Trans. Autom. Control*, **46**, 78–95.

[42] Tao G., Chen S., Joshi S. M. (2002). An adaptive actuator failure compensation controller using output feedback, *IEEE Trans. Autom. Control*, **47**, 506–11.

[43] Mihankhah, A., Salmasi, F. R., Salahshoor, K. (2013). Partial and total actuator faults accommodation for input-affine nonlinear process plants, *ISA Transactions*, **52**(3). 351–357.

[44] Dydek, Z. T., Annaswamy, A. M., Lavretsky, E. (2010). Adaptive control and the NASA X-15-3 flight revisited, *IEEE Control Syst.* **30**(3), 32–48.

[45] Yucelen, T., Calise, A.J. (2010). Kalman filter modification in adaptive control. *J. Guid. Control Dyn*. **33**(2), 426–439.

[46] Hovakimyan, N., Cao, C., Kharisov, E., Xargay, E., Gregory, I.M. (2011). L1 adaptive control for safety-critical systems, *IEEE Control Syst*, **31**(5), 54–104.

[47] Shi, Z., Zhao, L. (2017). Robust model reference adaptive control based on linear matrix inequality, *Aerosp. Sci. Technol.* **66**, 152–159.

[48] Yang, Y., Chen, X., Li, C. (2015). Transient performance improvement in model reference adaptive control using $H\infty$ optimal method, *J. Franklin Inst.*, **352**(1), 16–32.

[49] Nguyen, N. T., Krishnakumar, N. (2008). An Optimal Control Modification to Model-Reference Adaptive Control for Fast Adaptation. *AIAA Guidance, Navigation and Control Conference and Exhibit*.

[50] Sun, W., Zhang, Y., Huang, Y., Gao, H., Kaynak, O. (2016). Transient-Performance-Guaranteed Robust Adaptive Control and Its Application to Precision Motion Control Systems, *IEEE Trans. Ind. Electron.*, **63**(10), 6510–6518.

[51] Gruenwald, B., Yucelen, T. (2015). On transient performance improvement of adaptive control architectures. *Int. J. Control*, **88**(11), 2305–2315.

[52] Gibson, T.E., Annaswamy, A.M., Lavretsky, E. (2013). On adaptive control with closed-loop reference models: transients, oscillations, and peaking, *IEEE Access 1*, 703–717.

[53] Gibson, T.E., Annaswamy, A.M., Lavretsky, E. (2013). Adaptive systems with closed-loop reference-models, Part I: transient performance. *Am. Control Conf.*, 3376–3383.

[54] Wiese, D.P., Annaswamy, A.M., Muse, J.A., Bolender, M.A., Lavretsky, E. (2015). Adaptive output feedback based on closed-loop reference models for hyper-sonic vehicles, *J. Guid. Control Dyn.* **38**(12), 2429-2440.

[55] Guo, J. X., Tao, G., Liu, Y. (2011). A multivariable MRAC scheme with application to a nonlinear aircraft model, *Automatica*, **47**(4), 804–812.

[56] Tao G. (2014). Multivariable adaptive control: A survey, *Automatica*. **50**, 2737–2764.

[57] Johansson, K. H. (2000). The quadruple-tank process: a multivariable laboratory process with an adjustable zero, *IEEE Trans. Control Syst. Technol.* **8**(3), 456–465.

[58] Buciakowski, M., Rozprza-Faygel, M., Ochałek, J., Witczak, M. (2014). Actuator fault diagnosis and fault-tolerant control: Application to the quadruple-tank process. *J. Phys.: Conf. Ser.* **570**(8), 082002.

[59] Locatelli, A.; Schiavoni, N. (2011). Reliable regulation in decentralised control systems, *Int. J. Control*. **84**(3), 574–583.

[60] Locatelli, A., Schiavoni, N. (2009). Reliable regulation in centralized control systems. *Automatica*. **45**(11), 2673–2677.

[61] Gündeş, A. N., Mete, A. N., A. Palazoğlu. (2009). Reliable decentralized PID controller synthesis for two-channel MIMO processes. *Automatica*. **45**(2), 353–363.

[62] Zhang, Z., Chen, W. (2009). Adaptive output feedback control of nonlinear systems with actuator failure. *Inf. Sci.* **179**, 4249-4260.

[63] Tang, X. D., Tao, G., Joshi, S. M. (2003**).** Adaptive output feedback actuator failure compensation for a class of state-dependent nonlinear systems. *Proc. 42th IEEE Conf. Decision Control*, 1681–1686.

[64] Tang, X. D., Tao, G., Joshi, S. M. (2005**).** Adaptive output feedback actuator failure compensation for a class of non-linear systems. *Int. J. Adaptive Control Signal Process*. **19**, 419–444.

[65] Tang, X. D., Tao, G., Joshi, S. M. (2005). Adaptive output feedback actuator failure compensation using dynamic bounding: output regulation. *Proc. American Control Conf.* 3315–3320.

[66] X.D. Tang, G. Tao, S.M. Joshi (2005**).** Adaptive output feedback actuator failure compensation using dynamic bounding: output tracking and an application, *Proc. American Control Conf.* 3186–3191.

[67] Ioannou, P. A. Fidan, B. (2006). *Adaptive control tutorial*; SIAM :Philadelphia

[68] Slotine, J. J., Li, W. (1991). Applied nonlinear control. Prentice- Hall International INC. New Jersey.

[69] Tao, G. (2003). *Adaptive control design and analysis*, Wiley: Hoboken, NJ.

[70] Ioannou, P. A.; Sun, J. (1996). *Robust Adaptive Control*; Prentice-Hall: Upper Saddle River, NJ.

[71] Tao, G., Chen, S. H., Tang, X. D., Joshi, S. M. (2004). *Adaptive control of systems with actuator failures*. Springer-Verlag: London.

[72] Hsu, L., Battistel, A., Nunes, E. V. L. (2014**).** Multivariable MRAC Design Without Gain Symmetry Conditions Using a Stabilizing Multiplier. *IEEE Trans. Autom. Control*. **59**(4), 1041–1047.

[73] Alvarez, F., Attouch, H., Bolte, J., Redont, P. (2002). A second-order gradient-like dissipative dynamical system with hessian-driven damping: Application to optimization and mechanics. *Journal de mathématiques pures et appliquées*, **81**(8), 747–779.

[74] Arıcı, M., Kara, T. (2018). Improved Adaptive Fault-Tolerant Control for a Quadruple-Tank Process with Actuator Faults, *Industrial & Engineering Chemistry Research*. **57** (29), 9537-9553

[75] Attouch, H., Peypouquet, J., Redont, P. (2016). Fast convex optimization via inertial dynamics with Hessian-driven damping. *Journal of Differential Equations*, **261**(10), 5734–5783.

[76] Barkana, I., Teixeira, M. C. M., Hsu, L. (2006). Mitigation of symmetry condition in positive realness for adaptive control. *Automatica*, **42**(9), 1611-1616.

[77] Feedback Instruments .Coupled Tanks Installation & Commissioning Manual 33-041-IC. www.feedback-instruments.com.

PUBLICATIONS

[1] Arıcı, M., Kara, T. (2018). Improved Adaptive Fault-Tolerant Control for a Quadruple-Tank Process with Actuator Faults, *Industrial & Engineering Chemistry Research*. **57** (29), 9537-9553

[2] Kara, T., Arıcı, M. (2017). State Feedback Switching Control of an Underactuated Planar Manipulator with Partial Feedback Linearization, *Süleyman Demirel Üniversitesi Fen Bilimleri Enstitüsü Dergisi*, **21**(3), 703-710.

[3] Arıcı, M., Kara, T. (2017). Model Reference Adaptive Control of a Quadruple Tank Process with Actuator Faults, ELECO 2017 10th International Conference on Electrical and Electronics Engineering.

[4] Özkan, S., Kara, T., Arıcı, M. (2017). Modelling, Simulation and Control Of Quadruple Tank Process, *ELECO 2017 10th International Conference On Electrical And Electronics Engineering*.

[5] Arıcı, M., Kara, T. (2016). Adaptive Fault Tolerant Control for Liquid Tank Process, *International Journal of Applied Mathematics, Electronics and Computers*, **4**, 111-117.

[6] Arıcı, M., Kara, T. (2016). Adaptive Fault Tolerant Control for a Liquid Tank Process, *3rd International Conference on Advanced Technology & Sciences.*

[7] Arıcı M., Arslan, A. O. (2015). Self-tuning speed control of permanent magnet DC motor, *9th International Conference on Electrical and Electronics Engineering (ELECO*).

[8] Arıcı, M., Kara, T. (2013). Eksik Tahrikli Robot Manipülatörün Durum Geri Beslemeli Kontrolü, Otomatik Kontrol Ulusal Toplantısı (TOK2013).

CIRRICULUM VITAE

PERSONAL INFORMATION

Surname, Name: ARICI, Mehmet

Nationality: Turkish (Republic of Turkey)

Date and Place of Birth: 21 October 1986, Gaziantep

Phone: +90 342 317 2112

email: mehmetarici@gantep.edu.tr

EDUCATION

Degree	Institution	Year of Graduation
MS	Gaziantep University	2013
BS	Karadeniz Technical University	2010

WORK EXPERIENCE

Year	Place	Enrollment
2011-Present	Gaziantep University	Research Assistant